



AMERICAN UNIVERSITY OF BEIRUT

ENHANCING THYMOQUINONE'S ANTICANCER  
POTENTIAL BY COMBINATORIAL, CONJUGATIONAL  
AND NANOFORMULATION APPROACHES

by  
ISABELLE HILAL FAKHOURY

A dissertation  
submitted in partial fulfillment of the requirements  
for the degree of Doctor of Philosophy  
to the Department of Biology  
of the Faculty of Arts and Sciences  
at the American University of Beirut

Beirut, Lebanon  
September 2016

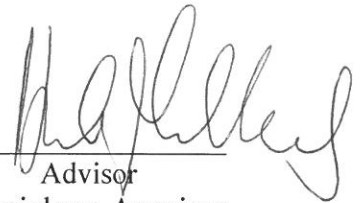
AMERICAN UNIVERSITY OF BEIRUT

ENHANCING THYMOQUINONE'S ANTICANCER  
POTENTIAL BY COMBINATORIAL, CONJUGATIONAL  
AND NANOFORMULATION APPROACHES

by  
ISABELLE HILAL FAKHOURY

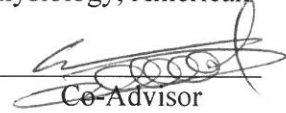
Approved by:

\_\_\_\_\_  
Dr. Hala Gali-Muhtasib, Professor  
Department of Biology, Department of Anatomy, Cell Biology, Physiology, American  
University of Beirut, Lebanon



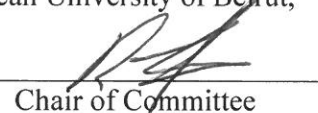
Advisor

\_\_\_\_\_  
Dr. Walid Saad, Assistant Professor  
Department of Chemical and Petroleum Engineering, American University of Beirut,  
Lebanon




Co-Advisor

\_\_\_\_\_  
Dr. Rabih Talhouk, Professor  
Department of Biology, American University of Beirut, Lebanon



Chair of Committee

\_\_\_\_\_  
Dr. Kamal Bouhadir, Associate Professor  
Department of Chemistry, American University of Beirut, Lebanon



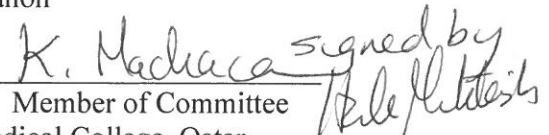
Member of Committee

\_\_\_\_\_  
Dr. Diana Jaalouk, Assistant Professor  
Department of Biology, American University of Beirut, Lebanon



Member of Committee

\_\_\_\_\_  
Dr. Khaled Machaca, Professor  
Department of Physiology and Biophysics, Weill Cornell Medical College, Qatar



K. Machaca signed by  
Hala Gali-Muhtasib

Member of Committee

Date of dissertation defense: April 25th, 2016

# AMERICAN UNIVERSITY OF BEIRUT

## THESIS, DISSERTATION, PROJECT RELEASE FORM

Student Name:     Fakhoury         Isabelle         Hilal      
                                    Last                                    First                                    Middle

Master's Thesis                       Master's Project                       Doctoral Dissertation

I authorize the American University of Beirut to: (a) reproduce hard or electronic copies of my thesis, dissertation, or project; (b) include such copies in the archives and digital repositories of the University; and (c) make freely available such copies to third parties for research or educational purposes.

I authorize the American University of Beirut, three years after the date of submitting my thesis, dissertation, or project, to: (a) reproduce hard or electronic copies of it; (b) include such copies in the archives and digital repositories of the University; and (c) make freely available such copies to third parties for research or educational purposes.

---

Signature

Date

This form is signed when submitting the thesis, dissertation, or project to the University Libraries

## ACKNOWLEDGMENTS

Over the past five years, I have received support and encouragement from a great number of people inside and outside AUB.

Dear Dr. Muhtasib, thank you for being my advisor, my instructor and my mentor. Your guidance, patience and kindness have made my experience a truly pleasant and enjoyable journey. Thank you for teaching me that focus and setting one's priorities are the keys to success. I wish you all the success and happiness in the world.

Thank you, Dr. Saad, for introducing me to the world of nanoparticles and their wide range of possible applications. I am forever indebted to your valuable teachings and help in planning and troubleshooting the experiments.

Thank you, Dr. Bouhadir, for your generosity in supplying materials needed for the project as well as for always being available to discuss and answer my questions. In addition, I would like to acknowledge Dr. Ali Kobeissi and Antranik Jonderian from your lab for their cooperation.

Dear Dr. Talhouk, I am very thankful to have taken your Advanced Cell and Molecular Biology course as well as your seminar courses. I have learned a new thing every time we met and I am forever grateful. Thank you for accepting to be the president of my thesis committee. It made me extremely happy because I have great admiration not only for your scientific and professional skills and rank, but also for your cheerful personality and wonderful easy-going character.

Dear Dr. Jaalouk, one gets to meet a professor like you only once in her lifetime. It has been an honor and a privilege. I can't thank you enough. Instead I hope that one day, I'll become a scientist of whom you are proud.

Thank you Dr. Machaca for accepting to be on my thesis committee and for your valuable contribution as committee member.

I would also like to thank Dr Raghida Abou-Merhi, Mrs. Salwa Makkouk, Ms. Maha Kaissi, Mrs. Ghida Itani, Mrs. Rania Osta, Mrs. Rita Khalil, the store room staff, Dr. Mouneimneh and all the members of the Kamal Shair Central Research Science Laboratory, Lamis Aaraj, Rabab el Eit, Sara Ghadban, Mohamad Sakr and all my course instructors for their help, as well as the Swedish Research Council, the FAS KS-CRSL and the FAS Dean's office for their financial support.

My recognition and gratitude go to all my friends from our lab and the biology department for the unforgettable happy moments we shared. Special thanks goes to Maamoun, Racha, Carla, Hala, Nasab, Angela, Rasha, Makram, Amr, Mohamad, Elia, Mike, Dana, Bilal, Rana, Mohammad, Farah, Dima and Rayan. To my tutorial students, Farah, Bassel, Danielle, Dana and Elia, you have taught me more than I could have ever imagined, this work would not have been possible without you. Also, thank you my non-biologist, non-AUBite friends, Madona, Rima, Katia, and Manal for your impact on my life.

Finally, Dad, Maurice, Jean-Pierre and Funny, you are my happiness and my most precious assets. Thank you for being by my side, thank you for being my family.

Last but not least, this thesis is dedicated to my "everything"; my mother.

# AN ABSTRACT OF THE DISSERTATION OF

Isabelle Hilal Fakhoury for Doctor of Philosophy  
Major: Cell and Molecular Biology

Title: Enhancing Thymoquinone's Anticancer Potential by Combinatorial, Conjugational and Nanoformulation Approaches

Thymoquinone (TQ), is the major bioactive component of *Nigella sativa* black seed oil. Our laboratory has long been investigating TQ's anticancer potential as well as its mechanism of action in both solid and non-solid tumors. Our results show that TQ modulates signaling pathways that are key to cancer progression, inhibits cancer cell viability in all cancer cell lines tested, while sparing the normal cells. The development of TQ however, is hindered by several factors including its hydrophobicity and limited bioavailability, its binding to non-specific targets which abrogate its activity and by the resistance of specific cell lines to treatment with TQ. In this project, we attempted to enhance TQ's anticancer activity by using combinatorial, conjugation and nanoparticle approaches.

Multi-drug regimens are commonly recommended for overcoming chemoresistance of cancer cells to a specific drug. Furthermore, combination treatment can potentially inhibit cancer viability without using high drug doses which cause severe toxic side effects. Doxorubicin (Dox) is a clinically approved drug for the treatment of a wide range of cancers including leukemia and lymphomas. However, high doses of the Dox have been associated with cardiotoxicity. To this aim, TQ was tested in combination with low doses of Dox in an adult T-cell leukemia (ATL) model. ATL is an aggressive malignancy of mature activated CD4<sup>+</sup> T-cells infected with the human T-cell lymphotropic virus type I (HTLV-1). We evaluated the effects of TQ and Dox combination treatment on cell death and cell cycle of HTLV-1 positive and negative cancer cells using MTT, trypan blue and propidium iodide (PI). Our data shows resistance of the HTLV-1 positive cancer cell line to treatment with Dox. However, co-treatment with TQ and Dox triggers cell death in both HTLV-1 positive and negative cancer cell lines. Specifically, the combination enables the use of low Dox concentrations to achieve the same viability inhibition effects as those observed in cells treated with high doses of Dox alone. TUNEL assay on Jurkat cells (HTLV-1 negative)

and HuT-102 cells (HTLV-1 positive) suggest that TQ and Dox combination treatment triggers cell death by apoptosis.

Next we sought to use nanotechnology to improve TQ delivery and accumulation at tumor sites. In this study, we describe the synthesis of polymeric TQ-NP using polystyrene-polyethylene oxide (PS-PEO) and Flash Nanoprecipitation (FNP). PS-PEO NP is a biocompatible diblock copolymer which has been used for the formulation of different NP including multifunctional NP. Passive targeting NP have been designed for use against solid and metastatic solid tumors. Hence, we characterized the NP and assessed their anticancer potential in a breast cancer model comprising of cell lines with different aggressiveness status as well as different gene expression profiles. In addition, cell-TQ-NP interaction was investigated to determine the cellular fate of the NP after intake. Specifically the dynamics and mechanism of TQ-NP uptake as well as the subcellular biodistribution of the particles in the different breast cancer cells were evaluated. Endocytosis, the main route of entry of NP to the cells was also assessed using different inhibitors of endocytosis as well as co-localization techniques. TQ-NP were stable with average diameter size of 100 nm. %EE and %LC of TQ-NP were high (approximately 80% and 50%, respectively). *In vitro*, TQ-NP had equal or enhanced anticancer activity compared to TQ, in MCF-7 and aggressive MDA-MB-231 breast cancer cell line with no significant cytotoxicity of the blank NP noted. Fluorescent TQ-NP uptake mechanism was both time and concentration-dependent. MDA-MB-231 cells exhibited more uptake of TQ-NP as compared to MCF-7 cells. Treatment with inhibitors of endocytosis revealed the involvement of caveolin-mediated endocytosis in TQ-NP uptake. This was further suggested by subcellular localization findings with the early and late markers of endocytosis.

Finally, to overcome cancer cells resistance to treatment with TQ, we prepared TQ pyrimidine hydrazides derivatives that have two additional functional groups in comparison to TQ: carbocyclic nucleosides and acylhydrazone. Both groups were chosen based on their wide range of biological activities including their antitumor potential. We hypothesized that the conjugated active classes as well as the new molecular structure can alter the binding of TQ to inhibitors which abrogate its activity and thus enhance its overall anticancer potential. To test this hypothesis high-throughput screening was performed using the PharmMapper server to identify the potential molecular targets of TQ and TQ derivatives. Comparative analysis revealed that many targets were common between TQ and the derivatives. However, unlike TQ, the derivatives were able to bind H-Ras, a small G protein of the Ras family of GTPases involved in the regulation of cell division. Furthermore, the derivatives did not bind bovine serum albumin (BSA) or NADPH quinone oxidoreductase 1 (NQO1) proteins and hence could potentially escape the inhibitory effects of these targets.

Altogether, these findings describe several approaches for the enhancement of TQ's anticancer potential. Currently, testing TQ derivatives and Dox combination treatment, as well as formulating and understanding Dox-NP and TQ derivatives NP are in preparation. Ultimately, we aim to combine and test the effectiveness of combining nanotechnology and combination therapy.

# CONTENTS

ACKNOWLEDGEMENTS .....	v
ABSTRACT.....	vi
LIST OF ILLUSTRATIONS.....	xii
LIST OF TABLES.....	xv
LIST OF ABBREVIATIONS.....	xvi

## Chapter

I. LITERATURE REVIEW .....	1
A. Introduction .....	1
B. Cancer Models.....	3
1. ATL Carcinogenesis.....	3
a. Types .....	4
b. Incidence .....	5
c. Risk Factors .....	6
d. Conventional Treatment.....	6
2. Breast Carcinogenesis .....	7
a. Types .....	9
b. Incidence .....	10
c. Risk Factors .....	12
d. Conventional Treatment.....	13
C. Nanoparticles (NP) .....	14
1. Flash Nanoprecipitation (FNP) .....	15
2. Stability of NP .....	16
3. Advantages of NP Encapsulated Drugs .....	18



4. NP and Cancer .....	19
5. Passive Targeting of NP to Tumors .....	20
6. Active Targeting of NP to Tumors.....	21
7. Physiological Barriers to NP Delivery to Tumor Tissue .....	22
8. Cellular Uptake of NP .....	23
a. Macropinocytosis .....	25
b. Clathrin-Mediated Endocytosis (CME) .....	26
c. Caveolin-Mediated Endocytosis.....	27
d. Clathrin and Caveolin Independent Endocytosis .....	27
D. Thymoquinone .....	28
1. Thymoquinone against Leukemia and Breast Cancer.....	32
a. Mechanisms of Action .....	32
i. Cell Cycle Arrest and Apoptosis.....	32
ii. p53 Independent Apoptosis.....	34
iii. Other Pathways .....	36
2. TQ in Combination.....	37
3. TQ Derivatives .....	39
4. Thymoquinone and Nanoparticles (TQ-NP).....	40
a. Activity and Biocompatibility .....	42
i. Polymeric TQ-NP.....	42
ii. Nanostructured Lipid Carriers TQ-NP (TQ-NLC) .....	44
iii. Liposomal TQ-NP (TQ-LP) .....	44
iv. Other.....	45
b. Drug Release, Uptake and Distribution .....	46
E. Hypothesis and Aims .....	47

## II. COMBINATORIAL EFFECTS OF THYMOQUINONE ON THE ANTICANCER ACTIVITY OF DOXORUBICIN IN ADULT T-CELL LEUKEMIA .....

A. Abstract .....	51
B. Introduction .....	52
C. Materials and Methods .....	54
1. Materials.....	54
2. Cell Culture .....	55
3. Drug Preparation and Cell Treatment .....	55
4. Viability Assay .....	56
5. Cell Cycle Analysis .....	56
6. TUNEL Assay .....	57
7. ROS Analysis .....	57

8. Rhodamine Staining .....	58
9. Protein Extraction and Western Blotting .....	58
10. Statistical Analysis .....	59
D. Results .....	59
1. TQ and Dox Combination Treatment Efficiently Inhibits Jurkat and HuT-102 cells.....	59
2. Combination Treatment Triggers Cell Cycle Arrest and Apoptosis .....	63
3. Oxidative Stress Occurs in Response to Treatment with the Combination .....	65
4. The Mitochondria is Disrupted in Response to Treatment with the Combination.....	67
5. Involvement of Molecular Modulators in Cell Death .....	68
E. Discussion.....	70

### III. UPTAKE, DELIVERY AND ANTICANCER ACTIVITY OF THYMOQUINONE NANOPARTICLES IN BREAST CANCER CELLS .....

A. Abstract .....	74
B. Introduction .....	75
C. Materials and Methods .....	77
1. Materials.....	77
2. Cell Culture .....	78
3. Preparation of TQ-NP .....	79
4. Characterization of TQ-NP .....	79
5. Quantification of TQ .....	80
6. Viability Assay .....	81
7. Cellular Uptake .....	82
8. Uptake Mechanism.....	83
9. Subcellular Localization.....	83
10. Statistical Analysis .....	84
D. Results .....	85
1. FNP Generates Stable TQ-NP with High %EE and %LC .....	85
2. TQ-NP Are Equally or more Active than TQ in Breast Cancer Cells and Non-Toxic to Non-Tumorigenic Breast Cells.....	87
3. NR-loaded TQ-NP Are Internalized by the Cells in a Time and Concentration-Dependent Manner .....	89

4. TQ and TQ-NP Take Different Routes for Entry into the Cells .....	93
5. Caveolin and Clathrin-Dependent Endocytosis Play a Role in TQ-NP Uptake .....	98
6. NP Can Be Processed by Endosomes and Lysosomes.....	98
E. Discussion .....	102
<b>IV. SYNTHESIS, PRIMARY BIOEVALUATION AND COMPUTATIONAL ANALYSIS OF THYMOQUINONE PYRIMIDINE DERIVATIVES .....</b>	<b>109</b>
A. Abstract .....	109
B. Introduction .....	110
C. Materials and Methods .....	112
1. Materials .....	112
2. Cell Culture .....	112
3. TQ Derivatives Synthesis.....	113
4. Characterization of TQ Derivatives .....	113
5. Viability Assay .....	113
6. Protein Target Prediction by PharmMapper.....	114
7. Systems Biology.....	114
8. Statistical Analysis .....	115
D. Results.....	115
1. TQ Pyrimidine Hydrazides Derivatives Synthesis.....	115
2. TQ Derivatives Enhance TQ's Anticancer Potential .....	117
3. Protein Target Prediction of TQ and TQ Derivatives .....	117
4. Targets Ontology .....	121
E. Discussion .....	125
<b>V. DISCUSSION AND PERSPECTIVES .....</b>	<b>129</b>
<b>BIBLIOGRAPHY .....</b>	<b>137</b>

## ILLUSTRATIONS

Figure		Page
1.	Breast architecture, onset and progression of breast cancer.....	9
2.	Differences between free drug delivery and NP-encapsulated drug delivery.....	21
3.	Mechanisms of endocytosis.....	25
4.	Cancer hallmarks modulated by TQ.....	29
5.	Key signaling pathways and molecules modulated by TQ.....	30
6.	Dox inhibits the viability of Jurkat and HuT-102 cells in a dose-dependent manner.....	60
7.	TQ and Dox combination treatment inhibits cell viability if Jurkat and HuT-102 cells.....	61
8.	Low doses of Do in combination with TQ inhibit Jurkat and HuT-102 cell viability.....	62
9.	The combination treatment induces cell death.....	64
10.	The combination treatment induces cell death by apoptosis.....	65
11.	The combination treatment induces ROS production.....	66
12.	The combination treatment disrupts the mitochondrial membrane potential.....	68
13.	TQ and the combination treatment modulate key molecular targets	69
14.	TQ-NP have round morphologies.....	86
15.	TQ-NP are stable over time.....	86
16.	TQ-NP are active in vitro against breast cancer cells.....	88

17.	TQ-NP are not toxic to normal breast cells.....	89
18.	TQ-NP are internalized in MCF-7 and MDA-MB-231 breast cancer cells.....	90
19.	TQ-NP uptake is concentration-dependent.....	92
20.	Qualitative assessment of concentration-dependent TQ-NP uptake.....	93
21.	TQ-NP uptake is time-dependent.....	94
22.	Fast TQ-NP uptake by breast cancer cells.....	95
23.	Fast TQ-NP uptake by MDA-MB-231 breast cancer cells correlates with enhanced anticancer potential.....	96
24.	TQ-NP compete with NR-TQ-NP.....	97
25.	TQ-NP uptake by caveolin-mediated endocytosis pathway.....	99
26.	TQ-NP colocalization with caveolin in MCF-7 and MDA-MB-231 breast cancer cells.....	100
27.	TQ-NP colocalization with transferrin in MCF-7 and MDA-MB-231 breast cancer cells.....	101
28.	TQ-NP colocalization with EEA-1 in MCF-7 and MDA-MB-231 breast cancer cells.....	102
29.	TQ-NP colocalization with Lamp-1 in MCF-7 and MDA-MB-231 breast cancer cells.....	102
30.	Synthesis of TQ derivatives.....	116
31.	Representation of TQ derivatives structures and molecular weights.....	117
32.	TQ pyrimidine hydrazides derivatives enhance TQ's anticancer potential.....	118
33.	Common targets among the different compounds.....	121
34.	Biological processes of TQ derivatives common targets.....	123
35.	Protein classes of TQ derivatives common targets.....	123

36.	Molecular functions of TQ derivatives common targets.....	124
37.	Pathways and networks modulated by TQ derivatives common targets...	128
38.	Model for TQ-NP uptake.....	135

## TABLES

Table		Page
1.1.	TQ-NP types, characteristics and methods of preparation.....	41
3.2.	TQ-NP have high entrapment efficiency (%EE) and loading capacity (%LC).....	86
4.3.	Classification of the top 10 disease-related targets for TQ and TQ derivatives.....	119
4.4.	Comparative gene ontology analysis.....	124

## ABBREVIATIONS

### Measurement Units and Symbols

$\alpha$	Alpha
$\beta$	Beta
$\kappa$	Kappa
$^{\circ}\text{C}$	Degree Celsius
h	hour
min	Minutes
KDa	Kilodalton
$\mu\text{M}$	Micromolar
$\mu\text{g/ml}$	Microgram per milliliter
mg	Milligram
nM	Nanomolar
%	Percent
/	Per
$\pm$	Plus or minus
x	Times

### Text Terms

%EE	Entrapment efficiency
%LC	Loading capacity
ACN	Acetonitrile



ADK	Adenosine kinase
AIs	Aromatase inhibitors
ANOVA	Analysis of variance
AP	Adaptor protein
ATL	Adult T-cell leukemia
Au	Gold
AZT	Zidovudine
Bcl-2	B-cell lymphoma 2
BRCA	Breast cancer type susceptibility protein
BSA	Bovine serum albumin
Cav	Caveolin
CD	Cyclodextrin
CLIC	Clathrin independent carrier
CME	Clathrin-mediated endocytosis
CS	Chitosan
DAPK1	Death-associated protein kinase 1
DCIS	Ductal carcinoma in situ
DMSO	Dimethyl sulfoxide
DNA	Deoxyribonucleic acid
Dox	Doxorubicin
ECM	Extracellular matrix
ED <sub>50</sub>	Effective dose 50
EDTA	Ethylenediaminetetraacetic acid
EE	Early endosomes

EEA-1	Early endosome antigen 1
EMT	Epithelial to mesenchymal transition
EPR	Enhanced permeability and retention
ER	Estrogen receptor
FACS	Fluorescence activated cell sorter
FBS	Fetal bovine serum
FITC	Fluorescein isothiocyanate
FNP	Flash nanoprecipitation
FRET	Fluorescence resonance energy transfer
GEEC	GPI-anchored protein-enriched early endosomal compartment
HINT1	Histidine triade nucleotide binding protein 1
HLA	Human leukocyte antigen
HPLC	High performance liquid chromatography
HSCT	Hematopoietic stem cell transplantation
HTLV-1	Human T-cell lymphotropic virus
IC <sub>50</sub>	50%-Inhibitory concentration
IDC	Invasive ductal carcinoma
IFN- $\alpha$	Interferon alpha
IL-2	Interleukin 2
Lamp-1	Lysosomal-associated membrane protein 1
Lck	Lymphocyte-specific tyrosine kinase 1
LDH	Lactate dehydrogenase
LP	Liposomes
MAPK	Mitogen associated protein kinase

MFI	Mean fluorescence intensity
MIVM	Multiple inlet vortex mixer
MMPs	Matrix metalloproteases
MP2K1	Mitogen activated protein kinase kinase 1
MPS	Mononuclear phagocytic system
MTT	3-(4,5-Dimethylthiazol-2-yl)-2,5-diphenyltetrazolium bromide
MVB	Multi-vesicular bodies
NAC	N-acetyl cysteine
NCI	National cancer institute
NEP	Neprylisin
NF- $\kappa$ B	Nuclear factor kappa B
Nio	Niosomes
NLC	Nanostructured lipid carriers
NP	Nanoparticles
NR	Nile red
NR-TQ-NP	Nile red thymoquinone nanoparticles
P/S	Penicillin-streptomycin
Pac	Paclitaxel
PAK1	p21-activated kinase 1
PANTHER	Protein analysis through evolutionary relationships
PBMCs	Peripheral blood mononuclear cells
PBS	Phosphate buffered saline
PEG	Polyethylene glycol
PHA	Polyhydroxyalkanoates

PHV	Poly([R]-3-hydroxyvalerate)
PI	Propidium iodide
PLGA	Poly(lactic-co-glycolic acid)
PR	Progesterone receptor
PS	Polystyrene
PVDF	Polyvinylidene fluoride
Rap-2A	Ras-related protein
ROS	Reactive oxygen species
SD	Standard deviation
SE	Standard error
SEM	Scanning electron microscope
SiRNA	Small interfering RNA
SLN	Solid lipid nanoparticles
SNK	Student-Newman-Keuls
STRING	Search tool for the retrieval of interacting genes/proteins
Tam	Tamoxifen
THF	Tetrahydrofuran
TNF $\alpha$	Tumor necrosis alpha
Topo	Topotecan
TQ-NP	Thymoquinone nanoparticles
TUNEL	Terminal deoxynucleotidyl transferase dUTP nick end labeling
UHRF-1	Ubiquitin-like, containing PHD and RING finger domains, 1
VEGF	Vascular endothelial growth factor
WHO	World health organization

# CHAPTER I

## LITERATURE REVIEW

### **A. Introduction**

Chemotherapy remains the most common procedure for the treatment of cancer. However, a great number of cancer patients exhibit mild to severe side effects in response to chemotherapy. This is mainly due to the toxicity of the anticancer agent against healthy tissues and organs. Chemotherapy further suffers from non-selective targeting of cancerous tissues and from tumors resistance to treatment. Non-targeted drug administration for instance, limits the dose which can be safely administered to patients, lowers the therapeutic efficacy and increases the chances of relapse. Tumor heterogeneity and prolonged drug administration regimens on the other hand, have been associated with adaptation of the tumors to the drugs and with chemoresistance (Gottesman, 2002).

Several strategies have been developed to overcome chemotherapy limitations including combination treatment, drug encapsulation and synthesis of improved drug derivatives among others. Combination treatment with two or more anticancer agents with distinct mechanisms of action have been shown to synergistically enhance the therapeutic efficacy and decrease resistance of cancer cells as well as the risk of relapse (Lehar et al., 2009). Furthermore, drugs in combination allow the targeting of a larger pool of genetically heterogeneous tumors.

Drug encapsulation enables localized high-concentration targeting of chemotherapeutics to tumor sites. Specifically, nanoparticles (NP) can be used to

control drug release, increase drug solubility, half-life circulation time, bioavailability, biodistribution as well as drug targeting and uptake (Petschauer et al., 2015). The concentration and dose of drug which can be safely administered to patients can thus be augmented while reducing the damage to healthy cells as well as patients' recovery period. Altogether, targeted drug delivery by NP lowers the systemic toxicity and side effects of the anticancer drug and improve treatment outcome.

Synthesis of drug derivatives allows the design of specific structural modifications in promising anticancer agents. The derivatives can enhance the pharmacokinetics, biodistribution and membrane transport properties of the parent drug making it more potent and or less toxic (Singh et al., 2008).

Moreover, NP can be used for targeted co-delivery of multiple drugs (Hu et al., 2010). Additional therapeutic effect and minimum side effects can thus be achieved by combining nanotechnology and combination treatment.

Thymoquinone (TQ) is a promising anticancer molecule which we have been studying for more than 10 years. To enhance the chances of TQ translation to the clinic, and in light of the success of TQ nanoparticles (TQ-NP), TQ derivatives and TQ in adjuvant therapy, the focus of this work is to test TQ-NP-assisted combination therapy for effective cancer treatment.

In this chapter, we will describe the cancer models that we used for investigating the anticancer potential of TQ derivatives, TQ-NP and TQ in combination treatment. We will also introduce the field of nanotechnology and elaborate on the anticancer properties of TQ. Finally, we will discuss the advantages of TQ in combination, TQ encapsulation and TQ derivatives in the different cancer models.

## **B. Cancer Models**

Previously in our lab, we demonstrated that TQ induces apoptosis in malignant T-cells by generation of reactive oxygen species (ROS) (Dergarabetian et al., 2013). Hence we chose the Adult T-cell leukemia (ATL) model that we formerly studied for investigating the anticancer potential of TQ in adjuvant therapy. Furthermore, TQ in combination with Doxorubicin (Dox) had not been tested against ATL although it had been tested against acute lymphoblastic leukemia and breast cancer (Brown et al., 2014; Effenberger-Neidnicht and Schobert, 2011). The effects of TQ-NP and TQ derivatives on the other hand, were tested against a breast cancer model. As discussed later on in this chapter, solid tumor models including metastatic tumors constitute a more suitable environment than non-solid tumors for drug delivery by NP. Finally, TQ derivatives can and will be assessed against the ATL model in future studies.

### ***1. ATL Carcinogenesis***

ATL is an aggressive rare form of T-cells malignancy that was initially described in Japan (Giam and Semmes, 2016; Goncalves et al., 2010). It is initiated by infection with the human T-cell lymphotropic virus type 1 (HTLV-1) (Giam and Semmes, 2016; Goncalves et al., 2010; Uozumi, 2010; Utsunomiya et al., 2015). The vast majority of people infected with HTLV-1 do not develop any disease. However, after a long latency period, 3-5% of HTLV-1 carriers develop ATL during middle age or later, at least 20 to 30 years after the onset of HTLV-1 infection.

ATL can be diagnosed by histopathological and molecular means through examination of peripheral blood, testing for HTLV-1 antibodies in the blood or HTLV-1

DNA in tumor cells. Furthermore, CD3, CD4, CD7, CD8, and CD25 can be analyzed for immunophenotypic diagnosis (Goncalves et al., 2010). Patients with ATL have elevated numbers of abnormal lymphocytes or characteristic cells called “flower cells” which have multi-lobed nuclei, condensed chromatin, small nuclei and basophilic cytoplasm. These cells infiltrate various tissues, including the lymph nodes, the skin, the spleen, the liver, the bone marrow and the central nervous system (Cook et al., 2013; Giam and Semmes, 2016; Goncalves et al., 2010; Uozumi, 2010; Utsunomiya et al., 2015). Other manifestations of ATL include skin neutrophilia, lymphadenopathy, hepatosplenomegaly, diffuse organ infiltration, immune suppression as well as hypercalcemia. ATL symptoms can range from lethargy to abdominal pain, diarrhea, cough, and ascites among others (Goncalves et al., 2010).

With a median survival of six months in the acute form, ATL remains a disease with poor prognosis (Uozumi, 2010; Utsunomiya et al., 2015).

#### a. Types

ATL is a heterogeneous disease which can be divided into five clinically different subtypes: acute, lymphoma, chronic, smoldering and cutaneous (Uozumi, 2010). These subtypes differ in terms of leukemic manifestation, organ involvement, serum lactate dehydrogenase (LDH) levels as well as corrected serum calcium levels (Utsunomiya et al., 2015). As a result, the symptoms, prognosis and patient survival rate differ between the subtypes. Poor prognosis is associated with high serum LDH and blood urea nitrogen and low serum albumin (Utsunomiya et al., 2015). Accordingly, acute and lymphoma types are the most aggressive, they can rapidly progress and



present very poor prognosis. Patients with acute ATL commonly show signs of adynamia; lymphadenomegalia; hepatosplenomegalia; multiple lesions and hypercalcemia (Uozumi, 2010). Their median survival rate ranges between 4-6 months. On the other hand, smoldering ATL symptoms including lesions are mild and no tumor mass involvement is reported (Utsunomiya et al., 2015). Thus smoldering ATL is considered a form of early stage ATL which can however lead to acute ATL over time (Giam and Semmes, 2016). The median survival rate of smoldering ATL can range up to 5 years.

b. Incidence

ATL remains a rare disease because only a small proportion of HTLV-1 carriers develop the disease. However, 10-20 million people are currently infected with HTLV-1 worldwide (Goncalves et al., 2010; Utsunomiya et al., 2015). Endemic regions include Japan, the Caribbean, Central Africa, South America, Melanesia and Iran. In recent years, a decrease in the prevalence of HTLV-1 carriers has been observed in endemic areas for ATL in Japan for instance. On the opposite, an increase in the prevalence of HTLV-1 carriers has been observed in non-endemic areas of Japan as well (Utsunomiya et al., 2015). These observations suggest that migration of HTLV-1 carriers is spreading the disease in non-endemic areas. The mortality of patients in both endemic and non-endemic areas in Japan has significantly decreased between 2000 and 2009 (Utsunomiya et al., 2015).

### c. Risk factors

HTLV-1 is more common in males, and individuals infected in childhood have higher risk to develop ATL. HTLV-1 can be transmitted through sexual intercourse, blood transfusion, sharing and re-use of contaminated syringes and needles and via breastfeeding from HTLV-1 positive mother to her child (Uozumi, 2010). Genital ulcers and sores can increase the chances of transmission of HTLV-1 by unprotected sex (Goncalves et al., 2010). Testing for HTLV-1 before blood transfusion has significantly reduced its transmission via direct intravenous exposure of the blood to the virus (Goncalves et al., 2010). Furthermore, studies suggest that cellular blood components but not plasma products present the highest risk to transmission of HTLV-1 by blood transfusion. Cold storage on the other hand lowers the risk because it reduces the chances of survival of HTLV-1 infected lymphocytes among others (Goncalves et al., 2010). The efficiency of HTLV-1 transmission by breastfeeding is estimated to be around 20%. This route is subject to many parameters which affect its efficiency including the viral load, the concordance of HLA class I type between mother and child, as well as the duration of breastfeeding (Goncalves et al., 2010).

### d. Conventional Treatment

Treatment regimens for ATL are based on the ATL subtype as well as the clinical factors at onset (Bazarbachi et al., 2011; Uozumi, 2010; Utsunomiya et al., 2015). For smoldering and indolent ATL the conventional treatment consists of a combined antiviral therapy with zidovudine (AZT) and interferon  $\alpha$  (IFN $\alpha$ ) (Bazarbachi et al., 2011; Uozumi, 2010; Utsunomiya et al., 2015). In addition, corticosteroids,

combination of various chemotherapeutic agents (including Dox), psolaren plus ultraviolet A, electron beam irradiation and surgery can be used for the treatment of ATL lesions, erythema and nodules/tumors (Uozumi, 2010; Utsunomiya et al., 2015). For aggressive chronic, acute and lymphoma types, the patients are given either conventional combination chemotherapy (LSG15) or antiviral therapy (AZT and IFN $\alpha$ ) (Uozumi, 2010). Recent data even suggests that AZT and IFN- $\alpha$  should be considered as a standard first-line therapy for ATL (Bazarbachi et al., 2011). For treating ATL, AZT and IFN $\alpha$  are generally used at doses of 900mg/day and 5-6 million IU/m<sup>2</sup>/day, respectively. The doses can be reduced after 30 days of treatment to 600mg/day and 3-5 million IU/day, respectively (Bazarbachi et al., 2011).

Alternatively, hematopoietic stem cell transplantation (HSCT) can be used to increase the survival rate of patients with ATL whereby about 40% of patients treated with HSCT achieve remission for 12-18 months as compared to a median survival rate of less than 12 months for patients without HSCT (Utsunomiya et al., 2015).

However, despite the significant benefits of the different treatments, most patients with acute ATL have high risks of relapse and their survival rates remain low.

## ***2. Breast Carcinogenesis***

The breast is composed of lobes, ducts and surrounding tissue. Every breast contains around 10 to 15 lobes formed of tens of thousands of lobules. The lobules are milk producing glands that are connected to each other by small ducts which join to form larger ducts that transport milk to the nipples (Allred, 2010). The lobules and ducts are lined by a layer of epithelial cells (luminal cells), myoepithelial cells and a basement

membrane which separates them from the surrounding microenvironment, also known as stroma (Bertos and Park, 2011). The stroma contains extracellular matrix elements, fibroblasts, adipocytes, immune cells as well as blood vessels. A normal breast tissue architecture is represented in Figure 1.

Around 75% of all breast cancers diagnosed thus far, are invasive ductal carcinoma (IDC). Invasive lobular carcinomas are diagnosed in 10% of breast cancer patients. On average, the survival rate for breast cancer patients is 10 years (Bertos and Park, 2011). It is now established that ductal carcinoma *in situ* (DCIS) is the immediate precursor of IDC. DCIS occurs when epithelial cells become cancerous, proliferate yet remain confined in the milk duct. This is commonly referred to as stage 0 cancer (Marshall, 2014). The progression from DCIS to IDC implicates an invasive stage where the cancerous cells breach the basement membrane which separates them from the surrounding tissues. From a cell and molecular perspective, cells of DCIS and IDC are very similar; the major difference however, is that the latter are invasive (Allred, 2010). The progression from DCIS to IDC is represented in Figure 1. IDC can give rise to metastatic cancers which are the main cause of cancer death worldwide.

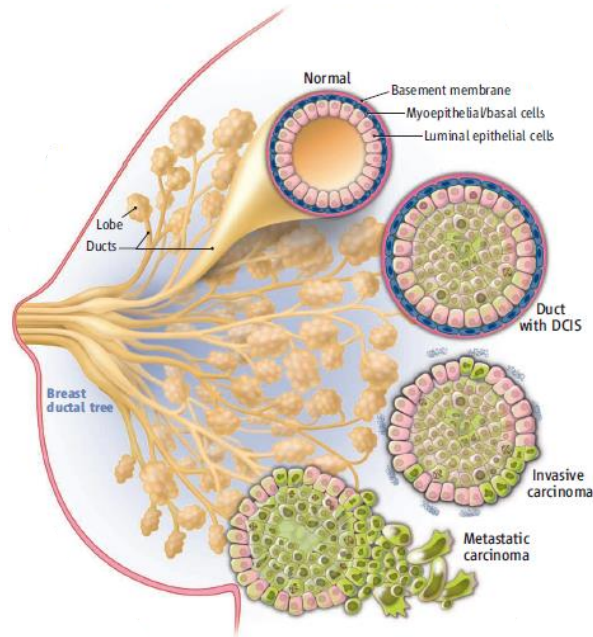


**Figure 1. Breast Architecture, Onset, and Progression of Breast Cancer.** Lobules are connected to the nipple by ducts. Ductal carcinoma is the most abundant type of breast cancer. DCIS is the precursor of IDC (Reproduced with permission from Marshall, 2014)

a. Types

Breast cancer is a complex and heterogeneous disease that is classified into five subtypes based on gene expression profiling, histological examination, tumor grade, lymph node status, the expression of the estrogen receptor alpha ( $ER\alpha$ ), the progesterone receptor (PR) and the human epidermal growth factor receptor 2 (HER2) (Holliday and Speirs, 2011). The subtypes also differ in terms of response to treatment. Briefly, luminal A breast tumors have ER, lack HER2 and often express PR. Luminal B subtypes are similar to luminal A in terms of ER and PR expression, but also express HER2. Both luminal subtypes respond to hormonal therapy and chemotherapy and HER2 positive cancers respond to HER2 targeted therapy (Bertos and Park, 2011; Holliday and Speirs, 2011). Aggressive HER2 subtypes lack ER and PR. They represent 10%–20% of all diagnosed breast cancers but respond well to HER2 targeted therapy.

Basal-like breast cancers are triple-negative as they lack ER, PR and HER2. Most BRCA1 breast cancers are basal-like and therefore do not respond to HER2 targeted therapies such as tamoxifen, trastuzumab and aromatase inhibitors (AIs). Claudin-low subtype have only been recently distinguished from basal-like subtype as they have been both previously classified as triple-negative cancers. Similar to the basal-like subtype, claudin-low lack ER, PR and HER2 but they differ by their low levels of expression of claudins and E-cadherin (Holliday and Speirs, 2011). From a prognostic point of view, the status of PR does not seem to have a significant clinical impact (Bertos and Park, 2011). ER positive cancers, however, have the best prognosis as they respond well to hormonal therapy. HER2 positive cancers have also a good prognosis because of the development of HER2 targeted therapy. The basal-like and claudin-low have the worst prognosis.

#### b. Incidence

Worldwide: According to the World Health Organization (WHO), cancer figures among the leading causes of mortality with approximately 8.2 million cancer-related deaths in 2012, or the equivalent of 4.5% of all deaths worldwide. Breast cancer, responsible for 521,000 deaths, is the most common type of cancer reported in women, and the fifth deadliest cancer (World Health Organization, 2015). Breast cancer of males accounts for 0.8% to 1% of all breast cancer deaths in the world (Nounou et al., 2015). In most developed countries, breast cancer incidence rates are below 40 per 100,000 women, but Western Europe has a significantly higher incidence rate of 89.7 per 100,000 women. With 19.3 per 100,000 women, Eastern Africa has a significantly

lower record of breast cancer incidence rate (World Health Organization, 2016). The survival rates however increase from less than 40% in low-income countries to 60% in middle-income countries, respectively. North America, Sweden and Japan record the highest survival rate with over 80% chance of survival (Coleman et al., 2008). Overall, 58% of breast cancer-related deaths take place in less developed countries.

In the Arab countries: Breast cancer is also the most common cancer in women and constitutes 13-35% of all cancers (El Saghir et al., 2007). The median age at presentation is 49-52 years, which is lower than that reported in the developed countries (63 years).

In Lebanon: Analysis of the 3.6 million cancer cases reported in the 2004 Lebanese National Breast Cancer Registry revealed that breast cancer is the leading cancer among Lebanese females. Specifically, 38.2%, i.e., more than one third, of all reported cancer cases in Lebanese females, were breast cancer. Compared to regional and Western countries, Lebanon had the highest breast cancer as proportion of all reported tumors. It was closely followed by Egypt (37.6%) and Jordan (36.2%). Lebanon also scored the highest age-specific incidence rates worldwide for the age groups 35–39 (behind Israeli Jews), 40–44 and 45–49 years. Finally, the median age at diagnosis for Lebanese females; 52.5 years was similar to that of Mexico, Jordan and Palestine. However, Lebanon's median age at diagnosis was much lower than that of USA and Western Europe (61-63 years) but higher than that of Saudi Arabia, Kuwait and Egypt (45-47 years) (Lakkis et al., 2010).

The above study highlights two major aspects: First, Lebanese women have higher incidence rates and age-specific incidence rates of breast cancer in comparison with other Arab or Western countries. Second, compared to developed Western

countries, Lebanese females have younger median ages at diagnosis. Whether these observations result from ethnic genetic differences and/or demographic differences remains unknown, especially that the study does not offer insights on cancers' genomic profiles, clinical or pathological characteristics, or the different treatments used. However, earlier work which included data from 1,320 patients seen at AUBMC between 1990 and 2001, revealed that younger women had worse prognosis and low survival in spite of having a higher than expected positive hormone receptor status, and receiving more aggressive chemotherapy namely, anthracycline-based adjuvant chemotherapy and equivalent adjuvant tamoxifen hormonal therapy (El Saghir et al., 2006).

Despite the high incidence rates of breast cancer, Lebanon and the Arab countries have only 84 radiation therapy centers, 256 radiation oncologists and 473 radiation technologists (El Saghir et al., 2007). By comparison, the USA, whose population is equivalent to that of the Arab world, has 1,875 radiation therapy centers, 3,068 radiation oncologists and 5,155 radiation technologists (El Saghir et al., 2007). Such difference clearly highlights the need for medical development in Lebanon and the Arab region.

### c. Risk Factors

Several genetic and environmental risk factors have been associated with breast cancer. For instance, mutations in BRCA1 and BRCA2 genes are associated with a higher risk of developing breast cancer. Family history of breast cancer incidence further increases the risk by two folds. Other genes have been associated with breast



cancer including PR, ER, HER2, PTEN, ATM, LKB1, DNA repair genes, TNF- $\alpha$ , Hsp70, and glutathione s-transferase family of genes (Nounou et al., 2015). Other factors have also been linked to increasing breast cancer incidence and death rate. For instance, 21% of all breast cancer deaths worldwide have been attributed to alcohol, overweight and obesity as well as physical inactivity (Danaei et al., 2005). On the other hand, a systematic review and meta-analysis study has shown that oral contraceptives, hormonal replacement therapy and diabetes mellitus significantly increase the risk of breast cancer by up to 10% to 23%. In contrast, women who breastfed had 10% lower risk of breast cancer in comparison to women who didn't (Anothaisintawee et al., 2013).

#### d. Conventional Treatment

Mastectomy is performed in cases where a detected breast tumor has already become invasive. In localized tumors, breast cancer conservation surgery is performed. Commonly, neoadjuvant therapy regimen is administered before surgery, to shrink the tumor, and radiation is applied after surgery to target any remaining cancerous cells. Depending on the breast cancer subtype, after surgery the patients receive adjuvant therapy which consists of chemotherapy, hormonal therapy or targeted therapy alone or in different combinations (Nounou et al., 2015).

Dox, paclitaxel (Pac), cyclophosphamide and capecitabine are approved chemotherapeutics for treatment of breast cancer (Wang et al., 2010). Dox is an anthracycline which inhibits DNA synthesis (Agudelo et al., 2016). Patients treated with Dox have high survival rates but can suffer from major side effects including

cardiotoxicity (Wang et al., 2010). Pac is a taxane which inhibits mitosis (Darwiche et al., 2007). Patients treated with Pac have a better response rate than those treated with Dox but exhibit lower overall survival rate. Capecitabine and cyclophosphamide are DNA alkylating agents which inhibit DNA synthesis. Cyclophosphamide is often used in combination with Pac or Dox to increase the survival rate. Capecitabine has high clinical outcome in metastatic cancers but patients treated with capecitabine can suffer from cardiotoxicity side effects (Wang et al., 2010).

### **C. Nanoparticles (NP)**

NP are organic or inorganic particles that have sizes in the range of 10-1000 nm. They are subdivided into nanocapsules and nanospheres. Nanocapsules have a solid shell and a hollow body while nanospheres are entirely solid. NP can be spherical or non-spherical depending on their type (Allouche, 2013). There are many different types of NP, including liposomes, micelles, dendrinanocapsules and antibodies (Allouche, 2013; Gupta et al., 2010; Lammers et al., 2012; Nair et al., 2010). Polymers are commonly used for the preparation of liposomes, micelles, dendrimers and capsules. Examples of widely used natural polymers include albumin, gelatin, dextran, pullulan and chitosan (CS). Poly(lactic-co-glycolic acid) (PLGA), polyethylene glycol (PEG), polystyrene (PS), poly(cyano)acrylate, and polyethylenimine are among the most used synthetic polymers (De Jong and Borm, 2008). In addition, various ligands can be easily attached to the polymer or incorporated in the NP, such as antibodies, tumor-specific peptides and fluorescent dyes. NP are prepared by bottom-up or top-down approaches which are based on grinding, or precipitation, respectively (Allouche, 2013; Nekkanti et

al., 2012; Swami et al., 2012). Furthermore, NP preparation methods can be divided into two-step procedures and one-step procedures. The two-step procedures include emulsion and emulsification (Allouche, 2013). Emulsion consists of the mixing of two or more immiscible liquids obtained in the presence or absence of a surface active agent. A nanoemulsification step is therefore required for converting nanodroplets into NP. Precipitation induced by solvent removal, solvent evaporation, solvent diffusion, salting-out, gelation of the emulsion droplets, polymerization in emulsion, conventional emulsion polymerization and many more techniques can be used to generate NP from emulsion (Allouche, 2013). Two-step approaches are challenging because they depend on the production of defined morphologies. In addition, many emulsifications require high energy. As for the one-step methods of NP preparation, commonly used techniques include nanoprecipitation, desolvation, self-assembly, nanogelation and supercritical drying among others (Allouche 2013).

### ***1. Flash Nanoprecipitation (FNP)***

Flash nanoprecipitation (FNP) is a rapid precipitation technique for the formation of NP by copolymer stabilization (Saad and Prud'homme, 2016). It was developed at Princeton University in 2003. This one-step procedure for the preparation of organic NP does not require an emulsification step. Like nanoprecipitation, FNP is among the easiest, most economical and reproducible means for preparing polymeric NP. It differs from traditional nanoprecipitation methods however by the dynamics of the process which involves a rapid mixing time shorter than the time needed for NP formation (Johnson, et al. 2003). The kinetics of NP formation are driven by externally

applied forces, i.e., a controlled flow of anti-solvent. FNP requires a confined mixing chamber to rapidly mix the solute with a non-solvent for supersaturation and precipitation of the particles (Saad and Prud'homme, 2016). Mixing is performed in multiple inlet vortex mixer (MIVM) (D'Addio et al., 2012). Stabilization of the nucleating particles is achieved by stabilizing polymers. The NP formed by FNP are not in an equilibrium state, they are in a kinetically frozen state. The advantage of this system is that it enables flexibility in controlling the size and loading of the particles (Johnson and Prud'homme, 2003; Johnson et al., 2003; Saad and Prud'homme, 2016).

FNP has been used to prepare NP for imaging, targeting and drug optimization purposes. In addition, multifunctional NP engineered for therapeutic and imaging purposes have also been prepared by FNP. Finally, multiple drugs have been delivered by NP prepared by FNP (Saad and Prud'homme, 2016).

## ***2. Stability of NP***

NP stability in solution depends on several parameters including the components' nature, solubility, concentration and/or ratio, temperature, precipitation rate, and charge. (Lammers et al., 2012). In other terms, NP stability depends on the factors governing the interaction of NP with each other and with the surrounding solvent. In precipitation and stabilization methods of preparation, NP are formed once the solute reaches supersaturation in the solvent and starts nucleating and growing. By increasing the concentration of solute in the system, the free energy of the solute increases. On the other hand, when the solute nucleates, its free energy decreases but the surface energy increases because the solution has two phases: 1- the solvent liquid

phase and 2- the solid particle (D'Addio et al., 2012). At equilibrium, the difference in free energy of the system is equal to zero. However, when this difference is not equal to zero, the particles will be unstable, which leads to aggregation or crystallization of the solute. Instabilities can occur from continuing nucleation and growth (kinetically favorable), coagulation and Ostwald ripening (Hwang et al., 2012). The main trigger behind Ostwald ripening is that small sized particles have high surface area and consequently, are thermodynamically unfavorable for having significantly high surface energy as compared to that of bulk solution (Hwang et al., 2012). Aggregation or crystallization of the solute thus becomes favorable since it can increase the particles' sizes and reduce their surface area and the free energy (Hwang et al., 2012). Ostwald ripening is the process which favors growth of large particles at the expense of small ones due to the difference in chemical potential (Mateo-Mateo et al., 2012). It is stimulated by the high polydispersity of the NP formulation (Davis et al., 1981; Tadros et al., 2004), and it describes a process where the total surface free energy of an emulsion is decreased as a result of the reorganization of monomers from smaller to larger droplets. Notably, Ostwald ripening can be suppressed by incorporation of low water soluble monomers or by addition of ultrahydrophobes given that this process highly depends on the saturation solubility near the different sized particles. Aside from the Ostwald ripening effect, collision between NP can also alter the size distribution of NP dispersions. Brownian motions cause the collision of NP together all the time. Hence, interactions can occur between charged NP and cause repulsion (Electrostatic) or attraction (Van Der Waals) which can lead to aggregation. The Zeta potential which represents the net charge difference between the solvent and the particles is a measurement that can predict NP stability, with large Zeta potentials (negative or

positive) favoring NP stability and small ones favoring aggregation. Surfactants are commonly used to confer electrostatic stability for NP formulations. Other than charge stabilization, various molecules including amphiphilic diblock polymers are used to confer steric stabilization.

### ***3. Advantages of NP Encapsulated Drugs***

Chemotherapy suffers from systemic toxicity, poor bioavailability and low targeting of drugs to tumors. This is in part due to the rapid degradation of the drugs or their excretion (Lammers, 2012). Toxicity arises because most administered anticancer drugs are taken up by healthy tissues and organs and only a small percentage of the remaining drugs is able to reach the tumor. Chemotherapeutic drugs also usually target rapidly growing healthy cells including hair follicles, bone marrow and gastrointestinal tract cells, resulting in unwanted adverse effects. NP are drug delivery systems designed to overcome the problems posed by administration of chemotherapeutic drugs, by enhancing drug activity and limiting side effects on the body. Mainly, encapsulation of water-insoluble drugs increases their dissolution, retention and bioavailability upon administration. NP can also inhibit drugs from diffusion to normal tissues as well as prevent their rapid metabolism (Gupta et al., 2010; Mohanraj and Chen, 2006; van Vlerken and Amiji, 2006). Moreover, because of the deregulated and leaky nature of tumor vasculature along with the poor lymphatic drainage near the tumor sites, NP are retained and accumulate near the tumors which decreases exposure of non-specific sites to the drug and prevents subsequent side effects or non-specific body reactions to the treatment (Gupta et al., 2010; Mohanraj and Chen, 2006; van Vlerken and Amiji, 2006).

#### ***4. NP and Cancer***

NP have been researched for the diagnosis as well as the treatment of cancer. So far, only therapeutic NP have been approved for use in the clinic. In 1995, the first nanoparticle for the treatment of cancer was FDA approved. Doxil®, a PEGylated liposomal formulation of Dox, was approved for the treatment of HIV-related Kaposi's sarcoma (Nounou et al., 2015; Ryan and Brayden, 2014). This formulation was more advantageous than free Dox in enhancing the pharmacokinetics, biodistribution and circulation time of the drug as well as enabling more drug accumulation in the tumor. Since then, 11 NP-based formulations have been approved for use in the clinic for the treatment of various cancers, and over 30 different formulations have reached clinical trials for cancer treatment (Lammers et al., 2012). In the past 10 years also, around 72 NP designed for the diagnostic or treatment of breast cancer have been patented (Nounou et al., 2015). It is worth noting that while different drug carrier types have reached the clinic or have been approved for the treatment of cancer, no active targeting formulation has so far been approved. Abraxane®, Myocet® and Doxil® are currently approved for the treatment of breast cancer (Ryan and Brayden, 2014). Abraxane® is an albumin-based nanoparticle formulation of Pac. Myocet® is a non-PEGylated liposomal formulation of Dox. Doxil® is a PEGylated liposomal formulation of Dox with methoxy PEG. NP formulations are more efficient in inhibiting disease progression and increasing the survival of patients. Furthermore, patients receiving NP formulations experience lower toxicity than those receiving the free drugs (Pinder and Ibrahim, 2006; Ryan and Brayden, 2014).

### ***5. Passive Targeting of NP to Tumors***

Solid tumors commonly have leaky vascular architectures. The leakiness of the vessels increase the permeability to the NP which can extravasate towards the tumor through the gaps between the endothelial cells. Overgrowth of cancerous cells also compresses the lymphatic vessels and results in poor lymphatic drainage from the tissue and thus more retention of the NP. (Lammers et al., 2012; Nair et al., 2010). The extravasation/retention of NP at the tumor site is known as the enhanced permeability and retention effect (EPR). This type of targeting of NP is referred to as passive targeting since the NP are not actively guided to the tumors; instead they accumulate at the tumor sites because of the histological and anatomical properties of those tumors (Figure 2). The tumor density and interstitial pressure as well as the vasculature vary between cancers, nonetheless they limit and control the rate and extent of drug delivery. The EPR effect can thus vary depending on the tumor stage and the heterogeneity of the tumor vasculature. However, the EPR effect is now recognized as the main mode of targeting of NP. Passive targeting of NP has also been successful in enhancing drugs activity as compared to free drugs. In fact, all FDA-approved NP, and the majority of NP in clinic rely on passive targeting as means of enhancing drug activity and limiting side effects on normal tissues (Ryan and Brayden, 2014).



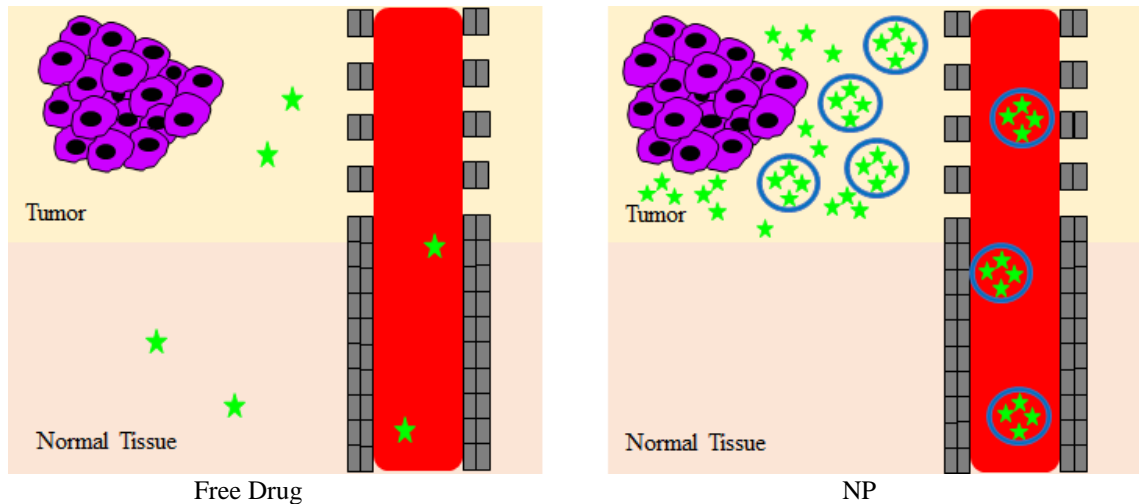


**Figure 2. Differences between Free Drug Delivery and NP Encapsulated Drug Delivery.** 1- Small amount of free drug can be administered intravenously while NP can encapsulate large amounts of drugs. 2- Free drug can diffuse through the endothelial cells to the normal tissues, but NP can't because of their size. 3- Only small amount of free drug can reach the tumor while NP will be passively targeted to the tumors. Passive targeting of NP to tumors relies on the EPR effect.

### **6. Active Targeting of NP to Tumors**

Cancer cells express specific antigens on their cell surface. NP can thus be targeted against those cancer markers to increase the specificity to cancer cells in addition to the retention and accumulation at the tumor site. Targeting is achieved by conjugation of the NP to ligands which are selective to tumor cells (Brannon-Peppas and Blanchette, 2004). Antibodies are among the most commonly used ligands for active targeting although peptides, lipoproteins and other molecules can be used. The internalization of the ligand leads to the internalization of the carrier and consequently the delivery of the cargo. Many antibodies have been approved for the treatment of cancer including Herceptin® which blocks HER2 receptor for the treatment of HER2 positive metastatic breast cancers (Brannon-Peppas and Blanchette, 2004). However, no active targeting NP has yet been approved and only a limited number has reached

clinical trials. Nonetheless, several promising active targeting NP have been developed and tested against breast cancer at the pre-clinical stages. For instance, Doxil®, the approved liposomal formulation for Dox, has been conjugated to an antibody which binds HER2. The antibody was selected for its ability to get endocytosed in breast cancer cells. As a result, the anti-HER2-modified Doxil® formulation was more efficient than Doxil® in inhibiting the growth of BT474 breast cancer cells *in vitro* and in the mouse xenograft model (Nielsen et al., 2002). Alternatively, more studies are investigating the targeting of NP to endothelial cells as means of circumventing the barriers of interstitial transport of the NP as well as for blocking a key hallmark in the survival of tumors (Brannon-Peppas and Blanchette, 2004; Lammers et al., 2012; Reynolds et al., 2003).

### ***7. Physiological Barriers to NP Delivery to Tumor Tissue***

After administration, NP have to overcome biological, cellular and subcellular barriers to deliver the cargo efficiently (Elsabahy and Wooley, 2012; Lammers et al., 2012; Zamboni et al., 2012).

First, the biological barriers can be sub-divided into external and en-route barriers. The external barriers include the skin and mucus (Elsabahy and Wooley, 2012). En-route barriers comprise of the blood and extracellular matrix among others. Most NP are administered intravenously and thus circumvent the skin and mucus barriers. However, NP in circulation still need to escape clearance by the kidneys and liver, opsonization and binding to plasma proteins. In fact, it is now established that NP smaller than 10 nm tend to be cleared by the kidneys and the liver. Small NP cleared by

the kidneys are excreted in urine. NP that are cleared by the liver into bile end up excreted with feces (Elsabahy and Wooley, 2012; Lammers et al., 2012; Zamboni et al., 2012). On the other hand, opsonization leads to clearance of the NP by the mononuclear phagocytic system (MPS) (Elsabahy and Wooley, 2012; Lammers et al., 2012; Zamboni et al., 2012). The nature and composition of the NP determines whether it will trigger opsonization and attack by the MPS system or not. For instance, albumin, complement proteins and immunoglobulins are known to activate opsonization and trigger the immune response and clearance by the MPS system (Elsabahy and Wooley, 2012; Lammers et al., 2012; Zamboni et al., 2012).

Second, to reach the tumor, NP administered intravenously have to cross the blood vessels and penetrate the tumor interstitium. The blood vasculature, the density of the tumor and the interstitial fluid pressure are thus barriers to NP delivery. In the tumors, the NP transport occurs by diffusion (Elsabahy and Wooley, 2012; Lammers et al., 2012; Zamboni et al., 2012).

Cellular barriers regulate the uptake of the NP by the cells. NP uptake commonly involves endocytosis (Kou et al., 2013). NP escape from lysosomes to the cytoplasm is also required to avoid degradation of the drug load (Iversen et al., 2011). The mechanisms involved in endocytosis are detailed in the following sections.

## ***8. Cellular Uptake of NP***

Delivery of NP cargo into cells can be achieved by release and diffusion from NP to the cells, by kiss and run mechanism of the NP on the cell membrane or by endocytosis of the NP into the cells. The factors which favor the mechanism of uptake

or delivery of the cargo are poorly understood, but both the nature of the formulation and the cell type are thought to play a role. Polystyrene NP (PS NP) have been shown to deliver their cargo by kiss and run, i.e., without uptake of the NP inside the cells (Hofmann et al., 2014). Other studies have also demonstrated endocytosis-dependent uptake of PS NP (Ekkapongpisit et al., 2012). Endocytosis of NP however, remains the most common route for cargo delivery. Endocytosis is a cell process involved in the uptake of nutrients, macromolecules, and surface receptors among others (Iversen et al., 2011; Kou et al., 2013; Oh and Park, 2014; Xu et al., 2013). It can be divided into phagocytosis and pinocytosis. Phagocytosis is the uptake of large particles by specialized cells. Pinocytosis on the other hand is the uptake of fluids and solutes. Pinocytosis is further divided into macropinocytosis, clathrin-mediated endocytosis, caveolin-dependent endocytosis and clathrin and caveolin independent endocytosis (Figure 3). The composition of the endocytic vesicle is different among the different routes of endocytosis (Xu et al., 2013). The size, charge, hydrophobicity, shape of the NP as well as cell type are factors which can favor uptake by one mechanism of endocytosis over another. Unlike diffusion, endocytosis is an active process which requires energy for the invagination of the membrane, packaging of the NP and pinching of the endocytic vesicle containing the cargo (Iversen et al., 2011; Kou et al., 2013; Oh and Park, 2014; Xu et al., 2013).

Endocytic vesicles can fuse with each other or with an early endosome (EE). Trafficking of the EE will determine the cargo's fate. The EE can recycle the cargo into the extracellular space, or to the intracellular components. The EE also goes through maturation to late endosome. This maturation process is marked by a decrease of pH. The late endosome can then fuse or mature into a lysosome. The acidic pH of the

lysosomes contributes to the degradation of the cargo (Iversen et al., 2011; Kou et al., 2013; Oh and Park, 2014; Xu et al., 2013).

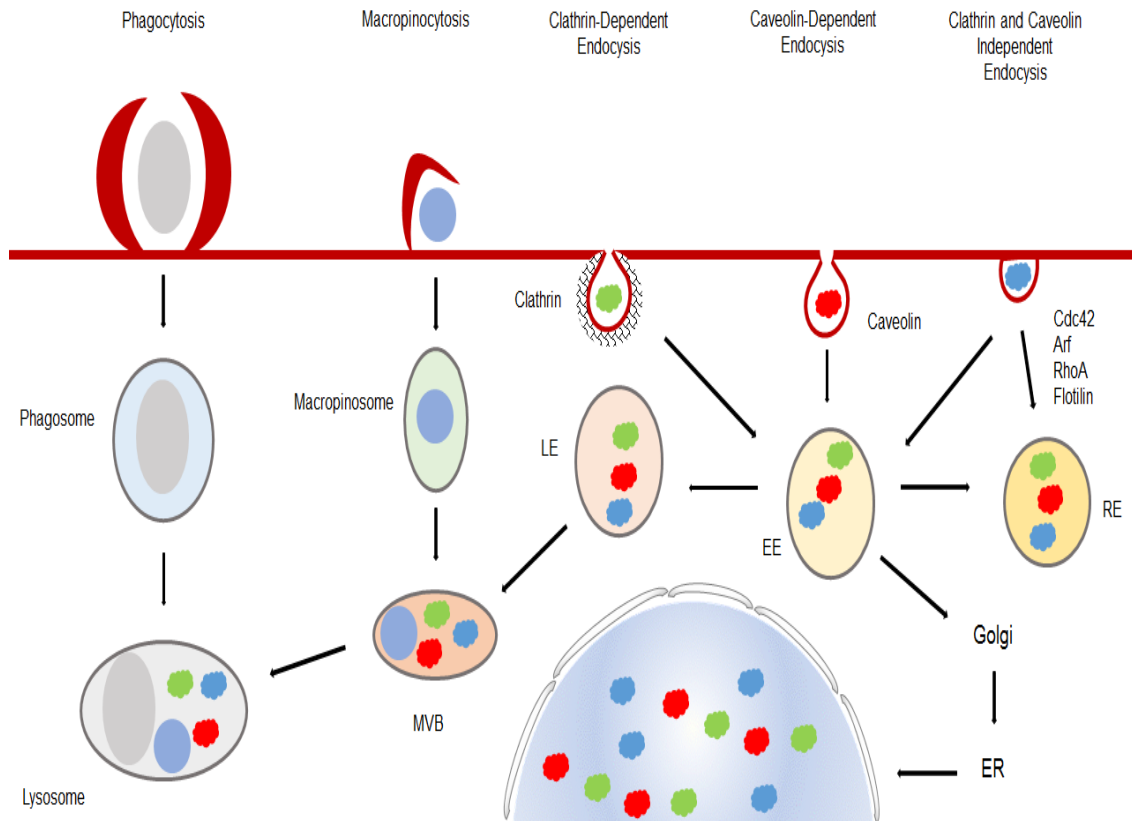


**Figure 3. Mechanisms of Endocytosis.** Endocytosis comprises phagocytosis and pinocytosis. Pinocytosis is subdivided into macropinocytosis, clathrin-dependent endocytosis, caveolin-dependent endocytosis, and clathrin and caveolin independent endocytosis. EE: Early endosomes; RE: Recycling endosome; LE: Late Endosome, MVB: Multi-vesicular body, ER: Endoplasmic Reticulum

#### a. Macropinocytosis

Macropinocytosis is the uptake of large volumes of fluids and solutes. Most cells except brain cells and endothelial cells use micropinocytosis. The vesicles formed during micropinocytosis are called macropinosomes (Iversen et al., 2011; Kou et al.,

2013; Oh and Park, 2014; Xu et al., 2013). With diameters between 0.5-10  $\mu\text{m}$ , macropinosomes are the largest endocytic vesicles. Macropinocytosis is a clathrin independent process which can be initiated spontaneously or by the activation of receptor tyrosine kinases including p21-activated kinase 1 (PAK1). Ras, Cdc42 and Rac1 as well as the PI3K pathway are also involved in macropinocytosis (Iversen et al., 2011; Kou et al., 2013). PAK1 induces actin polymerization which is required for the formation of ruffles for particle engulfing. GTPase of dynamin as well as PAK1 can assist with the separation of the macropinosomes from the membrane (Iversen et al., 2011). Macropinocytosis can be modulated by inhibiting tyrosine kinases or disrupting GTPases involved in actin remodeling. The fate of macropinosomes depend on the cell type (Iversen et al., 2011; Kou et al., 2013; Oh and Park, 2014; Xu et al., 2013).

b. Clathrin-mediated endocytosis (CME)

CME is the most studied mechanism of endocytosis. It is involved in the uptake of surface receptors and other cargo including LDL, transferrin, tyrosine kinase, as well as cholera toxin (Iversen et al., 2011; Kou et al., 2013; Oh and Park, 2014; Xu et al., 2013). CME is initiated by polymerization of clathrin at the cytosolic side of the membrane invagination facing the cargo. Dynamin and GTPases then pinch the membrane to release clathrin-coated vesicles (Iversen et al., 2011). The vesicles can be routed to the lysosomes or recycled depending on the receptor or internalized cargo (Iversen et al., 2011; Xu et al., 2013). Adaptor proteins including adaptor protein 2 (AP-2) and AP180, as well as epsin regulate endocytic vesicle formation and cytoskeleton rearrangement (Iversen et al., 2011).

### c. Caveolin-mediated endocytosis

Caveolin-mediated endocytosis is a clathrin independent mechanism of uptake. It involves caveolae, which are 50-80 nm large structures composed of cholesterol, sphingolipids, GPI-anchored proteins as well as caveolins (Iversen et al., 2011; Kou et al., 2013; Oh and Park, 2014; Xu et al., 2013). Caveolin-mediated endocytosis occurs in all cells but neuronal cells and leukocytes, where caveolin proteins are not expressed. There are three different caveolin isoforms, cav-1, cav-2 and cav-3. Cav-3 expression is muscle-specific while cav-1 and cav-2 are expressed in most non-muscle tissues. Caveolin-mediated endocytosis is a main route of entry of pathogens and viruses such as the SV40 virus and cholera toxin (Iversen et al., 2011; Kou et al., 2013; Oh and Park, 2014; Xu et al., 2013). Pathogens entering this pathway can escape lysosomal degradation. Caveolae cut-off from the membrane is mediated by dynamin (Iversen et al., 2011). Actin and microtubules then guide the caveolae in the cells for fusion with multi-vesicular bodies (MVB) or caveosomes. The fate of the cargo depends on this fusion which will either send the cargo to degradation in the lysosomes or to the endoplasmic reticulum and consequently, the cytosol and the nucleus, respectively.

### d. Clathrin and caveolin independent endocytosis

Clathrin and caveolin independent endocytosis can be divided into RhoA, Arf-6 and Cdc-42 mediated endocytosis. These mechanisms of uptake are not very well characterized. Some overlaps between these routes have also been reported. Cholesterol, dynamins, clathrin independent carrier (CLIC) and GPI-anchored protein-enriched early endosomal compartment (GLIC/GEEC) are key players in clathrin and caveolin

independent endocytosis (Iversen et al., 2011; Kou et al., 2013; Oh and Park, 2014; Xu et al., 2013).

#### **D. Thymoquinone**

TQ, or 2-methyl-5-isopropyl-1,4-benzoquinone is the main active constituent of *Nigella sativa* black seed oil. It has high reactivity to nucleophiles in addition to its redox cycling properties (Cremer et al., 1987; El-Najjar et al., 2011a). TQ has a wide range of therapeutic activities among which anti-inflammatory and anticancer properties (Schneider-Stock et al., 2014). TQ's anticancer potential has been demonstrated against many cancer models; including a number of multi-drug resistant cell lines which exhibit resistance to clinically used drugs (Worthen et al., 1998). Moreover, major organs such as the kidneys, the liver, and the heart in addition to other normal cells appear to be unaffected, resistant or even protected by TQ administration (Schneider-Stock et al., 2014). Extensive studies of TQ's anticancer activity have shown that TQ modulates nine of the ten cancer hallmarks (Figure 4). For instance, TQ disrupts cancer cell evasion from growth suppressors signals by targeting of cdks, cdk inhibitors, as well as cyclins (Gali-Muhtasib et al., 2004b; Li et al., 2010; Shoieb et al., 2003; Wirries et al., 2010). TQ also arrests cells at different phases of the cell cycle leading to growth inhibition by upregulation of the expression of p53 protein levels and its transcriptional target p21 (Alhosin et al., 2010; Arafa el et al., 2011; Gali-Muhtasib et al., 2004a; Kaseb et al., 2007; Roepke et al., 2007). Apoptosis triggered by TQ was shown to ROS generation, modulation of the B-cell non-Hodgkins lymphoma-2 (Bcl-2) protein family and activation of the intrinsic mitochondrial pathway (Badr et al., 2011; Das et al.,



2012; Woo et al., 2011). Several studies have further assessed the effect of TQ on inflammation which accounts for approximately 20% of all human cancers. Evidence suggests that TQ holds great potential for inhibiting pro-inflammatory mediators especially by regulating the TNF $\alpha$  – NF $\kappa$ B pathway (Chehl et al., 2009; El Gazzar et al., 2007; Sethi et al., 2008). TQ’s anti-angiogenic potential was also supported by its inhibitory effects on VEGF; a key pro-angiogenic molecule which enables oxygen and nutrient supplementation by stimulating the formation of new blood vessels from existing ones (Li et al., 2010; Ravindran et al., 2010; Yi et al., 2008). Finally, TQ was shown to target molecular markers involved in cancer invasiveness and metastasis including reduction of epithelial to mesenchymal transition (EMT) (Ahmad et al., 2013; Gali-Muhtasib et al., 2008b; Khan et al., 2015; Wu et al., 2011). In summary, TQ’s anticancer potential stems from its ability to disrupt critical steps for cancer survival and metastasis (Figure 5).

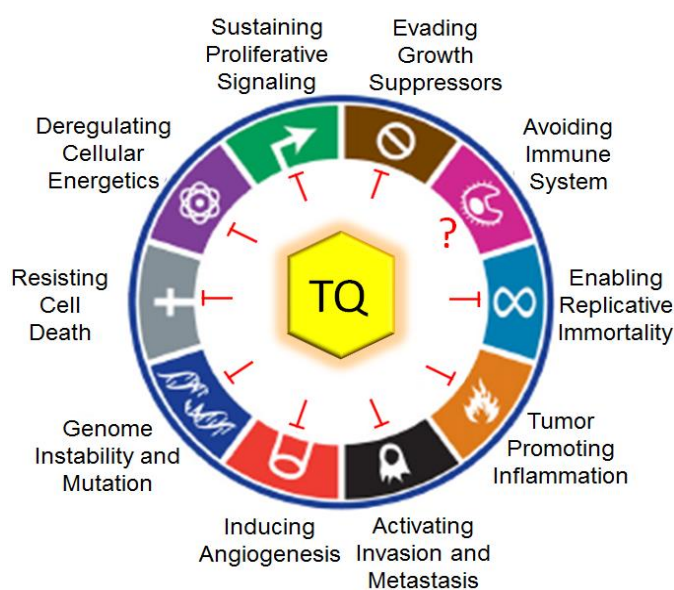


**Figure 4. Cancer Hallmarks Modulated by TQ.** TQ regulates nine of the ten cancer hallmarks described by Hanahan and Weinberg in 2011. The effects of TQ on avoiding

the immune system have not been investigated to date. Fakhoury, and Schneider-Stock, (equal contribution) et al., 2014

TQ toxicity has been assessed in several animal models in addition to a Phase I safety and clinical trial. TQ's LD<sub>50</sub> following oral and intraperitoneal administrations in mice were 870.9 mg/kg and 104.7 mg/kg, respectively, and 794.3 mg/kg and 57.5 mg/kg in rats (Al-Ali et al., 2008). Interestingly, in mice, TQ exhibited anticancer properties at subtoxic doses ranging between 5-20 mg/kg (Badary, 1999; Badary et al., 1997; Gali-Muhtasib et al., 2008b; Jafri et al., 2010). In addition, TQ oral administration to patients (23-92 years) who had failed or relapsed from therapy against a wide array of malignant tumors was well tolerated at doses ranging from 75 mg/day to 2,600 mg/day (Al-Amri and Bamosa, 2009).

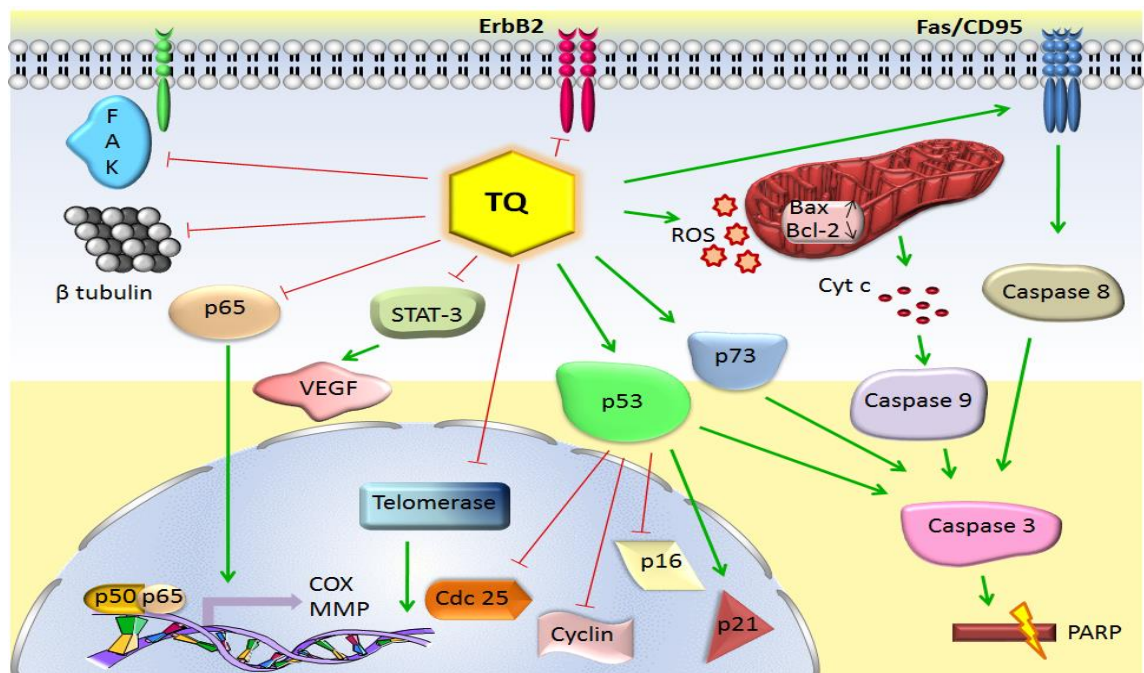


**Figure 5. Key Signaling Pathways and Molecules Modulated by TQ.** TQ prevents cancer cells from evading growth suppressors by targeting cdks (cdc 25 inhibition), cdk

inhibitors (p21 activation and p16 inhibition), as well as by inhibiting cyclins. It prevents replicative immortality by inhibiting telomerase activity. TQ also induces ROS and triggers p53 or p73-dependent apoptosis. Apoptosis by TQ occurs mostly via the intrinsic pathway through Bax upregulation and Bcl-2 downregulation, causing mitochondrial disruption, release of cytochrome c and caspase activation. Alternatively, TQ can trigger apoptosis through the extrinsic pathway through the FAS/CD95 death receptor. In addition TQ degrades  $\alpha/\beta$  tubulin in cancer cells leading to cell death. The modulation of inflammatory signals by TQ has also been evidenced: The mechanism involves inhibition of the NF $\kappa$ B pathway by blocking the nuclear translocation of p65 and downregulating the expression levels of genes coding for COX2 and MMP enzymes. Furthermore, TQ reduces angiogenesis by downregulating VEGF and deactivating STAT-3. Finally, TQ inhibits invasion and metastasis of cancer cells by downregulation of FAK and downregulating NF $\kappa$ B and MMPs. Fakhoury, and Schneider-Stock, (equal contribution) et al., 2014

TQ uptake mechanism and biodistribution remain poorly understood. However, a study investigating the distribution of an alkyne-labeled-TQ using streptavidin/biotin system has revealed its accumulation all over the nuclei of potoroo kidney cells (Effenberger-Neidnicht et al., 2011). The results were also confirmed by use of a highly specific visualization method based on alkyne-azide cycloaddition, and provided further evidence for specific localization of the TQ derivative in particular compartments of the nuclei as well as in the Golgi apparatus (Effenberger-Neidnicht et al., 2011).

TQ's biological activities, structural and pharmacological properties as well as its effects on cancer hallmarks are described in detail in our review entitled "Thymoquinone: fifty years of success in the battle against cancer models" (Schneider-Stock et al., 2014).

## **1. Thymoquinone against Leukemia and Breast Cancer**

TQ, TQ derivatives and TQ-NP have all been tested against leukemia and breast cancer models, alone or in combination. Cell cycle arrest and apoptosis are commonly triggered by TQ treatment simultaneously. In addition, examining the mechanisms involved in the inhibition of both hallmarks, TQ seems to modulate ROS levels as well as the AKT and DNA damage pathways.

### **a. Mechanisms of Action**

#### **i. Cell Cycle Arrest and Apoptosis**

The antiproliferative activity of TQ has been shown in HTLV-1 negative leukemia cells, namely Jurkat and CEM cell lines as well as HTLV-1 positive HuT-102 and MT-2 cells. The HTLV-1 cell lines were more sensitive to TQ than the HTLV-1 positive cells. ROS production and depletion of antioxidant enzymes in the HTLV-1 negative cells were also higher than in the HTLV-1 positive cells. In both types however, apoptosis occurred through the disruption of the mitochondrial membrane potential and cytochrome c release. Apoptosis was caspase-dependent and TQ was shown to activate caspases 3 and 9, as well as cleave PARP (Dergarabetian et al., 2013).

Another study confirmed the mitochondrial apoptosis mechanism in the acute lymphocyte leukemic cell line CEM. ROS generation, chromatin condensation and modulation of the Bcl-2, Bax, Hsp70 and caspases 3 and 8 levels were also implicated in the mechanism of cell death of CEM cells. The authors further revealed association of apoptosis with cell cycle arrest in the S phase. (Salim et al., 2013).

The same findings were also observed in murine WEHI-3 cells. Apoptosis was associated with cell cycle arrest in the S phase, chromatin condensation and modulation of the expression levels of Bcl-2, Bax and Hsp70. TQ further inhibited WEHI-3 cancer growth *in vivo* (Salim et al., 2014).

As for breast cancer, TQ was shown to cause cell cycle arrest of MCF-7 cells at the S or G2 phase depending on the concentration used (Motaghd et al., 2013). IC<sub>50</sub> of TQ in MCF-7 was around 25 µM at 72 h post-treatment (Effenberger-Neidnicht and Schobert, 2011; Motaghd et al., 2013).

In addition, TQ triggered G2/M cell cycle arrest as well as apoptosis in MCF-7/Dox resistant breast cancer cells. IC<sub>50</sub> of TQ in this cell line was 100 µM at 24 h. Cell cycle arrest was associated with DNA damage as evidenced by the increase in γH2AX, cyclin B1 and cdc25 expression levels. Apoptosis was evidenced by the disruption of the mitochondrial membrane potential, activation of caspases 3, 7 and 9 and cleavage of PARP as well as by the increase in the Bax/Bcl-2 ratio Mechanistically, TQ upregulated PTEN, p53 and p21 levels and inhibited the phosphorylation of AKT (Arafa el et al., 2011).

Similar observations were reported in another study investigating the effect of TQ in MDA-MB-468 and T-47D breast cancer cells. Accordingly, TQ activated PTEN and inhibited PDK1 leading to decreased phosphorylation and inhibition of AKT (Rajput et al., 2013a). Following AKT inhibition, phosphorylation and activation of downstream targets including GSK-3β 4E-BP1, eIF4E, S6R and p70S6K were also decreased. Decrease in cyclin D1, cyclin E and cyclin-dependent kinase inhibitor p27 levels further caused cell cycle arrest at the G1 phase. Apoptosis was also evidenced by the disruption of the mitochondria, release of cytochrome c, cleavage of caspase 3 and

PARP as well as the increase in apoptotic Bax and decrease of the anti-apoptotic Bcl-2, Bcl-xL and survivin (Rajput et al., 2013a).

Finally, TQ was shown to inhibit the growth of MDA-MB-435, MCF-7 and MDA-MB-231 breast cancer cells lines. The IC<sub>50</sub> for MDA-MB-231 was 50  $\mu$ M 24 h post-treatment with TQ. AKT phosphorylation was also inhibited in MDA-MB-231 cells, leading to DNA damage and release of cytochrome c, activation of caspases 3 and 7 and cleavage of PARP (Attoub et al., 2013). TQ also reduced the motility of MDA-MB-231 cells following wound assay and the invasion capacity of MDA-MB-231 and MDA-MB-231-18333 across matrigel (Attoub et al., 2013).

## ii. p53 Independent Apoptosis

Apoptosis in response to treatment with TQ has been reported in p53-null leukemic and breast cancer cell lines. In p53-null myeloblastic leukemic HL-60 cells for instance, TQ triggered apoptosis by activation of caspases 3, 8 and 9, PARP cleavage, increase in Bax/Bcl2 ratios as well as the release of cytochrome c. Caspase 8 activation was found to be upstream to cytochrome c release (El-Mahdy et al., 2005). Similarly, in acute lymphoblastic leukemic Jurkat cells, TQ induced G1 cell cycle arrest as well as apoptosis by generation of ROS, expression of the tumor suppressor p73 and cleavage of caspase 3. Knockdown of p73 abrogated mitochondrial apoptosis and cell cycle arrest. Furthermore, Ubiquitin-like PHD Ring (UHRF1), DNMT1 and HDAC1, which are involved in epigenetic regulation, were identified as the downstream targets of p73 (Alhosin et al., 2010).

This was further supported by another group which have shown the involvement of p73 and UHRF1 in cell cycle arrest and apoptosis in Jurkat cells. In fact, the increase in the expression levels of p73 led to a decrease in the expression levels of UHRF1 and PDE1A proteins. Furthermore, knockdown of PDE1A and re-expression of this protein proved that PDE1A acts upstream of UHRF1 whereby Jurkat cells growth inhibition and cell death were abrogated when PDE1A was knocked down and induced when PDE1A expression was restored (Abusnina et al., 2011).

As for breast cancer, Sutton et al. showed that TQ causes cell cycle arrest at the G1 phase, and apoptosis in MDA-MB-231 and MDA-MB-468 breast cancer cells with mutant p53 (Sutton et al., 2014). At 24, 48 and 72 h, MDA-MB-468 breast cancer cell line was more sensitive to treatment with TQ than the MDA-MB-231 breast cancer cells. Apoptosis was evidenced by cytochrome c release, caspases 8 and 9 activation as well as PARP cleavage and inhibition of XIAP. The anticancer potential of TQ also involved inhibition of AKT and upregulation of  $\gamma$ H2AX.

In addition, TQ triggered p53 independent apoptosis in T-47D, MDA-MB-231, and MDA-MB-468 breast cancer cells. MCF-7 cells possessing wild type p53 were resistant to treatment with TQ. Further investigations revealed that the NADPH quinone oxidoreductase 1 (NQO1); a flavoprotein involved in quinone detoxification, was responsible for breast cancer cells' resistance to TQ (Sutton et al., 2012).

This p53 independent apoptosis was further confirmed in another study which revealed that treatment with TQ had no effect on the level of expression of p53 in MCF-7 cells. However, apoptosis in response to TQ was associated with caspases 7, 8 and 9 activation, increase in Bax/Bcl-2 ratio, release of cytochrome c and disruption of the mitochondrial membrane potential (Woo et al., 2011). TQ also reduced invasiveness of

both MCF-7 and MDA-MB-231 breast cancer cells as evidenced by wound healing assay (Woo et al., 2011).

### iii. Other Pathways

TQ has also been shown to modulate different pathways involved in carcinogenesis. For instance, investigating the effects of TQ treatment on MCF-7 cells using cDNA microarray revealed that TQ downregulates genes involved in the estrogen and in the interferon pathways including cytochrome P450, UDP glucuronosyltransferase 1 family, and STAT1. By contrast, expression levels of caspase 10 and genes involved in p38 MAPK family was significantly upregulated (Motaghd et al., 2014). Interestingly caveolin 1 (cav-1) gene expression showed an upregulation by 1.5 fold.

Also, another study has shown that TQ activates PPAR- $\gamma$ , the main regulator of adipogenesis and lipid metabolism, in MCF-7 and MDA-MB-231 breast cancer cells (Woo et al., 2011). Further *in silico* analysis as well as expression of a dominant negative form of PPAR- $\gamma$  suggested that TQ binding to PPAR- $\gamma$  might be responsible for PPAR- $\gamma$  activation.

Nuclear factor kappa B (NF- $\kappa$ B) pathway was also involved in the response to TQ. In a model for myeloid leukemia, TQ inhibited NF- $\kappa$ B activation and suppressed the activation and phosphorylation of different kinases. TQ also inhibited antiapoptotic proliferative and antiangiogenic downstream targets to NF- $\kappa$ B including IAP1, IAP2, XIAP Bcl-2, Bcl-xL, survivin, cyclin D1, cox-2, c-Myc, MMP-9 and VEGF (Sethi et al., 2008).



TQ was also shown to degrade  $\alpha/\beta$  tubulin proteins in U87 human astrocytoma cell line U87 and in Jurkat cells but not in normal human fibroblasts. Tubulin degradation caused apoptosis in a p73 dependent manner (Alhosin et al., 2012).

Finally, based on *in silico* analysis, it was suggested that TQ binds to HDAC. As predicted, TQ inhibited HDAC in MCF-7 breast cancer cell line and reactivated p21 and Maspin, the downstream targets of HDAC. Bax/Bcl-2 ratio was also increased and cell cycle was arrested at the G2/M phase (Parbin et al., 2015).

## ***2. TQ in Combination***

Extensive evidence indicates that TQ used in combination with other active agents results in enhanced anticancer effects in leukemia and breast cancers cells *in vitro* and *in vivo* (Arafa el et al., 2011; Brown et al., 2014; Effenberger-Neidnicht and Schobert, 2011; Khalife et al., 2014; Rajput et al., 2013b; Sakalar et al., 2015; Sutton et al., 2014).

For instance, TQ and Dox both inhibit the growth of MCF-7 and MCF-7/TOPO breast cancer cells by apoptosis. TQ-Dox combination however, significantly increased growth inhibition of RAW leukemic cells as well as MCF-7 and MCF-7/TOPO breast cancer cells as compared to each drug alone (Arafa el et al., 2011; Brown et al., 2014; Effenberger-Neidnicht and Schobert, 2011). Similarly, co-treatment with cisplatin or docetaxel significantly enhanced the drugs anticancer potential in MDA-MB-468 breast cancer cell line (Sutton et al., 2014). TQ in combination with topotecan also synergistically induced cell death in U937 lymphoma cells (Khalife et al., 2014). Apoptosis signaling in response to the combination treatment was mediated

by the Bax/Bcl-2, p53, and caspases 3 and 9 proteins. In addition, TQ enhanced tamoxifen (TAM) induced apoptosis in MCF-7, T47D, MDA-MB-231 and MDA-MB-468 cells (Rajput et al., 2013b). In MCF-7 and MDA-MB-231 cells, TQ-TAM treatment was able to reduce invasion of the cells and alter the expression levels of cell cycle regulatory proteins as well as apoptotic proteins. Namely, XIAP was reduced in response to the treatment with TQ-TAM leading to apoptosis. Furthermore, XIAP was shown to act upstream of AKT in mediating TQ-TAM's anticancer response. The phosphorylation of AKT as well as that of its downstream targets, Bad and GSK-3 $\beta$ , was thus reduced in response to treatment with TQ-TAM. The efficiency of TQ-TAM combination treatment against breast cancer was also demonstrated in a xenograft model of MDA-MB-231 cells grown subcutaneously in nude mice. TQ-TAM reduced the expression levels of XIAP and the phosphorylation of AKT *in vivo* as well (Rajput et al., 2013b).

Furthermore, TQ and Pac combination was cytotoxic to 4T1 triple-negative breast cancer cells and Ehrlich tumor cells *in vitro* but not to mouse embryonic fibroblasts (Sakalar et al., 2015). The combination also deregulated the migration of 4T1 cells. *In vivo*, the combination inhibited the growth of ascites formed by intraperitoneal injection of Ehrlich tumor cells in mice (Sakalar et al., 2015). Expression levels of genes involved in the extrinsic (through Fas-I and Trail death receptors) and intrinsic (mediated by the mitochondria) apoptosis pathways were increased in 4T1 cells following treatment with the combination. JAK-STAT signaling was also activated. On the other hand, the combination reduced phosphorylation of p65 and AKT. Unexpectedly, treatment with TQ downregulated the expression levels of pro-apoptotic

proteins including caspases and increased the expression levels of VEGF (Sakalar et al., 2015).

TQ has also been investigated for use in combination with radiation therapy. TQ administration with a single dose of ionizing radiation (2.5 Gy) significantly sensitizes MCF-7 and T47D breast cancer cells (Velho-Pereira et al., 2011). TQ's chemo-radiation anticancer potential was mediated by cell cycle arrest and apoptosis (Velho-Pereira et al., 2011). Moreover, sensitization with TQ inhibited EMT-induced radiation (Rajput et al., 2015a). Mechanistically, TQ was able to restore TGF- $\beta$  in radiated breast cancer cells as well as prevent radiation-induced decrease in expression levels of E-cadherin, and increase in integrin, MMP-2 and MMP-9 expression levels (Rajput et al., 2015a).

### ***3. TQ Derivatives***

In parallel, different studies have conjugated TQ in attempt to enhance its activity. For instance, TQ was conjugated with fatty acids and investigated for its growth inhibition effect in different models including breast adenocarcinoma and leukemia (Breyer et al., 2009). In MCF-7/Topo, at 72 h after treatment, the IC<sub>50</sub> were 25  $\mu$ M and 30 nM for TQ or TQ conjugate, respectively. In HL-60 leukemic cells, the IC<sub>50</sub> at the same time point were 28  $\mu$ M and 2  $\mu$ M for TQ or TQ conjugate, respectively. The results clearly indicate an enhanced antitumor potential as compared to the native drug. The conjugates were also shown to trigger different response mechanisms than those initiated by TQ, specifically with regards to the kinetics of caspase activation (Breyer et al., 2009). Terpenes, known for their toxic and tumor suppressive properties, were also

conjugated with TQ and tested against MCF-7/Topo breast cancer cell line and HL-60 leukemic cell line among others (Effenberger et al., 2010). Similarly, some conjugates were more active than TQ and triggered apoptosis by disrupting the mitochondrial membrane potential and producing ROS. Finally, poloxin, a synthetic derivative of TQ, has also been tested against MDA-MB-231 breast cancer cell line (Yuan et al., 2011). *In vitro*, treatment with poloxin caused cell cycle arrest and induced apoptosis by destabilization of the centrosome and disruption of the mitotic spindle. Poloxin also inhibited tumor growth of MDA-MB-231 in a mouse xenograft model by triggering apoptosis (Yuan et al., 2011).

#### ***4. Thymoquinone Nanoparticles (TQ-NP)***

So far, several TQ-NP formulations have been tested against breast, colon, cervical and prostate cancers, as well as leukemia and multiple myeloma (Alam et al., 2012; Bhattacharya et al., 2015; Ravindran et al., 2010; Shah et al., 2011; Shah et al., 2010). Studies have shown that TQ-NP are more attractive candidates for clinical application than free TQ for two main reasons: 1- Enhanced activity including modulation of cancer hallmark targets *in vitro*, and 2- Increased bioavailability and distribution as compared to TQ *in vivo*. The types and characteristics as well as methods of preparation of the different TQ-NP are summarized in Table 1.

**Table 1: TQ-NP Types, Characteristics and Methods of Preparation**

Type	Method	Size in nm	%EE	%LC	Reference
PLGA-PEG	Nanoprecipitation	150-200	97	N/A	Ravindran et al., 2010
Modified PLGA	Emulsification solvent evaporation	100-200	10-35	N/A	Ganea et al., 2010
PHA-mPEG	Emulsification solvent evaporation	110-160	30-60	N/A	Shah et al., 2010
SLN	Ultrasonication	N/A	60	28	Pathan et al., 2011
PHV-mPEG	Modified emulsion-solvent evaporation	200	25	N/A	Shah et al., 2011
CS	Ionic gelation	150-200	60	31	Alam et al., 2012
SLN	Solvent injection	165	70	N/A	Singh et al., 2013
LP	Thin film hydration	100	50-90	N/A	Odeh et al., 2012
NLC	High pressure homogenization	75	N/A	N/A	Abdelwahab et al., 2013
CD	Self-assembly	445	N/A	N/A	Abu-Dahab et al., 2013
Myristic acid-chitosan	Self-assembly	150-200	N/A	N/A	Deghani et al., 2015
NLC	Hot preemulsion and crystallization	< 50	95-97	95-97	Ng et al., 2015
Au-Nio	Click chemistry	150	82		Rajput et al., 2015
Nanodrug	Ball milling	5-20	N/A	N/A	Randhawa et al., 2015
PEGylated	Nanoprecipitation	< 50	80-97	N/A	Bhattacharya et al., 2015

a. Activity and Biocompatibility

The anticancer potential of different types of TQ-NP have been investigated including the anticancer potential of polymeric, nanostructured lipid carriers (NLC), solid lipid nanocarriers (SLN), liposomal and niosomal TQ-NP among others.

i. Polymeric TQ-NP

TQ encapsulation in PLGA-PEG biodegradable nanoparticles, showed enhanced antiproliferative, anti-inflammatory and chemosensitizing effects of TQ-NP in comparison with free TQ. (Ravindran et al., 2010). Proliferation inhibition after 72 h was enhanced from 15% to 85% in colon cancer cells (HCT-116), from 30% to 88% in breast cancer cells (MCF-7), from 30% to 85% in prostate cancer cells (PC-3), and from 55% to 70% in multiple myeloma cells (U-266). Similarly, KBM-5 leukemia cell line was twice as sensitive to TQ-NP as compared to free TQ. Mechanistically, both TQ and TQ-NP inhibited NF- $\kappa$ B in KBM-5 cell line in a dose-dependent matter, with TQ-NP having greater effects as compared to the free drug. On the other hand, the pre-treatment of KBM-5 cells with TQ-NP prior to treatment with TNF $\alpha$  increased apoptosis from 18.7% to 24.8% as compared to pre-treatment with the free drug, suggesting a greater sensitizing potential for TQ-NP versus free TQ. Western blot analysis also showed greater effects of the combination of TQ-NP-TNF $\alpha$  in inhibiting NF $\kappa$ B, cyclin D1, MMP-9 and VEGF levels as compared to treatment with TQ-TNF $\alpha$ . The study finally assessed the effects of treatment with free or encapsulated drug on the cytotoxicity of KBM-5 cells, as well as on their sensitization to TNF $\alpha$  or Pac, showing significant

increase in toxicity in response to the NP as well as greater sensitization to both TNF $\alpha$  and Pac (Ravindran et al., 2010).

PEG-ylated TQ-NP were also efficient at inhibiting the proliferation of MCF-7 and HBL-100 breast cancer cells while being less toxic to peripheral blood mononuclear cells (PBMCs) than TQ. The mechanism of action of TQ-NP was p53-dependent. In response to treatment with TQ-NP, miR-34a expression levels were increased leading to downregulation of Rac1 and actin depolymerization. In consequence, TQ-NP disrupted the actin cytoskeleton which significantly decreased the rate of migration of MCF-7 breast cancer cells. Administered intravenously to tumor bearing mice *in vivo*, the NP also significantly reduced tumor volume and increased the survival rates of the animals. The role of p53 and cytoskeletal disruption in response to treatment with TQ-NP was also validated *in vivo*.

Similarly, another study reported that modified PLGA TQ-NP were more effective than TQ in inhibiting the proliferation of human breast carcinoma cells MDA-MB-231 at 96 h post-treatment (Ganea et al., 2010). The NP were also much more potent antioxidants, or ROS scavengers than TQ.

Finally, two amphiphilic TQ-NP formulations were synthesized using the polyhydroxyalkanoates (PHA)–monomethoxy PEG (mPEG) and the poly([R]-3-hydroxyvalerate)-block-mPEG (PHV-block-mPEG) diblock copolymers, respectively (Shah et al., 2011; Shah et al., 2010). The formulations were non-toxic upon evaluation on neuronal cells *in vitro*.

Beta-cyclodextrin was also used for the preparation of polymeric TQ-cyclodextrin NP (TQ-CD). Tested against MCF-7 breast cancer cells, TQ-CD were shown to enhance TQ's anticancer potential (Abu-Dahab et al., 2013). IC<sub>50</sub> following

treatment with TQ-CD or TQ for 72 h was around 5 and 25  $\mu\text{M}$ , respectively. TQ-CD NP were also less toxic to human periodontal fibroblasts.

ii. Nanostructured Lipid Carriers TQ-NP (TQ-NLC)

NLC of TQ were assessed for their anticancer activity against MCF-7 and MDA-MB-231 breast cancer cells and against Hela and SiHa cervical cancer cells (Ng et al., 2015). Blank NLC were non-toxic to normal and cancerous cell lines while TQ-NLC inhibited the growth of both breast and cervical cancers at 24, 48 and 72 h post-treatment. MDA-MB-231 cells were most sensitive to treatment with TQ-NLC. In comparison, TQ NLC were non-toxic to normal 3T3-L1 and Vero cell lines. In MDA-MB-231, TQ-NLC were shown to exert their anticancer potential by inducing apoptosis in addition to cell cycle arrest at the G2/M and S phase at 24 and 48 h.

In addition, treatment with TQ-NLC did not cause any toxicity to normal human liver cells (WRL-68) and the liver of rats (Abdel-Wahab, 2014). Examination of the stomachs, mucus production as well as histopathological evaluations further showed that TQ-NLC exhibit gastroprotective effects against ethanol-induced ulcers by modulation of Hsp70.

iii. Liposomal TQ-NP (TQ-LP)

TQ liposomal (TQ-LP) carriers have been also prepared, characterized and tested against MCF-7 and T47D breast cancer cell lines and normal periodontal ligament fibroblasts (Odeh et al., 2012). As expected, the drug carriers were effective in inhibiting the proliferation of cancer cells at 24 h post-treatment while having no toxic



effect on the normal fibroblast cell line. TQ-LP were however less potent in inhibiting cell viability than free TQ.

Niosomes, a special class of liposomes, were also used for the preparation of TQ-NP. Gold niosomes containing TQ and siRNA for AKT (siRNA-Au-Nio-TQ) were prepared and tested against tamoxifen resistant (MCF-7/TAM and T-47D/TAM) and AKT overexpressing (MCF7/AKT and T-47D/AKT) breast cancer cells *in vitro* as well as in a xenograft model of MCF-7/TAM (Rajput et al., 2015b). Treatment with siRNA-Nio-Au-TQ was more efficient in inhibiting the viability of all cancer cell lines as compared to treatment with TQ or with Nio-Au-TQ. Similar observations were obtained *in vivo*. The mechanism of action of the niosomes involved triggering apoptosis by inhibiting MDM-2 and induction of p53-mediated apoptosis.

#### iv. Other

The antioxidant activity and biocompatibility of gold NP containing *N. sativa* oil, *Calendula officinalis* extract, and lipoic acid were investigated in a cell-free system and in Vero cells (Guler et al., 2014). As expected, the NP exhibited more antioxidant activity than the free extracts and were biocompatible, as they did not affect Vero cells proliferation and viability. On the other hand, the NP stimulated wound healing of Vero cells.

## b. Drug Release, Uptake and Distribution

Two groups encapsulated TQ in SLN and investigated the *in vitro* and *in vivo* release profiles of TQ (Pathan et al., 2011; Singh et al., 2013). Pathan *et al.*, report a biphasic sustained release of TQ *in vitro* which comprises of an initial rapid release phase followed by a slower release. Upon quantification of TQ in the plasma of orally administered rats, they also show a two fold increase in bioavailability of TQ-SLN as compared to the parental drug (Pathan et al., 2011). Singh et al, also report a TQ-SLN formulation with *in vitro* controlled drug release properties versus a time-dependent release by TQ suspension. They also demonstrate more drug release (70% at 24 h) by the carriers that could be possibly facilitated by having more surface area than the suspension (45%). Similarly, a five-fold increase was noted in the plasma of orally administered rats. Furthermore, the amount of TQ in liver, spleen, kidneys, heart, brain and lungs was much higher upon SLN administration. The formulation also protected the liver against cirrhosis by lowering serum levels of liver damaging enzymes (AST ALT and ALP).

When formulated in CS-NP, TQ release was also sustained after an initial burst phase (Alam et al., 2012). *In vivo*, the NP distribution was assessed in different organs after intranasal or intravenous administration showing the system's capacity for high targeting of the brain after intranasal administration.

In rabbits, TQ NLC were shown to improve the pharmacokinetics of TQ with regards to the volume of distribution, clearance, maximum concentration reached in the blood, and elimination time, among others (Abdel-Wahab, 2014).

The uptake of TQ-NP remains poorly understood with only three studies addressing this question. So far, reports indicate that gold NP containing *N. sativa* oil

and *C. officinalis* extract labeled with FITC accumulate around the nucleus of Vero cells (Guler et al., 2014). It has also been shown that siRNA-Au-Nio-TQ exhibit a time-dependent uptake with maximum uptake observed at 120-180 min, which coincides with the time at which the Nio escape the lysosomal compartment (Rajput et al., 2015b). Finally, the uptake of PEG-ylated TQ-NP was shown to be mediated by clathrin-dependent endocytosis (Bhattacharya et al., 2015).

## **E. Hypothesis and Specific Aims**

Tumor resistance, toxic side effects and low tumor targeting are three main factors which limit the translation of new anticancer agents to the clinic. Previous work at our laboratory suggests that TQ is a potent anticancer molecule (Dergarabetian et al., 2013; El-Baba et al., 2014; El-Najjar et al., 2010; Gali-Muhtasib et al., 2004a; Gali-Muhtasib et al., 2008a; Gali-Muhtasib et al., 2008b; Gali-Muhtasib et al., 2006; Roepke et al., 2007). Literature supports our findings and further provides evidence for the potential of TQ in combination, of TQ-NP and of TQ derivatives in different cancer models (Schneider-Stock et al., 2014). For instance, TQ-Dox combination treatment was found to enhance TQ's activity and reduce Dox toxicity to normal tissues *in vitro* and *in vivo* (al-Shabanah et al., 1998; Badary et al., 2000; Brown et al., 2014; Effenberger-Neidnicht and Schobert, 2011; Elsherbiny and El-Sherbiny, 2014; Nagi and Mansour, 2000). This combination treatment efficiency however, has not been tested against aggressive ATL. The same, improvement of drug activity was observed when structural modifications were used to produce different TQ derivatives although the mechanism of action as well as the molecular targets of the derivatives remain poorly

understood (Banerjee et al., 2010a; Breyer et al., 2009; Effenberger et al., 2010; Wirries et al., 2010; Yusufi et al., 2013). Several TQ-NP also enhanced the free drug's anticancer activity as well as its bioavailability and biodistribution. However, a number of TQ-NP formulations suffered from large diameter sizes which do not conform to the size recommendations of the National Cancer Institute (NCI) (Abu-Dahab et al. 2013; Alam et al. 2012; Ravindran et al. 2010; Shah et al. 2011). Low entrapment efficiency (%EE) and loading capacity (%LC) were also some drawbacks of those preparations (Alam et al. 2012; Ganea et al. 2010; Shah et al. 2010). In addition, some TQ-NP did not enhance the activity of free TQ (Bhattacharya et al. 2015; Odeh et al. 2012). Moreover, no thorough studies have addressed the mechanism of uptake of TQ-NP and the fate of the particles after cellular intake. Finally, to our knowledge, TQ-NP assisted combination therapies or TQ derivatives formulations and combination have not been tested yet.

We therefore hypothesize that nanoparticle-mediated combination of two active molecules with distinct modes of action can overcome multiple mechanisms of drug resistance, increase tumor targeting as well as lower drug toxicity to normal tissues. To test this hypothesis, we first aim to develop and investigate the anticancer potential of the three commonly used methods for the enhancement of drug activity: combination, nanoparticles formulation as well as drug derivatives synthesis. Ultimately, we will combine the different approaches and determine the advantages, limitations as well as the anticancer mechanisms of action of the multiple systems used simultaneously.

The project consists of three main aims:

1) Investigating the anticancer potential of TQ in combination. To this aim, we will combine TQ with the clinically approved drug Dox, and assess the regimen's anticancer effects in an ATL model. We will attempt to a) Test if the combination treatment enables the use of non-toxic doses of Dox b) Assess the potential of TQ-Dox combination for enhancing cell death and preventing resistance of the tumors as compared to treatment with single drugs c) Understand the cellular mechanisms and molecular pathways that are involved in cell death by combination treatment.

2) Investigating the anticancer potential of TQ-NP. To this aim, we will prepare TQ-NP by FNP and test the formulation against a breast cancer model to a) Characterize the TQ-NP prepared using FNP b) Determine if TQ encapsulation enhances the anticancer activity of the free drug c) Study the dynamics and mechanism of uptake of TQ-NP by the cells to understand the link between the intracellular fate and activity of the NP. Taking into account the critical role that the environment of solid metastatic tumors plays with regards to the EPR effect, we chose to assess the anticancer potential of TQ-NP in a breast cancer model comprising of both non-aggressive and aggressive metastatic cells.

3) Investigating the anticancer potential of TQ derivatives. Each TQ pyrimidine hydrazide derivative will have a carbocyclic nucleoside and an acylhydrazone functional group added to TQ's original structure. The derivatives will be tested against breast cancer model to a) Determine if the modifications to the structure of TQ can enhance the molecule's anticancer potential b) Screen for the mechanisms and pathways involved in the response to TQ and TQ derivatives c) Compare the potential molecular targets between TQ and TQ derivatives in an attempt

to understand the advantages and inconveniences linked to the structural modification introduced to the TQ structure.

The following three chapters dedicated to each of the aims, will be presented as separate studies prepared in the form of articles. We will discuss the findings of all studies in the last chapter. The outcomes of these projects combined will contribute to the understanding of TQ from combinatorial, nanotechnology and conjugation perspectives. This step is critical for proceeding with the testing of TQ-NP-based combination chemotherapies. We aspire to be the first to merge two or more approaches for the enhancement of TQ activity and thus potentially overcome this molecule's limitations.

## CHAPTER II

# COMBINATORIAL EFFECTS OF THYMOQUINONE ON THE ANTICANCER ACTIVITY OF DOXORUBICIN IN ADULT T-CELL LEUKEMIA

### **A. Abstract**

Doxorubicin (Dox) is a clinically approved drug which suffers from drug resistance and cardiotoxicity. Recent studies have shown that thymoquinone (TQ) in combination with Dox can reduce Dox toxic side effects *in vitro* as well as *in vivo*. Both TQ and Dox have shown promising anticancer effects against aggressive adult T-cell leukemia (ATL), however the anticancer potential of TQ and Dox combination treatment has never been tested against ATL.

In this project, we hypothesized that co-treatment with TQ could enable the use of lower doses of Dox to achieve similar or enhanced anticancer activity as high doses of Dox alone. To test this hypothesis, the effects of TQ and Dox combination on cell death and cell cycle were evaluated by trypan blue and propidium iodide. TUNEL assay was used to investigate the mode of cell death. The levels of reactive species (ROS) were determined using DCFH assay, whereas the mitochondrial membrane potential was measured by rhodamine assay. Finally, the effects of the combination on the regulation of key proteins involved in cell cycle regulation and cell death were determined by Western blot.

The results reveal that the human T-lymphotropic virus (HTLV-1) positive HuT-102 cells are more resistant to treatment with Dox alone, than the HTLV-1 negative Jurkat cells. However, treatment with high doses of TQ and low doses of Dox simultaneously, enhances cell death in both cancer cell lines as compared to treatment with Dox alone. TUNEL assay on Jurkat and HuT-102 cells further indicates that the combination treatment causes cell death by apoptosis. Furthermore, an increase in ROS production was noted in response to treatment with TQ and the combination treatment in both Jurkat and HuT-102 cells. The oxidative stress however, was only shown to play a role in the disruption of the mitochondria of Jurkat cells. Similarly, caspase activation was involved in the disruption of the mitochondria of Jurkat cells. Finally, several key regulatory proteins whose expression levels or activation were modulated in response to treatment with the combination were identified in this study.

In conclusion, TQ in combination with Dox efficiently inhibits ATL leukemic cancer cell growth. The combination enables the use of low doses of Dox which can potentially lower the side effects of the drug. Nevertheless, *in vivo* studies are still warranted to assess the adjuvant chemotherapeutic potential of TQ in combination with Dox.

## **B. Introduction**

The human T-cell lymphotropic virus type I (HTLV-1) is the causative agent of adult T-cell leukemia/lymphoma (ATL), a disease with very poor prognosis (Cook et al., 2013). The anthracyclin doxorubicin (Dox), is an antibiotic first isolated from *Streptomyces peucetius*. Dox is commonly used in clinic to treat solid and



hematological tumors including acute leukemia (Octavia et al., 2012). However, reports of early onset of tumor resistance to treatment with Dox as well as severe complications in response to treatment with Dox remain major limitations in Dox chemotherapy (Octavia et al., 2012).

We have previously shown that thymoquinone (TQ) exhibits anti-neoplastic potential against a wide range of tumors including HTLV-1 positive cells (HuT-102 and MT-2) and HTLV-1 negative peripheral T-cell lymphomas (Jurkat and CEM) among others (Dergarabetian et al., 2013). Our findings also reveal that TQ in combination with arsenic and interferon alpha significantly inhibits the viability of ATL HTLV-1 positive and HTLV-1 negative cell lines (Manuscript in preparation). Many studies also indicate that TQ increases the anticancer efficacy of a wide number of clinically approved drugs in different tumor models. For instance, enhanced anticancer potential has been observed for TQ in combination with Dox, tamoxifen, 5-fluorouracil, gemcitabine, topotecan, epigallocatechin, cisplatin among others (Effenberger-Neidnicht and Schobert, 2011; Ganji-Harsini et al., 2016; Harpole et al., 2015; Kensara et al., 2016; Khalife et al., 2014; Mu et al., 2015; Wilson et al., 2015). Similarly, TQ has been successful in overcoming tumor chemoresistance to clinically approved drugs such as bortezomib, topotecan and Dox (Arafa el et al., 2011; Effenberger-Neidnicht and Schobert, 2011; Siveen et al., 2014). Specifically, TQ inhibited the viability of MCF-7/Dox resistant human breast cancer cell line by upregulation of PTEN (Arafa el et al., 2011). TQ also improved the anti-cancer potential of Dox in HL-60 myeloblastic leukemia and multi-drug-resistant MCF-7/TOPO breast cancer cells by ROS production and mitochondria associated apoptosis (Effenberger-Neidnicht and Schobert, 2011). In addition, at least three animal studies have presented evidence for a protective role of

TQ against Dox-induced cytotoxicity including protective effects against nephrotoxicity and cardiotoxicity (al-Shabanah et al., 1998; Badary et al., 2000; Nagi and Mansour, 2000). Furthermore, studies have reported non-toxic effects of TQ against a wide range of normal tissues among which PBMCs and cardiomyocytes (Brown et al., 2014; Schneider-Stock et al., 2014).

Combination therapy has emerged as a substitute to conventional treatments especially against tumors that are resistant to traditional chemotherapeutics or for reduction of drugs unpleasant side effects. In light of the promising potential of TQ in combination studies, we sought to combine the toxic chemotherapeutic drug Dox with TQ and investigate their anticancer potential in an ATL model. To this end, the cytotoxicity and anticancer potential of TQ and Dox were assessed in HTLV-1 positive HuT-102 and HTLV-1 negative Jurkat cells. We also investigated the mechanism of cell death and the combination treatment effect on ROS generation, the mitochondrial membrane potential as well as the expression levels of target proteins involved in cell cycle modulation and cell death.

## **C. Materials and Methods**

### ***1. Materials***

RPMI 1640 with 25mm HEPES and L-glutamine, fetal bovine serum (FBS), trypsin, penicillin-streptomycin (P/S), N-acetyl cysteine (NAC), Dulbecco's phosphate buffered saline (PBS), bovine serum albumin (BSA), and trypan blue were purchased from Sigma (St. Louis, Missouri, US). Propidium iodide (PI), and 1, 2-dimethylsulfoxide (DMSO) were obtained from Molecular Probes (Eugene, Oregon,

US). RNase A and protease inhibitor were ordered from Roche (Mannheim, Germany). Rhodamine 123 and CM-H2DFCDA were purchased from Invitrogen. PVDF membranes were obtained from Amersham Pharmacia Biotech (Amersham, England). Primary antibodies p53, p65 and the mouse and rabbit secondary antibodies were purchased from Santa-Cruz (Santa-Cruz, California, US). Bcl-2 primary antibody was obtained from Biosource (Camarillo, California, US). The GAPDH antibody was ordered from Biogenesis (Poole, UK). Primary antibodies for PARP and phospho p53 were purchased from Cell Signaling technology (Massachusetts, US). DC BioRad protein assay kit was ordered from BioRad (BioRad Laboratories, Hercules, CA).

## ***2. Cell Culture***

Jurkat and HuT-102 cells were cultured in RPMI 1640 medium containing 10% heat inactivated FBS and 1% P/S antibiotics. All cells were grown in a humidified incubator (95% air, 5% CO<sub>2</sub>) at 37 °C.

## ***3. Drug Preparation and Cell Treatment***

TQ and Dox, were dissolved in methanol and DMSO, respectively. TQ concentrations of 10 and 40 µM and Dox concentrations of 50 and 100 nM were prepared by serial dilution in the cell culture media. The final organic solvent concentration exposed to cells was less than 0.1 %. Unless otherwise specified, all cells were seeded at a density of 2 x 10<sup>5</sup> cells/ ml and 24 h later, at 50 % confluency, cells were treated with the desired conditions for 24 h or 48 h. For most studies, Jurkat cells

were treated with 10  $\mu$ M TQ, 50 nM Dox or their combination for 24 h while 40  $\mu$ M TQ, 100 nM and their combination were used for the treatment of HuT-102 cells for 48 h, respectively.

#### ***4. Viability Assay***

Trypan blue dye exclusion assay was used to evaluate the efficacy of separate or combined TQ and Dox treatments in inhibiting cell viability as compared with the control untreated cells. Cells were seeded in 12-well plates at a density of  $10^5$  cells/ml. At 50% confluency, cells were treated in triplicate with the different TQ and Dox concentrations as well as their combinations. At 24 h and 48 h post-treatment, cells were mixed with equal volumes of dye and mounted on a hemocytometer for counting under the microscope. Each sample was counted in triplicate.

#### ***5. Cell Cycle Analysis***

Jurkat and HuT-102 cells were seeded in 6-well plates at a density of  $2 \times 10^5$ /ml, and incubated overnight. After treatment (24 h for Jurkat, 48 h for HuT-102 cells), the cells were collected and washed twice with PBS, fixed in 70% ice-cold ethanol, and stored at  $-20$  °C overnight. Subsequently, cells were washed twice with PBS, incubated for 30 mins at  $37$  °C with 300  $\mu$ l PBS, 125  $\mu$ l RNase, and 25  $\mu$ l PI (1 mg/ml). Supernatants were then transferred to flow tubes and the samples were excited at 535 nm and the fluorescence recorded at 635 nm. For all flow analysis studies, a FACS scan flow cytometer from Becton Dickinson was used to record 10,000 ungated

events. Analysis of the events was performed using the Cell Quest software (Becton-Dickinson).

## **6. TUNEL Assay**

For TUNEL assay,  $2 \times 10^5$  cells were seeded in 6-well plates and incubated overnight before treatment. Fragmented DNA was quantified by the terminal deoxytransferase-mediated dUTP nick-end labeling assay (TUNEL). HuT-102 cells were collected 48 h post-treatment, washed twice with PBS, resuspended in 4% formaldehyde and incubated at room temperature for 30 min. Cells were then pelleted, washed with PBS, resuspended in 100  $\mu$ l solution containing PBS, 0.1% sodium citrate, and 0.1% Triton X-100 and incubated for 2 min on ice. After a second wash step, the cells were incubated for 1 h in 50  $\mu$ l TUNEL reaction mixture consisting of 45  $\mu$ l of the labeling solution and 5  $\mu$ l of the enzyme solution. After the incubation in the dark in a humidified atmosphere at 37 °C, the mixture was washed and the cells were suspended in 450  $\mu$ l PBS for flow cytometry analysis. The cells were excited using the 494 nm wavelength and the results recorded at the 521 nm wavelength.

## **7. ROS Analysis**

Generation of intracellular H<sub>2</sub>O<sub>2</sub> was measured using 5-(and-6)-chloromethyl-2',7'-dichlorodihydrofluorescein diacetate acetyl ester (CM-H2DCFDA) kit. At 50% confluency, cells were collected and washed with PBS then resuspended in 500  $\mu$ l RPMI medium containing 2% FBS and 10  $\mu$ M CM-H2DCFDA. The incubation was

performed at 37 °C, in the dark for 20 min. Subsequently, Jurkat and HuT-102 cells were treated for 1 h with TQ, Dox, the combination (with or without pre-treatment with 5 mM NAC for 2 h) or with H<sub>2</sub>O<sub>2</sub> (150 µM). The medium was then removed and the cells were washed twice and resuspended in 500 µl of PBS prior to analysis with a FACS scan flow cytometer. The cells were excited using the 494 nm wavelength and the results recorded at the 521 nm wavelength.

### ***8. Rhodamine Staining***

The mitochondrial membrane potential was measured using rhodamine 123; a green fluorescent dye which accumulates in active mitochondria with high membrane potential. Jurkat and HuT-102 cells were treated with TQ, Dox, the combination with or without pre-treatment with 5 mM NAC (2 h) or with 10 µM of the general caspase inhibitor pan caspase. After treatment (24 h for Jurkat, 48 h for HuT-102 cells), the cells were collected and the pellets were washed twice in rhodamine buffer. The cells were then stained for at 37 °C in the dark for 30 min using a rhodamine 123 dye solution (5 µM). Finally, the cells were washed and resuspended in the rhodamine buffer before analysis by flow cytometry. The cells were excited and 488 nm and the emission recorded at 525 nm.

### ***9. Protein Extraction and Western blotting***

For Western blot analysis, cells were seeded in T75 flasks, treated with the corresponding concentrations and collected at different time intervals after treatment.

The cell pellets were then lysed to extract the proteins. Protein concentration in the cell lysate was determined using the DC BioRad protein assay kit according to the manufacturer's instructions. BSA was used as a standard for protein quantification. The proteins were then resolved by SDS-PAGE on a 12 % denaturing polyacrylamide gel and transferred onto a PVDF membrane at 120 V for 2 h. The membrane was immunoblotted with the appropriate primary and secondary antibodies, reacted with enhanced chemiluminescence reagent and exposed to X-ray films for different time periods.

#### ***10. Statistical Analysis***

To determine the statistical significance between two samples, Two-sample t-test was used (Microsoft Office Excel). To determine the statistical significance between multiple samples, one way analysis of variance (ANOVA) test was used. Statistical significance was claimed when the p-value was  $< 0.05$ .

### **D. Results**

#### ***1. TQ and Dox Combination Treatment Efficiently Inhibits Jurkat and HuT-102 Cell Viability***

First, the effect of Dox on the viability of HTLV-1 negative Jurkat cells and HTLV-1 positive HuT-102 cells was assessed. Both cell lines were treated with Dox at concentrations ranging between 50-750 nM for 24 h and 48 h, respectively. The results in Figure 6 show a dose-dependent response of Jurkat and HuT-102 cells to treatment

with increased concentrations of the drug. The Jurkat HTLV-1 negative cell line was more sensitive than HTLV-1 positive HuT-102 cells with IC<sub>50</sub> of 250 nM and 50 nM at 24 h and 48 h respectively, as compared with 500 nM and 100 nM for the HuT-102 cell line at the same time points (Figure 6).

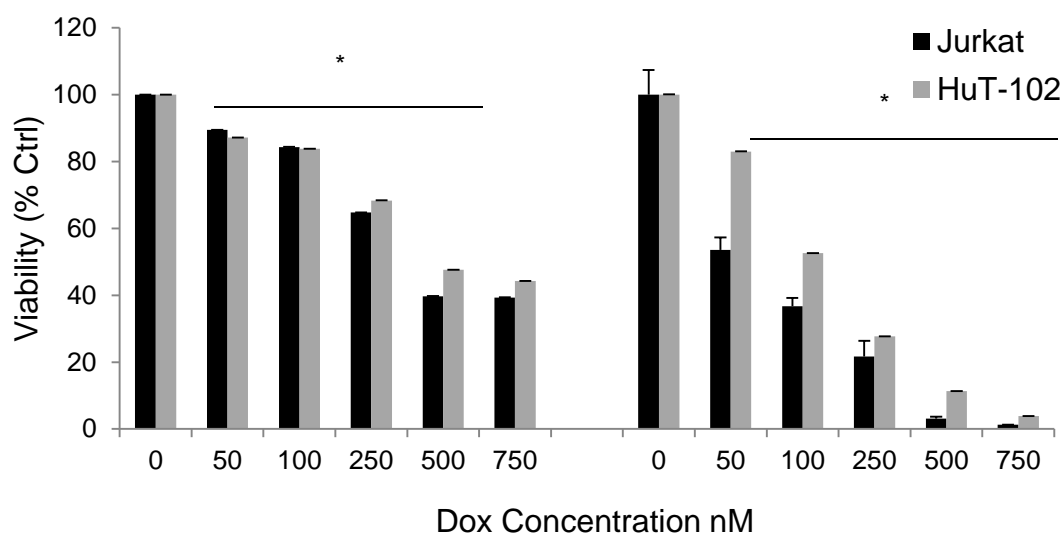


**Figure 6. Dox Inhibits the Viability of Jurkat and HuT-102 Cells in a Dose-Dependent Manner.** HTLV-1 negative Jurkat cells and HTLV-1 positive HuT-102 cells were treated with Dox (50-750 nM). At 24 and 48 h post-treatment, cell viability of Jurkat and HuT-102 cells was assessed by MTT assay and the values expressed as % control. Each value represents the mean  $\pm$  SD of two independent experiments (n =3). \* indicates p <0.05.

Next, different combination mixtures of Dox and TQ were tested for their growth inhibition effect against Jurkat and HuT-102 cells. Briefly, Dox at doses of 50 and 100 nM was combined with TQ at concentrations of 5 and 10  $\mu$ M for treatment of Jurkat cells and with TQ at concentrations of 10 and 40  $\mu$ M for treatment of the resistant HuT-102 cells. Cell viability was assessed at 24 h and 48 h post-treatment with the combination mixtures or the single treatments, and compared to the non-treated



control. As seen in Figure 7, all TQ and Dox combination treatment efficiently inhibited cell viability of Jurkat and HuT-102 cells as compared to the control.

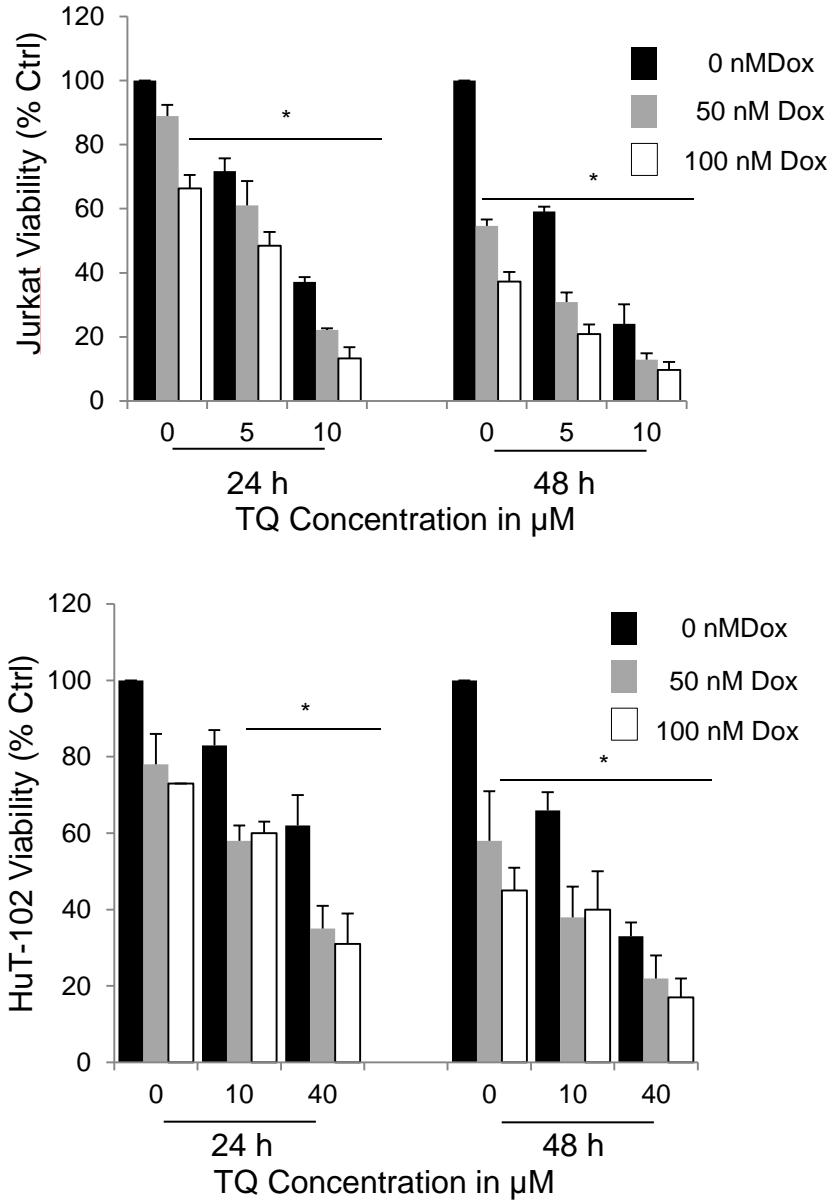


**Figure 7. TQ and Dox Combination Treatment Inhibits Cell Viability of Jurkat and HuT-102 Cells.** Jurkat cells (upper panel), were treated for 24 and 48 h respectively, with 5 and 10 μM TQ, 50 and 100 nM Dox or the combination of TQ and Dox. HuT-102 cells were treated at the same time points with 10 and 40 μM TQ, 100 and 250 nM Dox or the corresponding combinations. At the indicated time points, Jurkat and HuT-102 cell viability was assessed in triplicate by trypan blue excision

assay and the values expressed as % control. Each value represents the mean  $\pm$  SD of two independent experiments (n =3). \* indicates p <0.05.

We further investigated two combination mixtures which significantly inhibited cell viability while circumventing the need to use high doses of Dox to achieve the same effect. Specifically, the combination of 10  $\mu$ M TQ with 50 nM Dox was tested against Jurkat cells, and the combination of 40  $\mu$ M TQ and 100 nM Dox was tested against HuT-102 cells. Both combinations caused around 80% cell viability inhibition at 24 h and 48 h post-treatment in Jurkat and HuT-102 cells, respectively (Figure 8). In comparison, treatment of Jurkat cells for 24 h with TQ (10  $\mu$ M), or Dox (50 nM) causes around 60% and 8% inhibition, respectively (Figure 8). Similarly, treatment of HuT-102 cells for 48 h with TQ (40  $\mu$ M) or Dox (100 nM) only causes 60% and 40% growth inhibition, respectively (Figure 8).

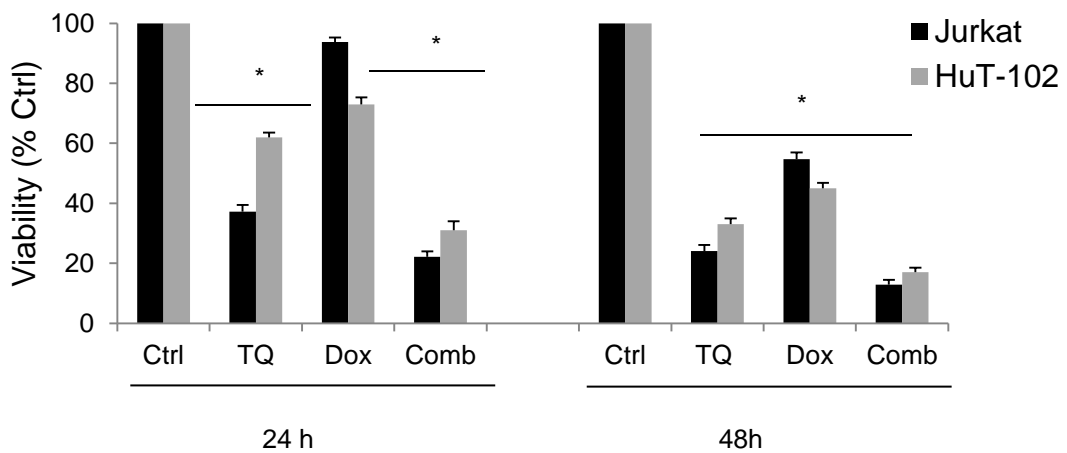


**Figure 8. Low Doses of Dox in Combination with TQ Inhibit Jurkat and HuT-102 Cell Viability.** Jurkat cells were treated with 10  $\mu$ M TQ, 50 nM Dox or their combination for 24 h. HuT-102 cells were treated with 40  $\mu$ M TQ, 100 nM Dox or the corresponding combination for 48 h. At the indicated time points, Jurkat and HuT-102 cell viability was assessed in triplicate by Trypan blue excision assay and the values

expressed as % control. Each value represents the mean  $\pm$  SD of two independent experiments (n =3). \* indicates p <0.05.

To understand the mechanism of action of the single drugs and their combination on Jurkat and HuT-102 cells, cell cycle analysis was performed (Figure 9). At 24 h post-treatment of Jurkat cells with 10  $\mu$ M TQ, there was a 25% increase in the Pre-G1 cell population. In comparison, treatment of Jurkat cells with Dox (50 nM) caused a 48% increase in the G2/M cell population. Similarly, 48 h post-treatment of HuT-102 cells with 40  $\mu$ M TQ, a 35% increase in the Pre-G1 cell population was observed. Treatment of the HuT-102 cells with 100 nM Dox caused 55% cell cycle arrest at the G2/M phase. The combination treatment of HuT-102 cells with both TQ (40  $\mu$ M) and Dox (100 nM) for 48 h caused 49% to accumulate at the Pre-G1 phase (Figure 9).

## ***2. Combination Treatment Triggers Cell Cycle Arrest and Apoptosis***

To determine if cell death triggered by the combination of TQ and Dox in HTLV-1 negative and positive cells, is due to apoptosis we performed a TUNEL assay. As shown in Figure 10, treatment of Jurkat cells for 24 h with 10  $\mu$ M TQ, or the combination of TQ (10  $\mu$ M) and Dox (50 nM) leads to 50% and 69% TUNEL positive cells, respectively. Treatment of Jurkat cells for 24 h with Dox alone (50 nM) however, does not significantly increase the % TUNEL positive cells as compared with the untreated control. Similarly, treatment of HuT-102 cells for 48 h with 40  $\mu$ M TQ, 100

nM Dox or their combination leads to 13%, 4% and 20% TUNEL positive cells, respectively (Figure 10).

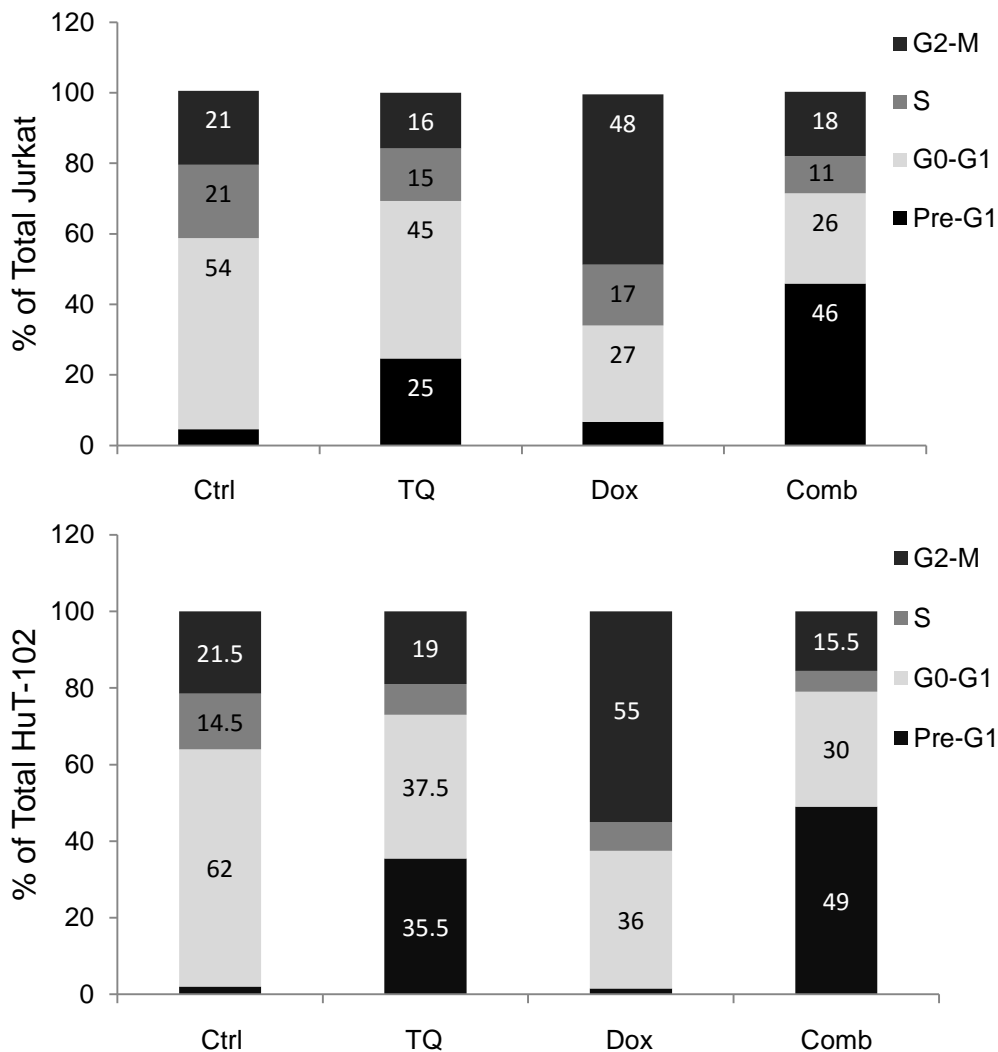


**Figure 9. The Combination Treatment Induces Cell Death.** Jurkat cells were treated with 10  $\mu$ M TQ, 50 nM Dox or their combination for 24 h. HuT-102 cells were treated with 40  $\mu$ M TQ, 100 nM Dox or the corresponding combination for 48 h. After treatment, the cells were harvested and the DNA was stained with PI for cell cycle analysis. % of Jurkat and HuT-102 cells in the Pre-G1, S, G0-G1 and G2-M phases of the cell cycle are illustrated. Values shown are representative of at least two experiments n = 1.

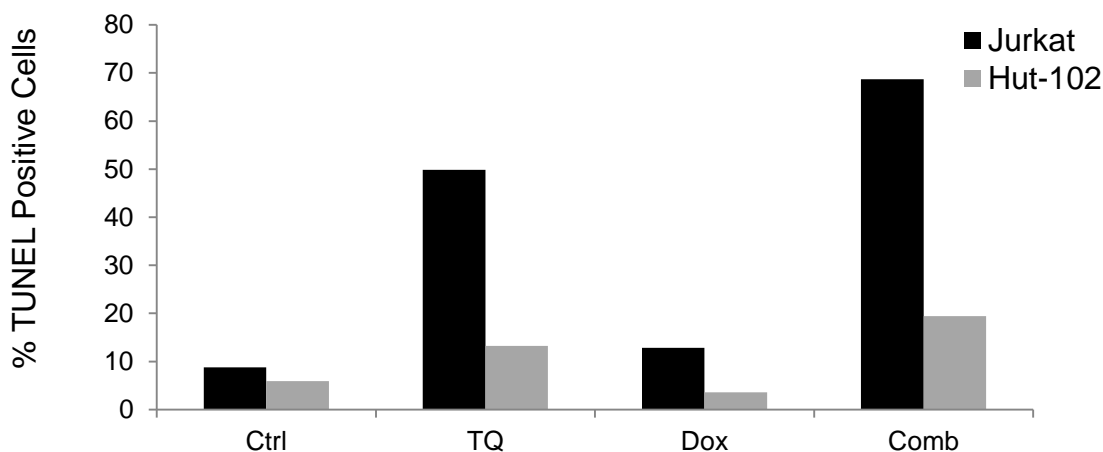


**Figure 10. The Combination Treatment Induces Cell Death by Apoptosis.** Jurkat cells were treated with 10  $\mu$ M TQ, 50 nM Dox or their combination for 24 h. HuT-102 cells were treated with 40  $\mu$ M TQ, 100 nM Dox or their combination for 48 h. After treatment, the cells were stained and apoptosis was detected by flow cytometry analysis. TUNEL assay was used to determine % apoptotic cells. The values illustrated are obtained from one experiment n = 1.

### ***3. Oxidative Stress Occurs in Response to Treatment with the Combination***

Having previously shown that TQ treatment induces apoptosis in Jurkat and HuT-102 cells by triggering the production of ROS and permeabilization of the mitochondrial membrane (Dergarabetian et al., 2013), we investigated the implication of ROS and the mitochondria in the response to treatment with the combination (Figures 11 and 12). To quantify ROS production, Jurkat and HuT-102 cells were treated with TQ, Dox or their combination for 1 h before treatment with the CM-H2DCFDA dye and flow analysis. Jurkat cells were treated with 10  $\mu$ M TQ, 50 nM Dox or their combination. HuT-102 cells were treated with 40  $\mu$ M TQ, 100 nM Dox or their combination. Quantification of ROS levels shows that both TQ and the combination treatment trigger ROS production in Jurkat cells while no significant ROS level is noted upon treatment with Dox. Both TQ and the combination treatment trigger around 40% increase in ROS production. In comparison, treatment with the positive control H<sub>2</sub>O<sub>2</sub>,

triggers around 60% oxidative stress. Moreover, pre-treatment of Jurkat cells with the strong antioxidant NAC before treatment with the combination was shown to completely abrogate ROS production (Figure 11). Similarly, ROS production was observed in response to treatment of HuT-102 cells with TQ or the combination which increased the oxidative stress by around 25%, respectively as compared to 40% in response to treatment with H<sub>2</sub>O<sub>2</sub> (Figure 11).

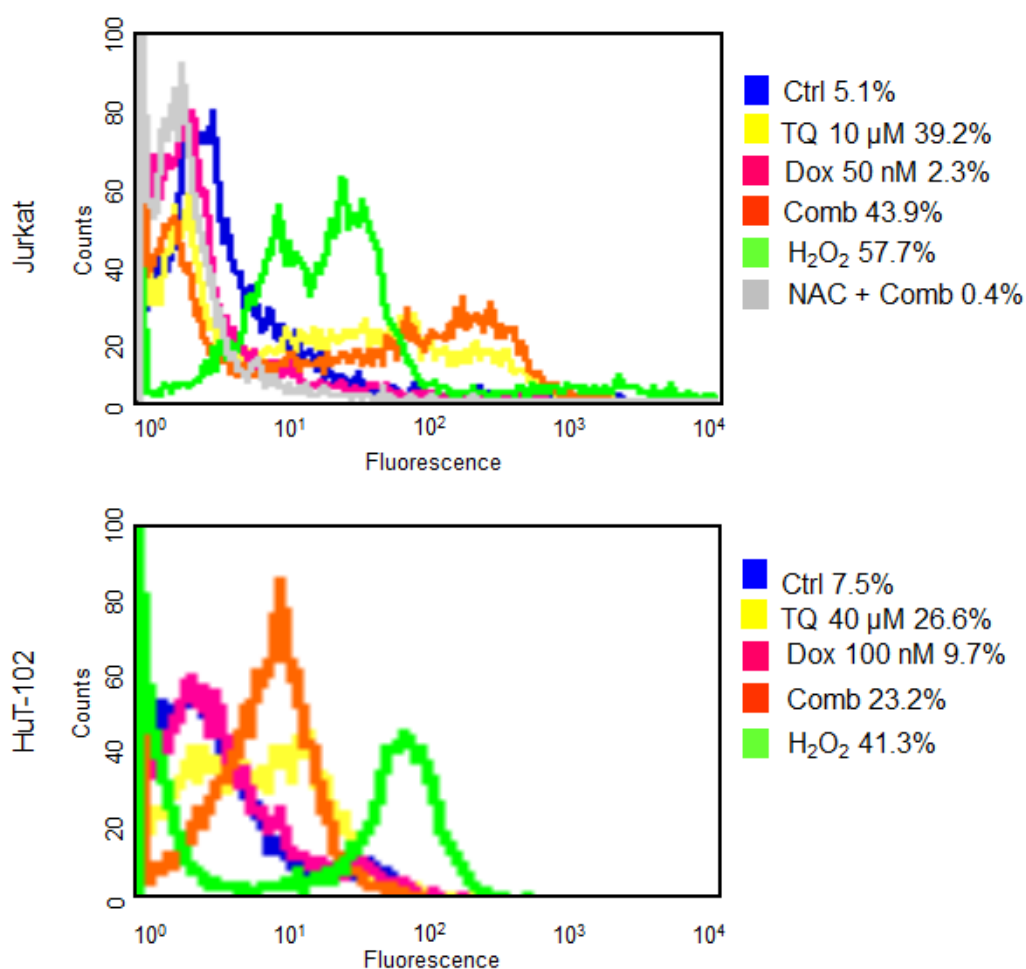


**Figure 11. The Combination Treatment Induces ROS Production.** Jurkat cells were treated with 10  $\mu$ M CM-H2DCFDA dye for 20 mins, and then they were treated for 1 h with 10  $\mu$ M TQ, 50 nM Dox, the combination treatment (with or without pre-treatment with NAC) or with H<sub>2</sub>O<sub>2</sub> (150  $\mu$ M). HuT-102 cells were treated with 10  $\mu$ M CM-H2DCFDA dye for 20 mins, and then with 40  $\mu$ M TQ, 100 nM Dox, their combination

or H<sub>2</sub>O<sub>2</sub> (150 μM) for 1 h. After treatment, the cells were collected and analyzed by flow cytometry. Representative histograms showing ROS production in Jurkat and HuT-102 cells are illustrated. ROS levels values are expressed as % increase as compared to the control. This experiment was repeated twice with n = 1.

#### ***4. The Mitochondria is Disrupted in Response to Treatment with the Combination***

The mitochondria is the main site for production of ROS. Moreover, high ROS levels can be associated with a disruption of the mitochondrial membrane potential. To assess the integrity of the mitochondrial membrane, Jurkat and HuT-102 cells were treated with TQ, Dox or their combination with or without pre-treatment with NAC (5 mM) or the general caspase inhibitor pan caspase (10 μM). After treatment, staining with rhodamine 123 dye was performed and the mitochondrial membrane potential was measured as percentage of accumulated fluorescent dye. Figure 12 indicates 31% and 55% increase in Jurkat cell population with disrupted membrane potential in response to treatment with TQ or the combination, respectively. The results also show that pre-treatment of the Jurkat cells with the antioxidant NAC or the caspase inhibitor prior to treatment with the combination decreases the population of cells with disrupted mitochondrial membrane potential by almost half. In fact only 26% and 22% cells show a decrease in the membrane potential following pre-treatment with NAC and the caspase inhibitor, respectively (Figure 12).

In contrast, treatment of the HuT-102 cells with the different conditions does not appear to have an effect on the mitochondria. In fact the data shows that the untreated control has an initial population of 13% cells with disrupted mitochondrial membrane potential. All treatments however lead to around 20% HuT-102 cells with decreased membrane potential (Figure 12).

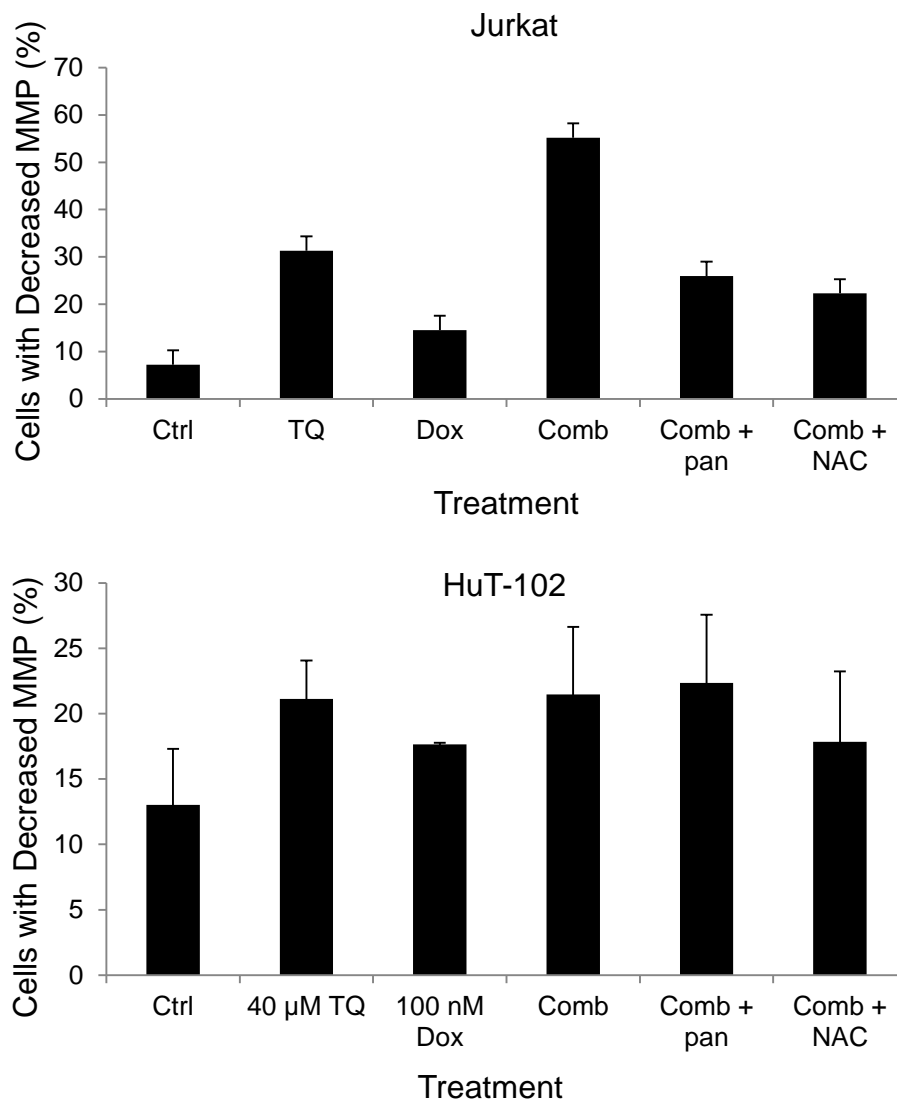


**Figure 12. The combination Treatment Disrupts the Mitochondrial Membrane Potential.** Jurkat cells were treated with 10  $\mu$ M TQ, 50 nM Dox, and their combination with or without pre-treatment with pan caspase (10  $\mu$ M) for 1 h or NAC (5 mM) for 2 h. HuT-102 cells were treated with 40  $\mu$ M TQ, 100 nM Dox or their combination with or without pre-treatment with pan caspase (10  $\mu$ M) for 1 h or NAC (5 mM) for 2 h. After treatment, the loss of mitochondrial membrane potential was determined by quantifying the rhodamine-123 dye retention by flow cytometry. Values shown are representative of two independent experiments n = 1.

### 5. Involvement of Molecular Modulators in Cell Death

To determine the mechanism behind cell death by combination treatment, we examined the expression levels of molecular targets involved in cell proliferation and



apoptosis. To this aim, HuT-102 cells were treated with 40  $\mu$ M TQ, 100 nM Dox or their combination for 48 h. As seen in Figure 13, treatment with TQ or the combination decreases the expression levels of the NF $\kappa$ B activator p65, increases the expression levels of the DNA damage marker H2AX histone protein, and leads to cleavage of PARP. None of the treatments had any effect on the expression levels of p53, Bcl-2 or the viral oncoprotein Tax. The phosphorylation of p53 was significantly decreased in response to treatment with TQ and the combination and on the opposite, Dox alone caused an increase in p-p53 (Figure 13).

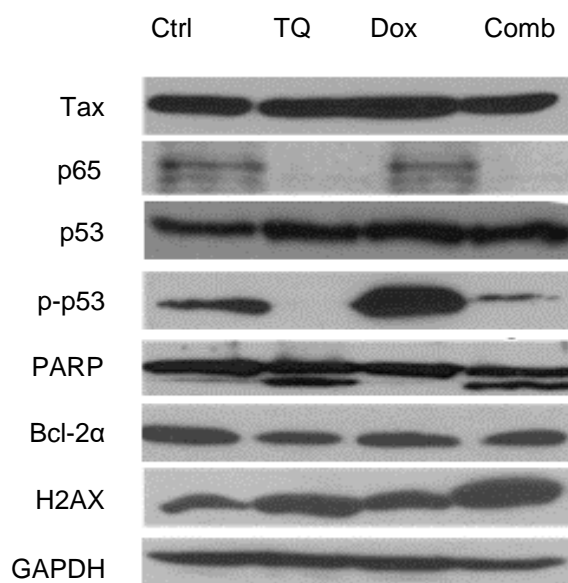


**Figure 13. TQ and the Combination Treatment Modulate Key Molecular Targets.** Jurkat cells were treated with 10  $\mu$ M TQ, 50 nM Dox or their combination for 24 h. HuT-102 cells were treated with 40  $\mu$ M TQ, 100 nM Dox or their combination for 48 h. After treatment, the cells were lysed and proteins were extracted for analysis by Western Blot. The figure shown represents one independent experiment of two.

## **E. Discussion**

To our knowledge, this is the first study assessing the anticancer potential of TQ and Dox combination treatment against an ATL model. Here, we show that TQ in combination with low doses of Dox significantly inhibits the viability of HTLV-1 negative and HTLV-1 positive cells and that the combination also enhances cell death in comparison to treatment with Dox alone. The findings also uncover and compare the mechanism of cell death triggered by the combination and the separate treatments in Jurkat and HuT-102 cells.

HuT-102 cells were more resistant to treatment with Dox than Jurkat cells. The  $IC_{50}$  obtained for both cell lines were similar to those observed in the literature whereby Dox  $IC_{50}$  in Jurkat cells was reported to be around 135 nM at 48 h post-treatment and >500 nM in HuT-102 cells at 24 h post-treatment (Georgakis et al., 2005; Muhleisen et al., 2014).

Higher concentrations and longer incubation times for Dox and TQ combination treatment were also required to efficiently inhibit the viability of HuT-102 cells. These differences between the HTLV-1 negative and HTLV-1 positive cell lines can be attributed to the genomic differences between the cells including the expression of the viral oncoprotein Tax whose role in conferring resistance to apoptosis for HTLV-1 positive cells is well established (Giam and Semmes, 2016). In fact, Tax plays an important role in initiating ATL and it activates many cellular pathways including the NF- $\kappa$ B pathway, as well as upregulates anti-apoptotic proteins, represses p53, and interferes with several cell cycle regulators leading to resistance to therapy (Kfoury et al., 2005; Yoshida, 2001).

The main advantage of the combination treatment is that it allowed to use low doses of Dox to achieve significant cell death. In fact, the combination of TQ with 50 nM Dox had an effect on the viability of Jurkat cells, similar to that of treatment of the cells with the 100 nM toxic Dox dose. The same was observed for the combination of TQ with 100 nM of Dox for the treatment of HuT-102 cells which had an effect similar to treatment of the cells with the 250 nM toxic Dox dose. Reducing Dox concentrations can potentially limit the undesirable toxicity of the drug against normal cells such as the peripheral blood mononuclear cells (PBMCs) and cardiomyocytes among others. We have previously established that treatment with TQ at doses of 40 and 100  $\mu$ M for 48 h only reduces cell viability of PBMCs by around 27% in comparison to 60% and 50% reduction in Jurkat and HuT-102 cell viability, respectively (Dergarabetian et al., 2013). This suggests that the TQ doses chosen for combination treatment of Jurkat cells (10  $\mu$ M for 24 h) and HuT-102 cells (40  $\mu$ M for 48 h) in this study have no or low toxic effects on normal PBMCs. Another group has also shown that the combination of TQ with Dox at concentrations which significantly reduce the viability of leukemic cells, have no or effects against cardiomyocytes (Brown et al., 2014). However, testing of the different combinations used in this project against PBMCs and cardiomyocytes is still warranted for a conclusive understanding of the effects of the treatment on the viability of normal cells.

Unlike treatment with Dox, treatment with TQ or the combination mediated cell death by apoptosis in both cell lines. This is consistent with the fact that Dox was used at low concentrations which are below the  $IC_{50}$  of Dox in Jurkat and HuT-102 cells at the indicated times points. Findings from another study further confirm that treatment

of Jurkat cells with 40 nM Dox for 72 h causes necrosis in these cells with very little percentage of apoptotic cells to be noted (Sugimoto et al., 2002).

Similarly, TQ and the combination treatment but not Dox were able to induce ROS production. Most cancer cells have high ROS levels which promote and maintain their high cell proliferation level. An increase in the ROS levels beyond a threshold however can result in growth arrest, senescence or even cell death by apoptosis. Both TQ and Dox cytotoxic effects are known to be partially mediated by pro-oxidation (Angsutararux et al., 2015; Schneider-Stock et al., 2014). However, in the described combination treatments, Dox used at low concentrations does not trigger ROS production. TQ's ability to interact with glutathione and other thiol-bearing enzymes, and deplete the intracellular thiols could thus account for the oxidative stress induced after treatment with TQ or the combination.

Our results further indicate that ROS produced in response to treatment with the combination disrupt the mitochondrial membrane potential in Jurkat cells. Disruption of the mitochondrial membrane potential usually results from swelling of the mitochondria and permeabilization of its membrane which are the early signs of intrinsic apoptosis or apoptosis through the mitochondrial route. The increase in the mitochondrial membrane potential after using an inhibitor of caspases confirms the association between cell death through caspases activation and the mitochondria, and suggest that the combination could be mediating cell death by apoptosis through the intrinsic pathway.

Western blot analysis further confirmed the implication of the apoptotic pathway in the response to treatment with the combination as well as revealed the implication of new pathways. For instance, cleavage of the caspase substrate PARP

from 116 kDa to 85 kDa is consistent with a caspase-dependent apoptosis and the findings after treatment with the general caspase inhibitor.

Bcl-2, Bax and other members of the Bcl-2 protein family are key players in the intrinsic apoptotic pathway. However, the levels of Bcl-2 were not affected by any of the treatments. Our data however does not offer enough information with regards to the ratio of Bax to Bcl-2 proteins which is responsible for the triggering of mitochondrial apoptosis.

Interestingly, TQ and the combination inhibited the NF- $\kappa$ B pathway by inhibition of the p65 and was shown to implicate the DNA damage response.

In summary, the combination treatment offers the possibility to use up to two folds lower doses of Dox while exhibiting the same cancer inhibition effect as the toxic doses. Although cell death is higher upon treatment with the combination as compared to treatment with the separate drugs, most of the mechanisms implicated in the response to treatment with TQ and Dox combination, namely apoptosis, ROS, disruption of the mitochondrial membrane potential and regulation of the expression of key molecular targets, seem to be similar to those observed with treatment with TQ alone. The effect of treatment with the two fold higher doses of Dox on these mechanisms was not investigated and should be performed to better understand the advantages or inconveniences of using lower doses of Dox in combination with TQ. Moreover, it is critical to assess the anticancer potential of the combination treatment in an ATL leukemia mouse model to test the efficacy of TQ as an adjuvant to conventional chemotherapy.

# CHAPTER III

## UPTAKE, DELIVERY AND ANTICANCER ACTIVITY OF THYMOQUINONE NANOPARTICLES IN BREAST CANCER CELLS

### **A. Abstract**

Thymoquinone (TQ) is a promising anticancer molecule but its development is hindered by its limited bioavailability. Drug encapsulation is commonly used to overcome low drug solubility, limited bioavailability and non-specific targeting. In this project, TQ nanoparticles (TQ-NP) were synthesized and characterized.

The cytotoxicity of the NP was investigated in non-tumorigenic MCF-10-A breast cells, while the uptake, distribution as well as the anticancer potential were investigated in MCF-7 and MDA-MB-231 breast cancer cells. Flash Nanoprecipitation (FNP) and dynamic light scattering (DLS) coupled with scanning electron microscopy (SEM) were used to prepare and characterize TQ-NP prior to measuring their anticancer potential by MTT assay. The uptake and subcellular intake of TQ-NP were evaluated by fluorometry and confocal microscopy.

TQ-NP were stable with a hydrodynamic average diameter size around 100 nm. Entrapment efficiency (%EE) and loading content (%LC) of TQ-NP were high (around 80% and 50%, respectively). *In vitro*, TQ-NP had equal or enhanced anticancer activity effects compared to TQ in MCF-7 and aggressive MDA-MB-231 breast cancer

cells, respectively, with no significant cytotoxicity of the blank NP. In addition, TQ and TQ-NP were relatively non-toxic to MCF-10-A normal breast cells. TQ-NP uptake mechanism was both time and concentration-dependent. Treatment with inhibitors of endocytosis suggested the involvement of caveolin in TQ-NP uptake. This was further confirmed by subcellular localization findings showing the colocalization of TQ-NP with caveolin and transferrin as well as with the early and late markers of endocytosis.

Altogether, the results describe an approach for the enhancement of TQ anticancer activity and uncover the mechanisms behind cell-TQ-NP interaction.

## **B. Introduction**

Thymoquinone (TQ), isolated 50 years ago from *Nigella sativa* black seed oil, has shown promising biological activities including antioxidant, anti-inflammatory and anticancer effects. The potential of translating TQ to the clinic is supported by the fact that it inhibits cancer onset, survival and progression and protects major organs from chemotherapy toxicity (Schneider-Stock et al., 2014). However, TQ's hydrophobic nature, poor solubility and low bioavailability, make its translation to the clinic challenging. Nanoparticle encapsulation of poorly soluble drugs is commonly used for increasing drug dissolution and bioavailability. These drug delivery systems have made significant clinical impact by improving the pharmaceutical efficacy and dosing of a variety of already approved drugs (Lammers et al., 2012). Nanoparticle formulation is a rapidly progressing field in cancer treatment (Brannon-Peppas and Blanchette, 2004; Lopez-Davila et al., 2012; Zamboni et al., 2012) as it can enhance drug accumulation in tumors, prevent rapid drug metabolism and lysosomal degradation, and lower the

exposure of normal tissues to the drug (Gupta et al., 2010; Mohanraj and Chen, 2006; van Vlerken and Amiji, 2006).

The decreased exposure of non-specific sites, or healthy tissues to the drug in NP reduces putative side effects and toxicity (Gupta et al., 2010; Mohanraj and Chen, 2006; van Vlerken and Amiji, 2006). The enhancement of drug accumulation near the tumor sites is mainly due to the deregulated and leaky nature of tumor vasculature, along with the poor lymphatic drainage. This enhanced permeability and retention effect (EPR) results in passive drug targeting to the tumors and this constitutes a major advantage for NP encapsulated drugs over free drugs. The ideal NP should be biocompatible, selective to tumors and rapidly and efficiently taken up and retained within the cancer cells for sufficient amount of time until it releases its cytotoxic drug cargo and exerts its therapeutic function (Kievit and Zhang, 2011; Shapira et al., 2011). Endocytosis is now recognized as the main route for NP entry into cells (Iversen et al., 2011; Oh and Park, 2014).

Several TQ-NP formulations have been described in the literature (Bhattacharya et al., 2015; Nair et al., 2010; Rajput et al., 2015b; Ravindran et al., 2010; Schneider-Stock et al., 2014). The studies mainly investigated the enhanced anti-inflammatory and anticancer activities of TQ-NP as compared to the free drug. The efficacy of NP formulations is determined by their cell processing mechanism. Several factors influence NP efficacy, including the time and concentration dynamics of NP uptake, the routes of entry, and the trafficking and intracellular distribution. Three studies have addressed TQ-NP-cellular interactions and cell trafficking mechanisms. Guler *et al.* imaged the uptake of FITC-labeled NP containing *N. sativa* and *Calendula officinalis* extracts by fluorescence microscopy (Guler et al., 2014). siRNA and TQ



encapsulated multicellular gold niosomes uptake was shown to be time-dependent with maximum uptake observed at 180 min, after the particles escaped the lysosomes (Rajput et al., 2015b). Bhattacharya *et al.* demonstrated that PEGylated TQ-NP uptake increased with concentration and was mediated by clathrin-dependent endocytosis (Bhattacharya et al., 2015).

In view of the gap in knowledge regarding TQ-NP interaction with the cells, this project aimed to design TQ-NP and investigate the uptake mechanism and dynamics as well as the TQ-NP fate after cellular trafficking. To this end, TQ was formulated in poly(styrene-*b*-ethylene oxide) (PS-PEO) NP using Flash nanoprecipitation (FNP) (Saad and Prud'homme, 2016). PS-PEO is a biocompatible non-toxic amphiphilic diblock copolymer (Ahmad et al., 2010; Cambon et al., 2013; Han et al., 2007). The cytotoxicity and anticancer potential was assessed in normal MCF-10-A breast cells, non-aggressive MCF-7 and highly aggressive MDA-MB-231 human breast cancer cell lines. The classical routes of entry of TQ-NP into cells and the intracellular distribution of the particles after uptake were investigated in the presence of specific inhibitors and markers of endocytosis.

## **C. Materials and Methods**

### ***1. Materials***

RPMI 1640, and Dulbecco's Modified Eagle Medium (DMEM) and DMEM-F12 cell culture media were purchased from Lonza (Verviers, Belgium). TQ, trypsin-EDTA, Dulbecco's phosphate buffered saline (PBS), horse serum, fetal bovine serum (FBS), penicillin-streptomycin (P/S), epidermal growth factor, hydrocortisone, insulin,

cholera toxin, DMSO, MTT (3-(4,5-Dimethylthiazol-2-yl)-2,5-diphenyltetrazolium bromide), trypan blue, methanol, acetonitrile (ACN) HPLC-grade, Nile red (NR), chlorpromazine hydrochloride, nystatin, genistein, and amiloride were purchased from Sigma Aldrich (St Louis, Missouri, USA). Hoechst stain was purchased from Molecular Probes, Invitrogen (Eugene, Oregon, USA). Tetrahydrofuran (THF) (99.8%) was obtained from Acros organics (New Jersey, USA). PS-PEO diblock copolymers were purchased from Polymer Source Inc. (Dorval, Montreal, Canada). Caveolin 1 N-20 rabbit polyclonal, transferrin H-65 rabbit polyclonal, EEA-1 E-8 mouse monoclonal IgG, and lamp-1 H4A3 mouse monoclonal IgG antibodies were purchased from Santa Cruz Biotechnology (Paso Robles, California, USA). Alexa Fluor 647 anti-rabbit IgG and Alexa Fluor 647 anti-mouse IgG antibodies were purchased from Abcam (Cambridge, UK).

## ***2. Cell culture***

MCF-10 normal breast cells were grown in DMEM/F-12 cell culture media supplemented with 1% P/S (with penicillin at 10 000 units and streptomycin at 10 mg/ml), 5% horse serum, 20 ng/ml epidermal growth factor, 0.5 mg/ml hydrocortisone, 100 ng/ml cholera toxin and 10 µg/ml insulin. MDA-MB-231 breast cancer cells were grown in RPMI 1640 cell culture media supplemented with 10% heat-inactivated FBS and 1% P/S. MCF-7 breast cancer cells were grown in DMEM cell culture media supplemented with 10% heat-inactivated FBS and 1% P/S. All cells were maintained in a humidified atmosphere of 5% CO<sub>2</sub> at 37°C. TQ was dissolved in methanol and then

diluted in media as needed such that the final methanol concentration did not exceed 0.1%.

### ***3. Preparation of TQ-NP***

TQ-NP were prepared by FNP using a multiple inlet vortex mixer (MIVM) and controlled flow rates (D'Addio et al., 2012). The formulations were composed of TQ and amphiphilic diblock copolymers of PS-PEO dissolved in 100% THF. TQ weight ratio to the polymer was 1:1 at a concentration of 50 mg/ml in the THF stream. The solution was rapidly mixed with water using a four-port MIVM with flow rates set at 12/108 ml/min (solvent/water). The flow rates were controlled using Harvard apparatus PHD2000 syringe pumps. Fluorescent TQ-NP were prepared as above, with addition of NR at a concentration of 0.1 mg/ml.

### ***4. Characterization of TQ-NP***

The hydrodynamic particle size was determined by dynamic light scattering (DLS) at 25°C using 90Plus/BI-MAS (BrookHaven Instruments Corporation (BIC), Holtsville, NY) and analyzed using the BIC particle sizing software in automatic mode. TQ-NP were dispersed in water (1:10) prior to recording the intensity of light scattered at 90° angle to an incident beam. The measured sizes represent the intensity-weighted average value of 3 runs.

To examine the morphology of the TQ-NP, 10 µl were deposited on the surface of clean silicon wafers. The silicon plates were air dried in a dark place at room

temperature for 24 h before viewing in InBeam mode by SEM (from TESCAN, VEGA 3 LMU with OXFORD EDX detector (INCA XMAW20)).

The entrapment efficiency (%EE) and the loading capacity (%LC) of TQ-NP were determined as follows: Amicon Ultra 30K Ultracel centrifugal filters purchased from Merck Millipore (Tullagreen, Carrigtwohill, IRL) were used according to the manufacturer's guidelines to separate free TQ from TQ in NP. The amount of TQ in the formulation (Total drug) and the amount of TQ in the NP were quantified by high performance liquid chromatography (HPLC). Equation (1) was used to determine the %EE:

$$(1) \%EE = (\text{Amount of TQ in NP} / \text{Total drug}) \times 100$$

To measure the %LC, 1 ml of formulation was centrifuged using the Amicon Ultra 30K Ultracel centrifugal filters. The recovered NP were dried by heating prior to weighing. The weight of the NP was integrated in Equation (2) to calculate the %LC:

$$(2) \%LC = (\text{Amount of TQ in NP} / \text{Nanoparticle weight}) \times 100$$

### ***5. Quantification of TQ***

TQ-NP formulations were dissolved in THF (100%) to ensure complete TQ solubilization prior to quantification by HPLC. Chromatographic analysis was conducted on an Agilent Technologies (Walborn, Germany) 1100 series instrument, comprised of a vacuum degasser, an autosampler, a quaternary pump and a diode array detector. Chromatographic separation was performed on a BDS HYPERSIL C<sub>18</sub> column (250 x 4.6 mm I.D) with 5 µm packing material purchased from Thermo Fisher Scientific (Germany). The samples were eluted at 25 °C using an isocratic mobile phase

of water (> 18 MΩ resistivity): ACN (45: 55% v/v) at a flow rate of 1 ml/min. The injection volume was 20 µl and analysis was performed at 254 nm wavelength with a total run time of 12 min. At these conditions, TQ elution time was 7.42 min. Data acquisition, data handling and instrument control were performed using the Chemstation software package (Agilent). The TQ concentration in the formulation was calculated from a TQ calibration curve obtained by plotting the peak area of the analytical standards 1.5, 3, 30, 75, 150, 300 and 500 µg/ml of TQ prepared in HPLC-grade ACN against their respective TQ concentrations. TQ is light and heat sensitive, therefore all samples were protected from light by aluminum foil and prepared on ice in order to avoid TQ degradation. Also, all samples were filtered through 0.2 µm syringe filter prior to HPLC analysis.

## **6. Viability assay**

Viable cells have the ability to reduce the MTT dye, a yellow tetrazole, into a purple insoluble formazan product the absorbance of which is recorded at 595 nm. MTT assay was used to determine the inhibitory effect of TQ, TQ-NP and blank NP on the viability of MCF-7 and MDA-MB-231 breast cancer cells and non-tumorigenic MCF-10-A breast cell line. Cells were seeded in 96 well plates at a density of 10,000 cells well as described previously (Woo et al., 2011). All treatments were performed at 50% confluency. At 24 h after treatment, the medium was removed and the cells were incubated overnight with an MTT solution (1 mg/ml prepared in PBS). The solution containing the MTT dye was removed the next day and replaced by isopropanol to dissolve the formazan crystal prior to measuring the colorimetric absorbance of the

different wells at 595 nm using a microplate reader (Sutton et al., 2012). Cellular viability was expressed as percentage of cell viability of treated cells relative to untreated controls.

### ***7. Cellular uptake***

Uptake of fluorescent TQ-NP was determined qualitatively by confocal microscopy and quantitatively by flow cytometry. For confocal microscopy analysis,  $10^5$  cells/ml were plated on cover slips in 6 well plates, in 2 ml of respective growth medium. After treatment with NR-TQ-NP at the indicated time points and concentrations, the cells were rinsed twice with PBS, and fixed at room temperature for 20 min in 4% formaldehyde solution. Hoechst (0.5  $\mu$ g/ml) was used to stain the nuclei before mounting on glass slide using FluorSave mounting reagent (Calbiochem). Imaging and visualization as well as Z-stack tomographic sections along the Z-axis were obtained using the Zen software of the Zeiss 710 Confocal microscope (Zeiss, Germany) and a 63x oil objective.

For fluorometry,  $10^5$  cells/ml were plated in 6 well plates in 2 ml of respective growth medium. At different time points after treatment with the corresponding amount of NR-TQ-NP, the cells were rinsed twice with PBS, trypsinized, harvested and then resuspended in 700  $\mu$ l PBS. The mean fluorescence intensity of cellular uptake was measured using a Fluorescence activated cell sorting (FACS) flow cytometer (Becton Dickinson BD, FACS Aria Cell Sorter, USA) operated at an excitation of 488 nm and an emission wavelength of 570 nm.

For the competition assay,  $10^5$  cells/ml were seeded in 6 well plates in 2 ml of respective growth medium. After overnight incubation, the cells were treated for 5 min with 50  $\mu\text{g/ml}$  NR-TQ-NP, 50  $\mu\text{g/ml}$  NR-TQ-NP + 50  $\mu\text{g/ml}$  TQ or 50  $\mu\text{g/ml}$  NR-TQ-NP + 50  $\mu\text{g/ml}$  TQ-NP prepared in PBS. After removal of treatment, the cells were rinsed with PBS, trypsinized, harvested and resuspended in 700  $\mu\text{l}$  PBS for fluorometry analysis.

### ***8. Uptake mechanism***

Cells were seeded in 6 well plates at a density of  $10^5$  cells/ml in 2 ml of respective growth medium and allowed to grow. On the day of treatment, the media was removed and the cells were separately incubated with PBS containing either chlorpromazine hydrochloride (10 mg/ml), genistein (50 mg/ml), nystatin (50 mg/ml), or amiloride (20 mg/ml) for 1 h before treatment with the fluorescent TQ-NP for 30 min. Finally, cells were washed twice with PBS, trypsinized, harvested, and resuspended in 700  $\mu\text{l}$  of PBS. Cells that were not treated with the inhibitors were used as control. The cellular uptake efficiency was determined using a FACS flow cytometer operated at an excitation wavelength of 488 nm and an emission wavelength of 570 nm.

### ***9. Subcellular localization***

Cells were plated on cover slips in 6 well plates at a density of  $10^5$  cells/ml. After overnight incubation in 2 ml of respective growth medium, the media was removed and the cells were treated for 30 min with 25  $\mu\text{g/ml}$  NR-loaded TQ-NP

prepared in PBS. After treatment, the cells were washed twice with PBS and fixed at room temperature for 20 min in 4% formaldehyde. The formaldehyde was then removed and the cells were washed three times in PBS before permeabilization in 0.2% Triton solution for 10 min. After two successive 5 min washes in PBS, the cells were blocked in 2% BSA for 2 h. Caveolin, transferrin, lamp-1 and EEA-1 antibodies were subsequently diluted (1:100) in 1% BSA and incubated separately with the cells overnight at 4°C. The next day, the primary antibodies were removed and the cells were washed twice before incubation for 1 h with mouse or rabbit secondary antibodies diluted (1:200) in 0.2% BSA. Finally, the secondary antibody was removed and the cells were washed twice in PBS before staining the nuclei with Hoechst (0.5 µg/ml). Coverslips were mounted on glass slides using FluorSave mounting reagent (Calbiochem). Imaging and visualization were done using a Zeiss 710 Confocal microscope (Zeiss, Germany) with a 63x oil objective.

### ***10. Statistical analysis***

All experiments were performed at least three times. Data are presented as mean  $\pm$  standard error (SE). Viability was analyzed by one-way analysis of variance (ANOVA) for comparison of several means with associated post-hoc Tukey, and Student-Newman-Keuls (SNK) tests (SPSS Version 16.0). Stability and uptake were analyzed by ANOVA with associated post-hoc Dunnett's test to compare to a control. Statistical significance was set at p-value  $\leq$  0.05.



## B. Results

### *1. FNP generates stable TQ-NP with high %EE and %LC*

TQ-NP were formulated using the PS<sub>1600</sub>PEO<sub>1800</sub> amphiphilic diblock polymer. The numbers in subscript denote the block molecular weight (g/mole). The concentration of both TQ and the polymer used for the preparation of the NP was 50 mg/ml (ratio 1:1). SEM images revealed that TQ-NP have a spherical shape and a smooth surface morphology (Figure 14). The hydrodynamic particle size of TQ-NP is presented in Table 2. Measurement of the hydrodynamic diameter by DLS showed that the formulation possessed an average diameter size of 100 nm (Table 2). The physicochemical properties which assess the amount of drug encapsulated in NP per amount of total drug (%EE) and the amount of drug encapsulated per NP weight (%LC) were also investigated. TQ-NP had around 80% drug %EE and around 50% drug %LC, respectively (Table 2).

The stability of TQ-NP formulation was investigated by monitoring the average diameter sizes over time. Up to 4 weeks, no significant change in the hydrodynamic particle size was noted (Figure 15).

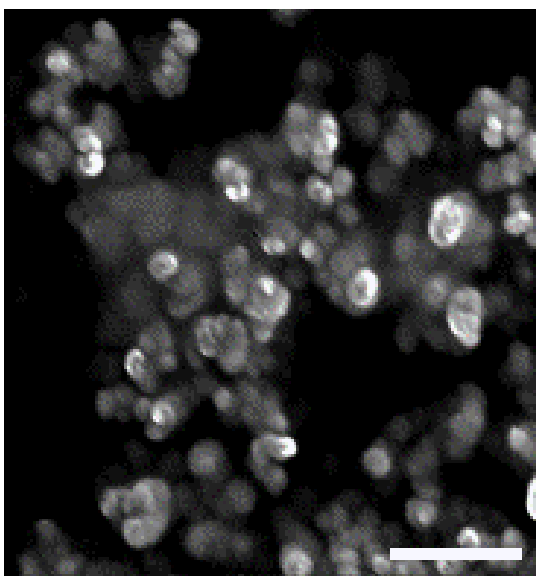


**Figure 14. TQ-NP Have Round Morphologies.** SEM image illustrating the morphology of TQ-NP was taken in InBeam mode after 10  $\mu$ l of NP were deposited on the surface of clean silicon wafers and air dried overnight. Bar = 500 nm.

**Table 2. TQ-NP Have High Entrapment Efficiency (%EE) and Loading Capacity (%LC).** Table showing the average hydrodynamic diameter size, the entrapment efficiency (%EE) and the loading capacity (%LC) of the different TQ-NP formulations. The data represents the mean of two independent experiments  $\pm$  SE (n = 2). The average hydrodynamic sizes were measured by dilution of 100  $\mu$ l of TQ-NP formulation in 2 ml water prior to analysis by DLS. %EE and %LC were calculated using equations 1 and 2, respectively as described in the materials and methods.

NP	Hydrodynamic Diameter (nm)	% EE	%LC
TQ PS <sub>1600</sub> PEO <sub>1800</sub>	94.1 $\pm$ 1.7	79.2 $\pm$ 0.2	50.5 $\pm$ 4.6
TQ PS <sub>1600</sub> PEO <sub>1800</sub> + NR	115.5 $\pm$ 0.1	79.9 $\pm$ 0.1	49.8 $\pm$ 0.3

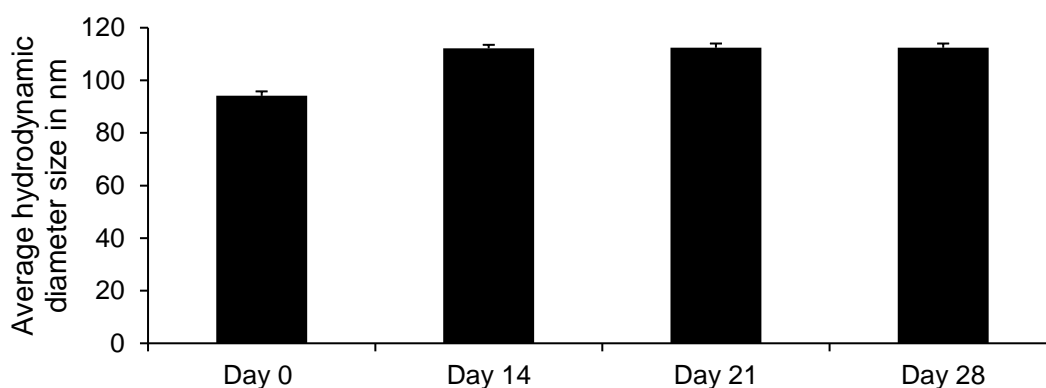


**Figure 15. TQ-NP Are Stable Over Time.** To determine the average hydrodynamic size of TQ-NP, 100  $\mu$ l of the solution was diluted in 2 ml water and the samples were measured by DLS. The size of TQ-NP was monitored over a period of four weeks. The data represents the mean of two independent experiments  $\pm$  SE (n = 2).

## ***2. TQ-NP are equally or more active than TQ in breast cancer cells and non-toxic to non-tumorigenic breast cells***

To investigate the anticancer potential of TQ-NP, cells were treated for 24 h with free TQ, TQ-NP, or blank NP at concentrations ranging between 10-100  $\mu\text{M}$  of TQ. There was a dose-dependent response to treatment with TQ or TQ-NP in both MCF-7 and MDA-MB-231 breast cancer cells (Figure 16). With  $\text{IC}_{50}$  of 30  $\mu\text{M}$  and  $>100 \mu\text{M}$ , respectively; the aggressive MDA-MB-231 breast cancer cell line was more sensitive to treatment with TQ in comparison to MCF-7. This was also the case in response to treatment with TQ-NP. Moreover, in MCF-7, there was clear enhancement of the anticancer activity of TQ-NP over free TQ at 50, 75, and 100  $\mu\text{M}$  starting 24 h with  $\text{IC}_{50}$  of 70  $\mu\text{M}$  (Figure 16 upper panel). In MDA-MB-231, TQ-NP were as active as free TQ (Figure 16 lower panel). Blank NP did not exhibit any toxicity to both cell lines as shown in Figure 16. In addition, when tested against normal MCF-10-A breast cell line, TQ and TQ-NP did not affect the viability of these cells up to 25  $\mu\text{M}$  (Figure 17). At 50  $\mu\text{M}$ , 24 h after treatment, TQ and TQ-NP slightly decreased cell viability with no significant difference between the viability of cells in response to treatment with free or encapsulated drug. As previously observed with the MCF-7 and MDA-MB-231 breast cancer cells, treatment of MCF-10-A normal cells with blank NP did not cause affect cell viability (Figure 17).

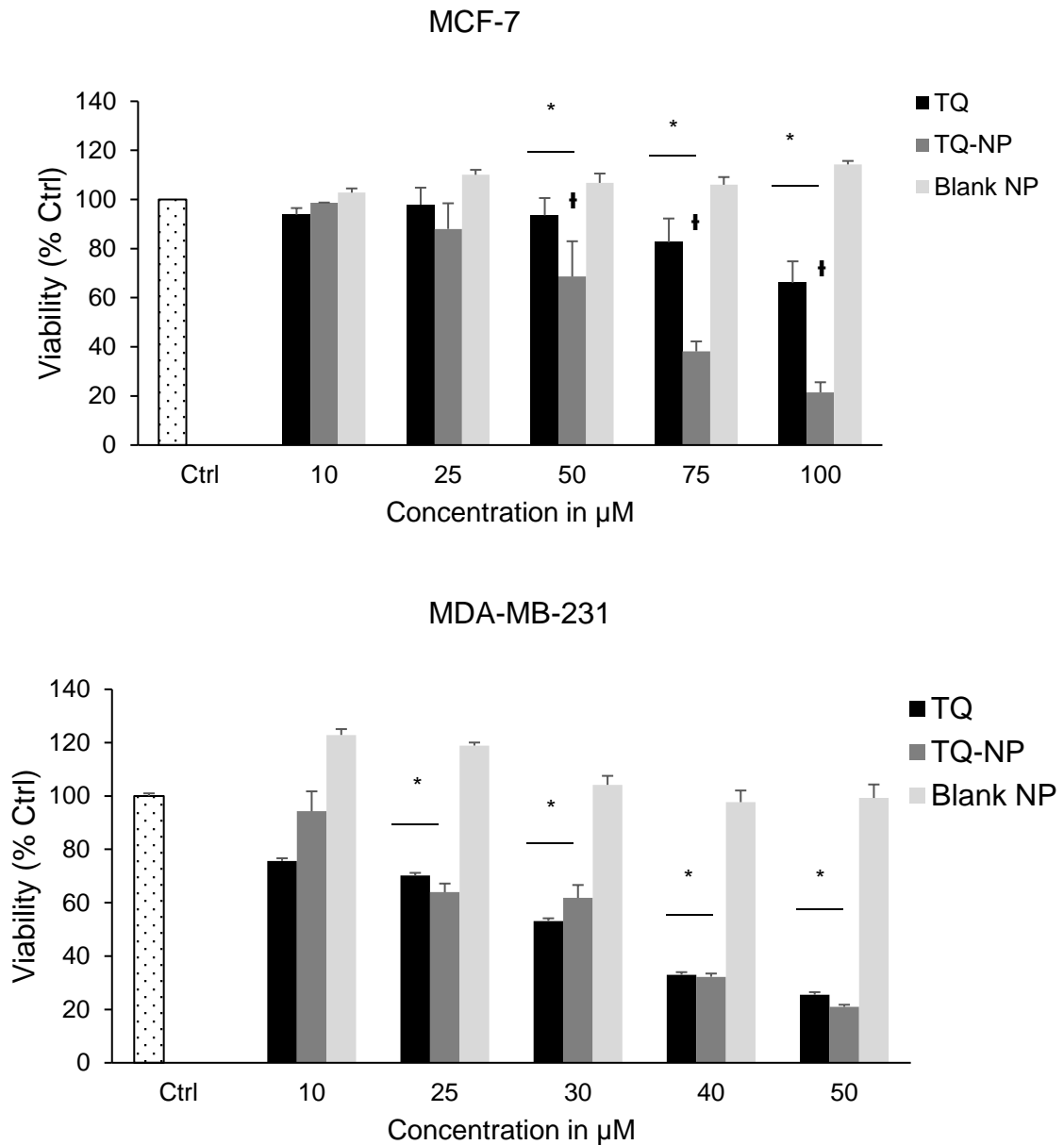


**Figure 16. TQ-NP Are Active *in vitro* against Breast Cancer Cells.** MCF-7 cells were treated with 10-100  $\mu\text{M}$  TQ, TQ-NP or blank NP. MDA-MB-231 cells were treated with 10-50  $\mu\text{M}$  TQ, TQ-NP or blank NP. Both cell lines were treated for 24 h and cell viability was measured by MTT. The values representing the mean  $\pm$  SE of two independent experiments ( $n = 3$ ) were normalized to the control. \* indicates  $p < 0.05$  with respect to the control. † indicates  $p < 0.05$  with respect to TQ.

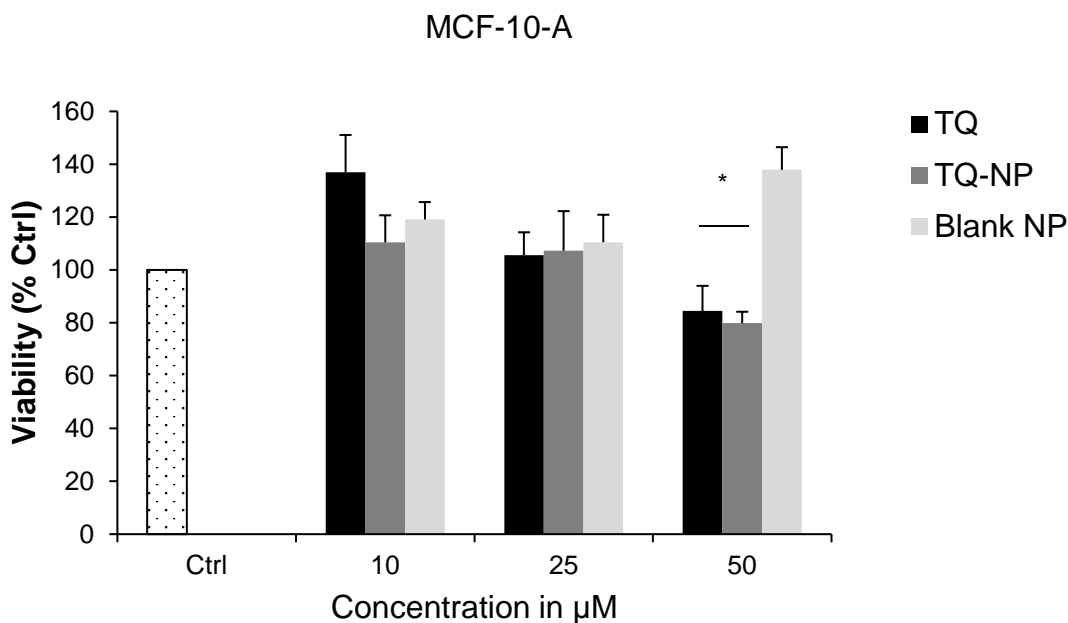


**Figure 17. TQ-NP Are not Toxic to Normal Breast Cells.** MCF-10-A cells were treated with 10-50  $\mu\text{M}$  TQ, TQ-NP or blank NP for 24 h. After treatment, cell viability was measured by MTT. The values representing the mean  $\pm$  SE of two independent experiments ( $n = 3$ ) were normalized to the control. \* indicates  $p < 0.05$  with respect to the control. † indicates  $p < 0.05$  with respect to TQ.

### ***3. NR-loaded TQ-NP are internalized by the cells in a time and concentration-dependent manner***

To study the cellular uptake of TQ-NP *in vitro*, NR fluorescent dye was incorporated into the NP formulation (0.1 mg/ml). Commonly used fluorescent dyes are hydrophilic, making them incompatible for use with FNP, which relies on imposing high supersaturation levels using water as an anti-solvent for precipitating hydrophobic solutes. Nile red is a hydrophobic dye previously used for the labeling and imaging of NP prepared by FNP (Akbulut et al., 2009). As such, TQ-NP containing NR were formulated by FNP. The TQ:NR weight ratio used was (500:1). The fluorescent dye had no significant effect on the size, stability or %EE and %LC of the TQ-NP formulation (Table 2). Subsequently, tomographic scans of both MCF-7 and MDA-MB-

MCF-7 and MDA-MB-231 cells after incubation with 10  $\mu\text{g/ml}$  of NR-loaded TQ-NP for 30 min, were performed to locate the NP in the cells (Figure 18). The different planes on the z-axis (Figure 18 lower small panels) as well as the three-dimensional reconstruction (Figure 18 upper panels) demonstrate that the NP are internalized by MCF-7 and MDA-MB-231 breast cancer cells and distributed in the cytoplasm and the nucleus.

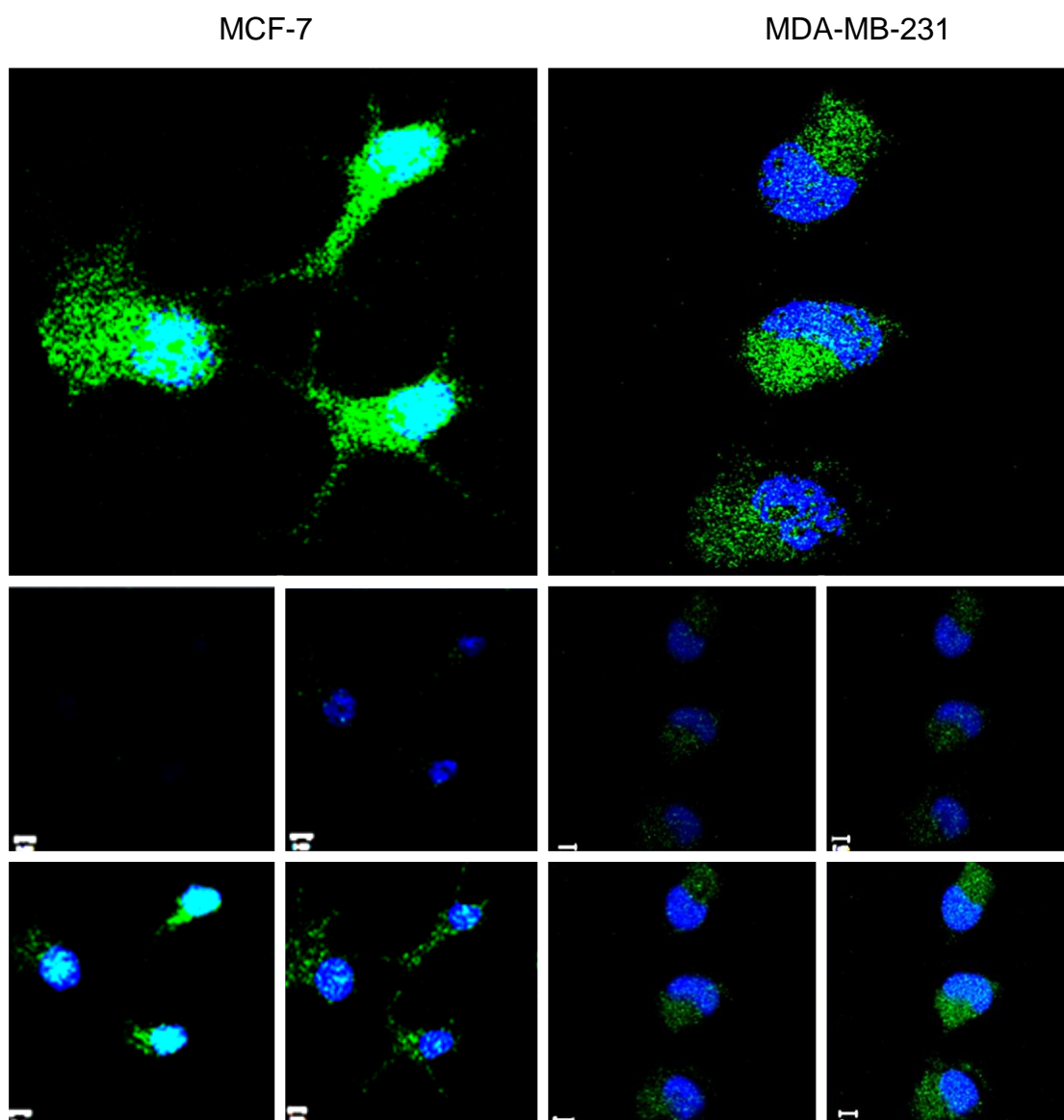


**Figure 18. TQ-NP Are Internalized in MCF-7 and MDA-MB-231 Breast Cancer cells.** MCF-7 and MDA-MB-231 breast cancer cells were incubated with 10  $\mu\text{g/ml}$  of

NR-loaded TQ-NP in growth medium for 30 min before being prepared for confocal imaging. Images were obtained using a Zeiss 710 confocal microscope and a 63x oil objective. Cells 3D spatial images were recreated by taking 21 slices on the z-axis; each slice having a thickness of 0.6  $\mu\text{m}$ .

Determining the maximum concentration of NP taken up by cells is also critical for the design of a treatment regimen for *in vivo* administration. To this aim, cells were treated for 30 min with either 10 or 25  $\mu\text{g/ml}$  of NR-loaded TQ-NP. As shown in Figure 19, the mean fluorescence intensity (MFI) was increased when the cells were incubated with higher particle concentration. The increase in uptake between the MFI was around 2 folds in both cell lines which is proportional to the difference in concentration. The MFI after treatment of cells with 50  $\mu\text{g/ml}$  of NR-loaded TQ-NP did not significantly increase as compared with cells treated with 25  $\mu\text{g/ml}$  of NR-loaded TQ-NP (data not shown). A similar result was obtained using confocal microscopy as means for qualitatively assessing NP uptake (Figure 20). The images further reveal a strong fluorescence in the cell cytoplasm and in the nucleus at both concentrations.

In addition, nanoparticles for chemotherapy need to be taken up by cells with a sufficiently high rate and extent. To assess the dynamics of this uptake, MCF-7 and MDA-MB-231 cells were incubated with 10  $\mu\text{g/ml}$  of NR-loaded TQ-NP for increasing amounts of time, starting from 5 to 60 min. At the indicated time points, the MFI of the cells was measured by flow cytometry. The data of the overlay in Figure 21 and the corresponding representative bar graph, indicate that an increase in the uptake between 5, 15, and 30 min as compared to the non-treated cells in both cell lines. Uptake did not increase between the 30 min and 60 min time points, indicating saturation is reached at

30 min. Hence these findings show that the TQ-NP enter the cells in a time-dependent manner until 30 min of incubation of the NP with the cells.

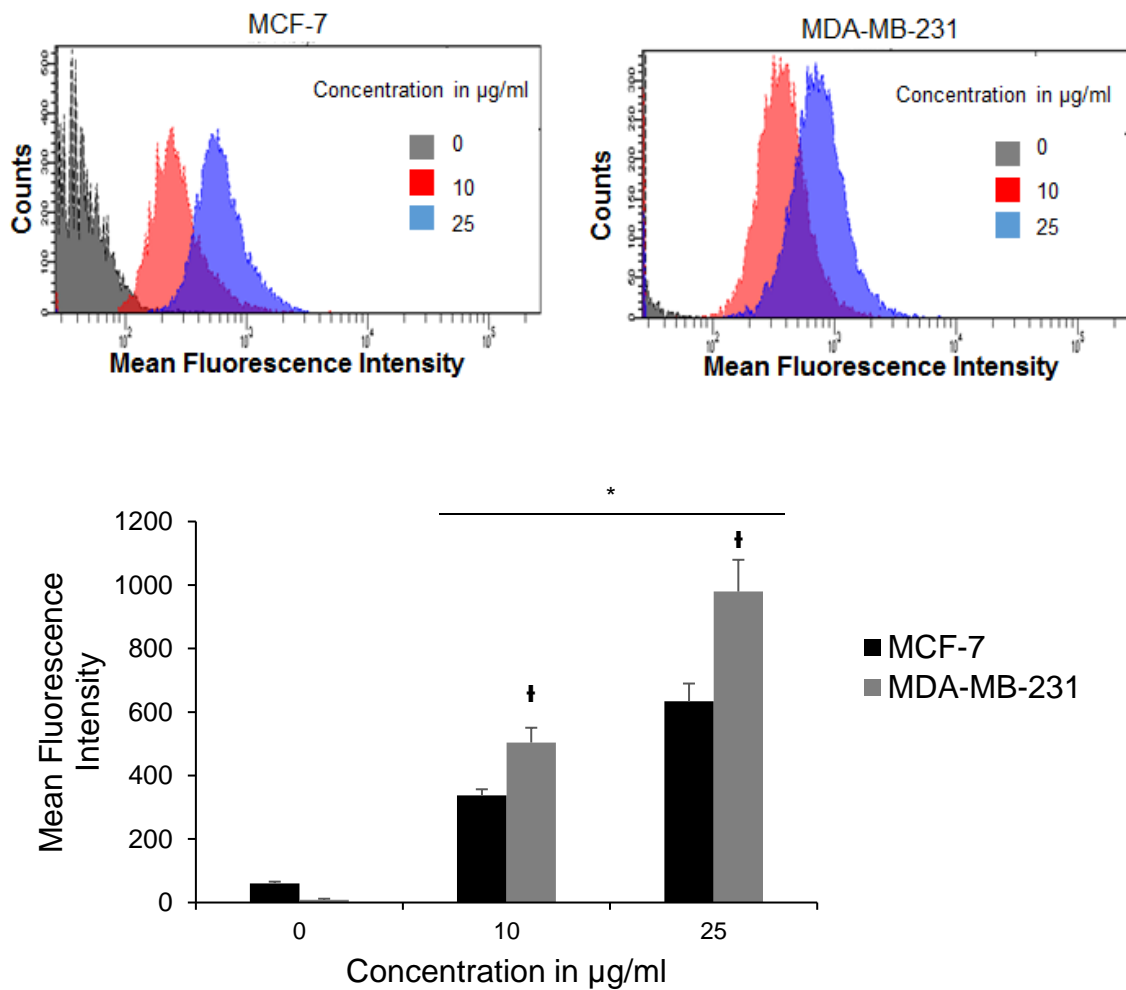


**Figure 19. TQ-NP Uptake is Concentration-Dependent.** Top: The effect of particle concentration on the cellular uptake of NR-loaded TQ-NP is shown as the mean fluorescence intensity of MCF-7 (left panel) and MDA-MB-231 (right panel) cells treated with 10 µg/ml or 25 µg/ml NR-loaded TQ-NP. NR-loaded TQ-NP were prepared in PBS and the treatment was done for 30 min at 37 °C. The fluorescence intensity was measured at the 488 nm excitation and 570 nm emission wavelengths. Bottom: Bar graph represents the concentration-dependent uptake of NR-loaded TQ-NP expressed as the average of the mean fluorescence intensity of MCF-7 and MDA-MB-231 cells  $\pm$  SE. The data represents two independent experiments (n = 3). \* indicates  $p < 0.05$  with respect to the control, † indicates  $p < 0.05$  with respect to cells treated with 10 µg/ml.



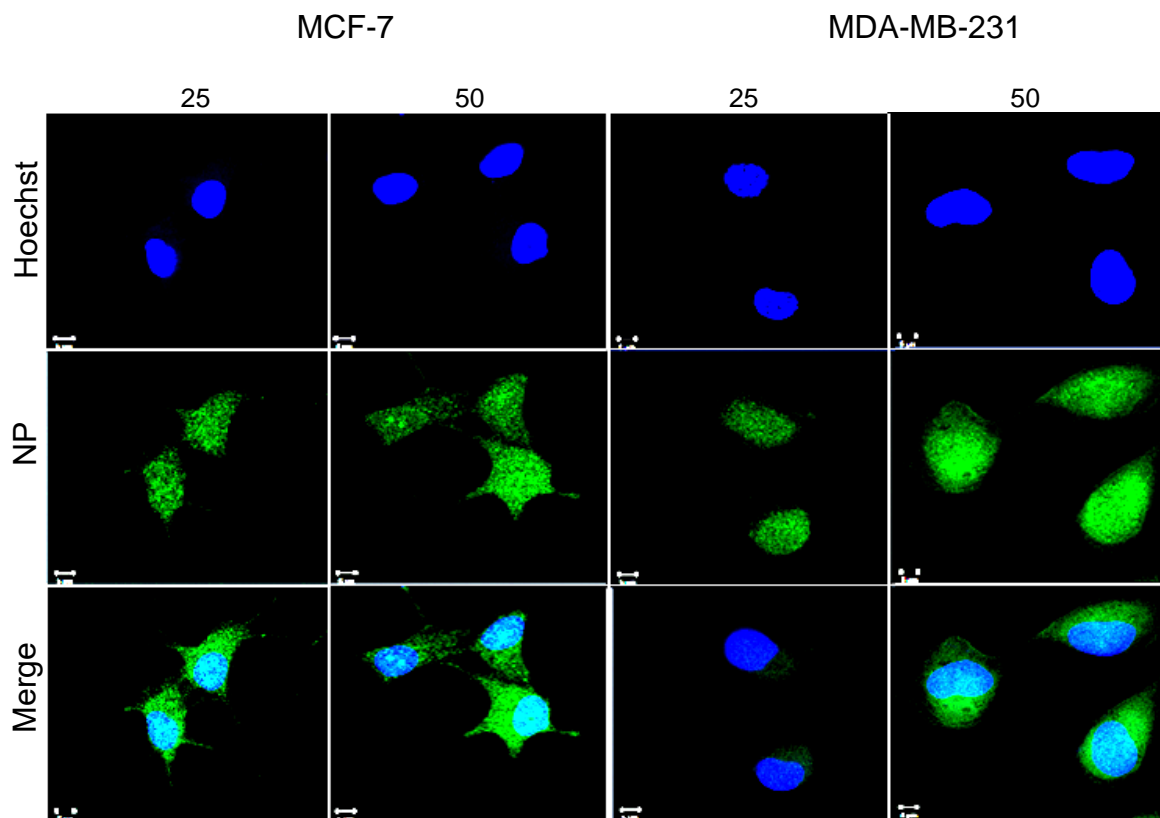


**Figure 20. Qualitative Assessment of Concentration-Dependent TQ-NP Uptake.** MCF-7 and MDA-MB-231 cells were incubated with 25  $\mu\text{g/ml}$  and 50  $\mu\text{g/ml}$  NR-loaded TQ-NP, respectively for 30 min at 37  $^{\circ}\text{C}$ . The nuclei are stained with Hoechst (0.5  $\mu\text{g/ml}$ ) (blue). The uptake of NP (green) is visualized by overlaying images obtained by NR filter and Hoechst filter using a Zeiss 710 confocal microscope and a 63x oil objective. Bar = 5  $\mu\text{m}$ .

#### **4. TQ and TQ-NP take different routes for entry into the cells**

To determine the amount of cells which incorporate TQ-NP following incubation of the cells with the different treatment conditions, the % positive cell population, in comparison to the untreated control was investigated (Figure 22). In both cell lines, the % positive cells, i.e. the population of cells which had incubated TQ-NP after treatment for 5 min were very high, whereby around 80% of MCF-7 cells and approximately 95% of MDA-MB-231 cells were positive. There was no significant

difference in the % positive cells between 5 and 30 min which reflects the fast uptake of NP by the cells which in majority, take up TQ-NP as early as 5 min.

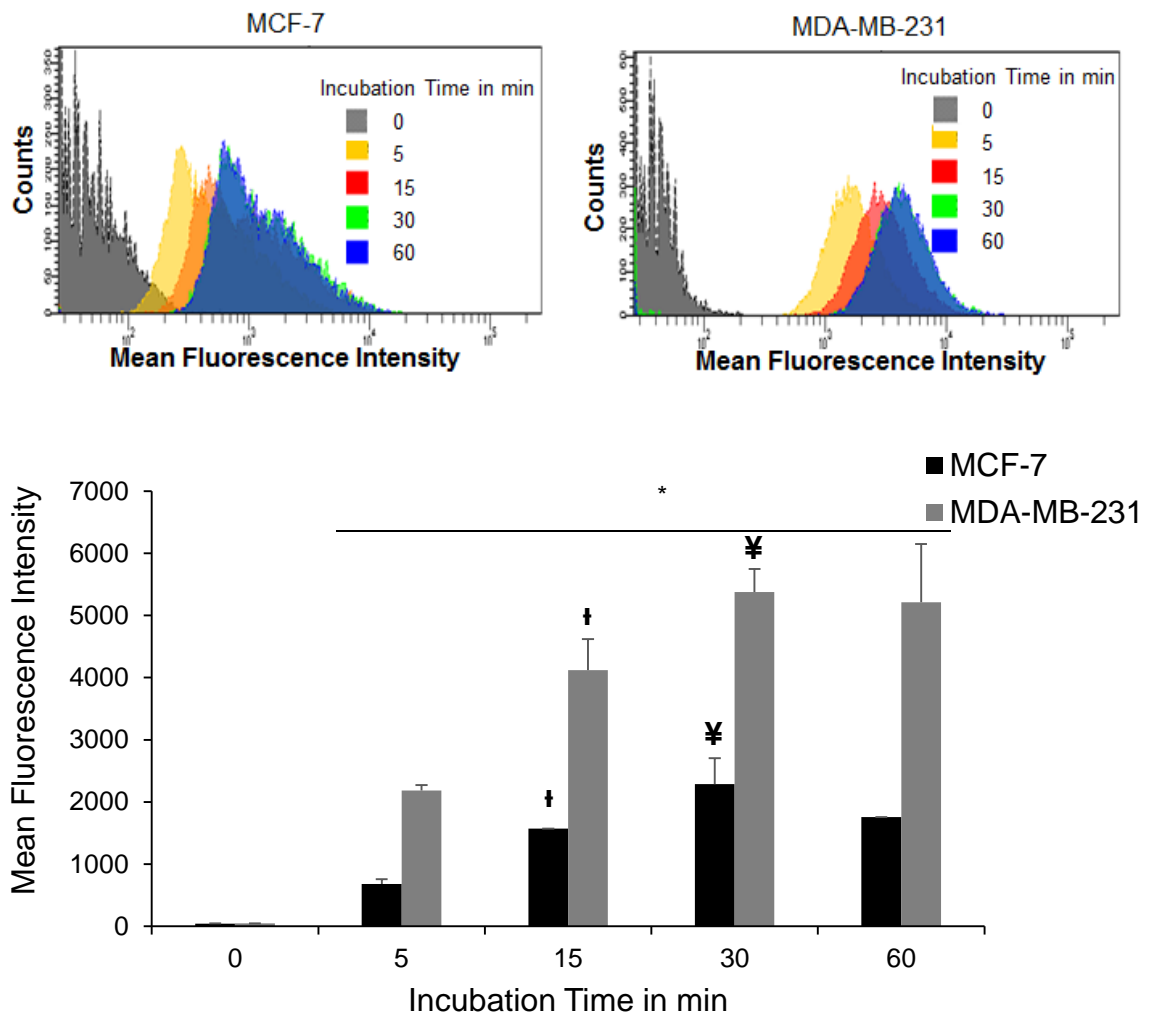


**Figure 21. TQ-NP Uptake is Time-Dependent.** Top: Dot plots showing the effect of particle incubation time on the cellular uptake of NR-loaded TQ-NP expressed as the mean fluorescence intensity of MCF-7 (right panel) and MDA-MB-231 (left panel) cells treated with 10  $\mu\text{g/ml}$  of NR-loaded TQ-NP for 0, 5, 15, 30 and 60 min (upper panel). The fluorescence intensity was measured at the 488 nm excitation and 570 nm emission wavelengths. Bottom: Bar graph showing the uptake of NR-loaded TQ-NP over time expressed as the average of the mean fluorescence intensity of MCF-7 and MDA-MB-231 cells  $\pm$  SE. The data represents two independent experiments ( $n = 3$ ). \* indicates  $p < 0.05$  with respect to the control, † indicates  $p < 0.05$  with respect to 5 min incubation time and ¥ indicates  $p < 0.05$  with respect to 15 min incubation time.

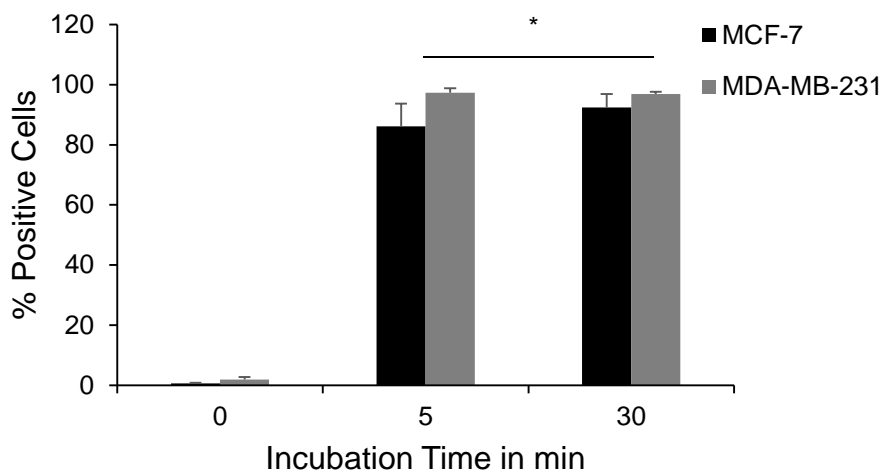


**Figure 22. Fast TQ-NP Uptake by Breast Cancer Cells.** MCF-7 and MDA-MB-231 breast cancer cells were incubated with 10  $\mu\text{g/ml}$  of NR-loaded TQ-NP for 5 and 30 min. The NP were prepared for flow cytometry. The fluorescence intensity was measured at the 488 nm excitation and 570 nm emission wavelengths. The %positive cell population of NR-loaded TQ-NP treated cells was determined in reference to the control untreated cells. The data represents the mean of two independent experiments  $\pm$  SE (n = 3). \* indicates  $p < 0.05$  with respect to the untreated control (0).

To test whether the fast uptake correlates with the anticancer potential of TQ-NP, MDA-MB-231 breast cancer cells were treated with 25  $\mu\text{M}$  TQ or TQ-NP for 30 min. The treatment was then removed and the cells were incubated with cell culture media after which cell viability was assessed at 24 h post-treatment (Figure 23). Both TQ and TQ-NP decreased cell viability of MDA-MB-231 breast cancer cells after treatment for 30 min and removal of treatment with TQ-NP causing more inhibition of cell viability. Specifically, Treatment of MDA-MB-231 breast cancer cells for 30 min with TQ-NP results in 40% cell death while treatment with TQ and removal of treatment only causes around 20% cell death in MDA-MB-231 breast cancer cells.

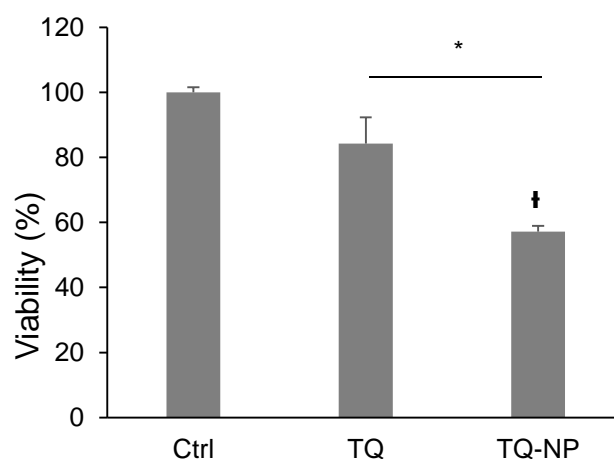


**Figure 23. Fast TQ-NP Uptake by MDA-Mb-231 Breast Cancer Cells Correlates with Enhanced Anticancer Potential.** MDA-MB-231 breast cancer cells were treated with 25  $\mu$ M of TQ, TQ-NP or blank NP. After 30 min incubation with the cells, the treatment was removed and replaced with cell culture media. Cell viability was assessed 24 h post-treatment by MTT assay. The values were normalized to the control. Each condition was done in triplicate and the experiment was repeated three times. The error bars represent the standard error. \* indicates  $p < 0.05$  with respect to the control. † indicates  $p < 0.05$  with respect to TQ.

To investigate if the difference in the dynamics of uptake of TQ and TQ-NP stems from a difference in the mechanism of uptake of free or encapsulated drug, a competition assay was performed. To this aim, MCF-7 and MDA-MB-231 breast cancer cells were treated for 5 min with 50  $\mu$ g/ml NR-loaded TQ-NP alone or in combination with either 50  $\mu$ g/ml of TQ or 50  $\mu$ g/ml of TQ-NP. The MFI was measured by fluorometry and the uptake profiles of the different treatment conditions were overlaid (Figure 24). NP uptake by MCF-7 and MDA-MB-231 cells is reflected by the shift of the mean fluorescent peak to the right as compared to the untreated control. When cells are treated with NR-loaded TQ-NP and competed with TQ, the MFI peak remains similar to that obtained with cells treated with NR-loaded TQ-NP alone. However, a clear MFI shift to the left is observed for cells treated with fluorescent and non-

fluorescent TQ-NP. Quantitatively, the competition accounts for 40% inhibition of uptake of fluorescent NP in both cell lines (Figure 24).

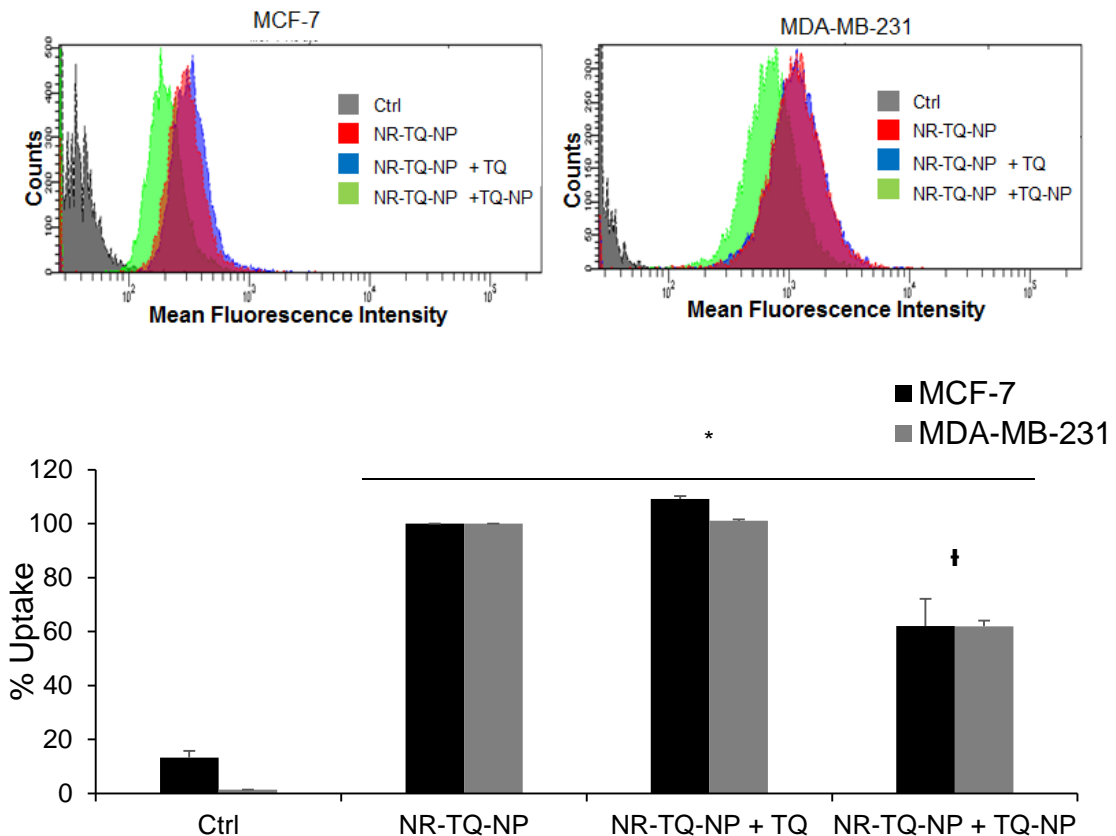


**Figure 24. TQ-NP Compete with NR-TQ-NP.** Top: Representative dot plots featuring the mean fluorescence intensity of control and treated MCF-7 and MDA-MB-231 breast cancer cells. Bottom: Bar graph showing the competition assay of the uptake of NR-loaded TQ-NP expressed as the average of the mean fluorescence intensity of MCF-7 and MDA-MB-231 cells  $\pm$  SE. The data represents two independent experiments ( $n = 3$ ). Cells were incubated for 5 min with 50  $\mu\text{g/ml}$  of NR-loaded TQ-NP, or a mixture of 50  $\mu\text{g/ml}$  of NR-loaded TQ-NP and 50  $\mu\text{g/ml}$  TQ, or a mixture of 50  $\mu\text{g/ml}$  of NR-loaded TQ-NP and 50  $\mu\text{g/ml}$  TQ-NP. The NP were prepared in PBS and the treatment was done at 37  $^{\circ}\text{C}$ . After incubation, the cells were prepared for flow cytometry analysis and the fluorescence intensity was measured at 488 nm excitation and 570 emission. \* indicates  $p < 0.05$  with respect to the control. † indicates  $p < 0.05$  with respect to NR-TQ-NP.

### ***5. Caveolin and clathrin-dependent endocytosis play a role in TQ-NP uptake***

Given that TQ can freely diffuse into the cells, endocytosis; the major route of uptake of NP was investigated to determine if it could be implicated in the uptake of TQ-NP. To this aim, different endocytosis inhibitors were used. Cells were pretreated with nystatin, genistein, chlorpromazine hydrochloride and amiloride, prior to treatment with NR-loaded TQ-NP. Nystatin depletes cholesterol and inhibits the formation of sag vesicles (Iversen et al., 2011). It is also a caveolae-mediated endocytosis inhibitor (Liu et al., 2014). Genistein inhibits several tyrosine kinases and enables the disruption of the caveolin-mediated endocytosis, or lipid rafts route (Iversen et al., 2011; Liu et al., 2014). Chlorpromazine hydrochloride is an inhibitor of Rho GTPases which prevents the formation of clathrin coated sag vesicles and thus disturbs the clathrin-mediated endocytosis (Iversen et al., 2011; Liu et al., 2014; Zeng et al., 2014). Finally, amiloride is a blocker of micropinocytosis which functions by lowering the pH close to the membrane and preventing Rac1 and cdc42 signaling (Iversen et al., 2011; Liu et al., 2014; Zeng et al., 2014). Treatment with genistein reduced the uptake of NP in MCF-7 cells by 20% as shown in Figure 25. The same trend was observed in MDA-MB-231 cells where this decrease was slightly more pronounced (around 30%) and where an inhibition of the uptake was also observed in response to treatment with chlorpromazine (Figure 25).

### ***6. NP can be processed by endosomes and lysosomes***

To rule out any non-specificity effect of the inhibitors of endocytosis, the internalization of TQ-NP was investigated. The cellular trafficking and biodistribution

of TQ-NP after entry into the cells was determined using the following markers: caveolin to label the caveolae, transferrin to detect the clathrin-coated pits as well as early and recycling endosomes, early endosome antigen 1 (EEA-1) to identify early endosomes and lysosomal associated membrane protein 1 (lamp-1) for lysosomes tracking. Overall images suggest that the NP colocalize with caveolin (Figure 26), transferrin (Figure 27), as well as with EEA-1 (Figure 28) and lamp-1 (Figure 29) in both cell lines.

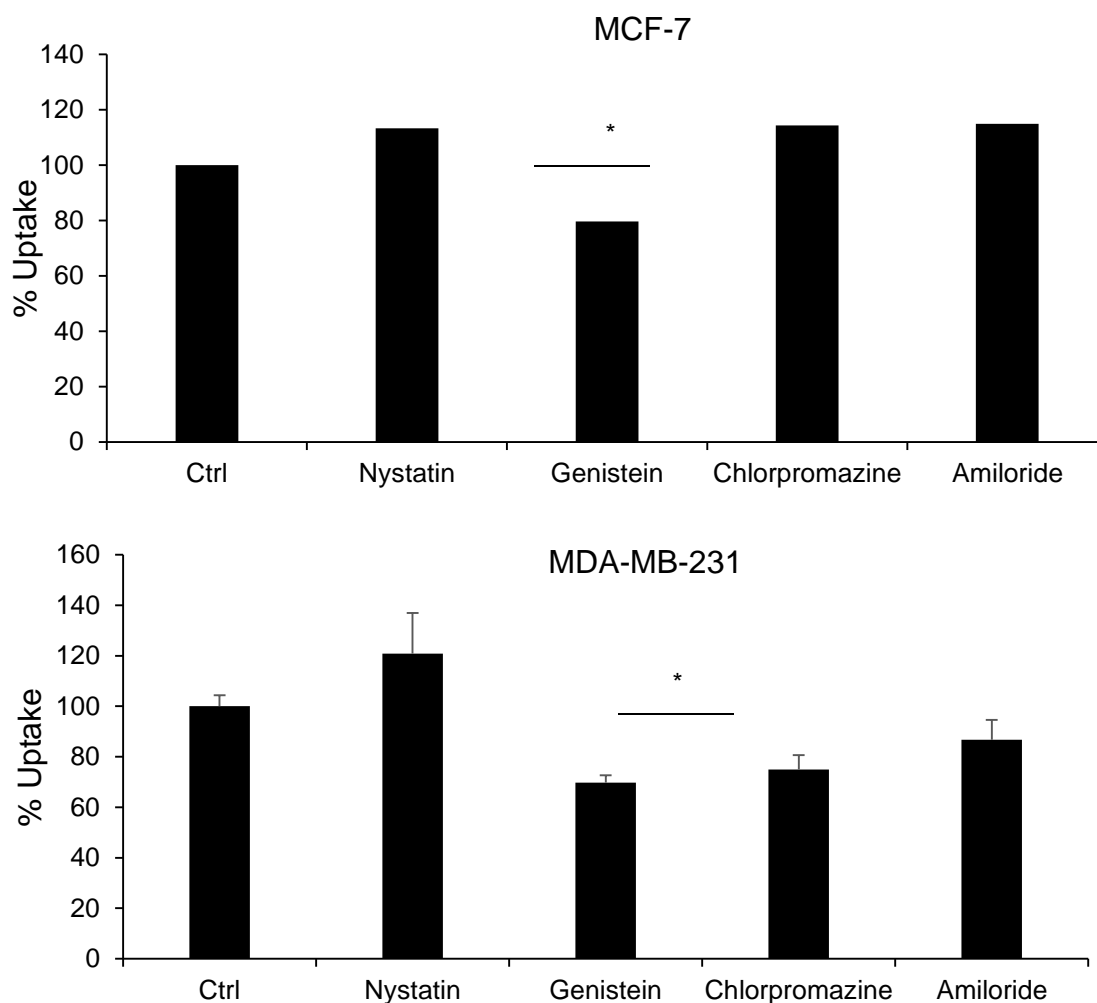


**Figure 25. TQ-NP Uptake by Caveolin-Mediated Endocytosis Pathway.** Effect of the inhibitors of endocytosis on the internalization of NR-loaded TQ-NP by MCF-7 (left

panel) and MDA-MB-231 (right panel). Cells were untreated (Ctrl) or pretreated with nystatin (50 mg/ml) genistein (50 mg/ml) chlorpromazine (10 mg/ml) or amiloride (20 mg/ml) for 1 h prior to treatment with NR-loaded TQ-NP (10  $\mu$ g/ml) for 30 min. After treatment, the mean fluorescence intensity of each condition was measured by flow cytometry. The uptake is expressed as percentage of the mean fluorescence intensity relative to the untreated control  $\pm$  SE. \* indicates  $p < 0.05$  with respect to the control.

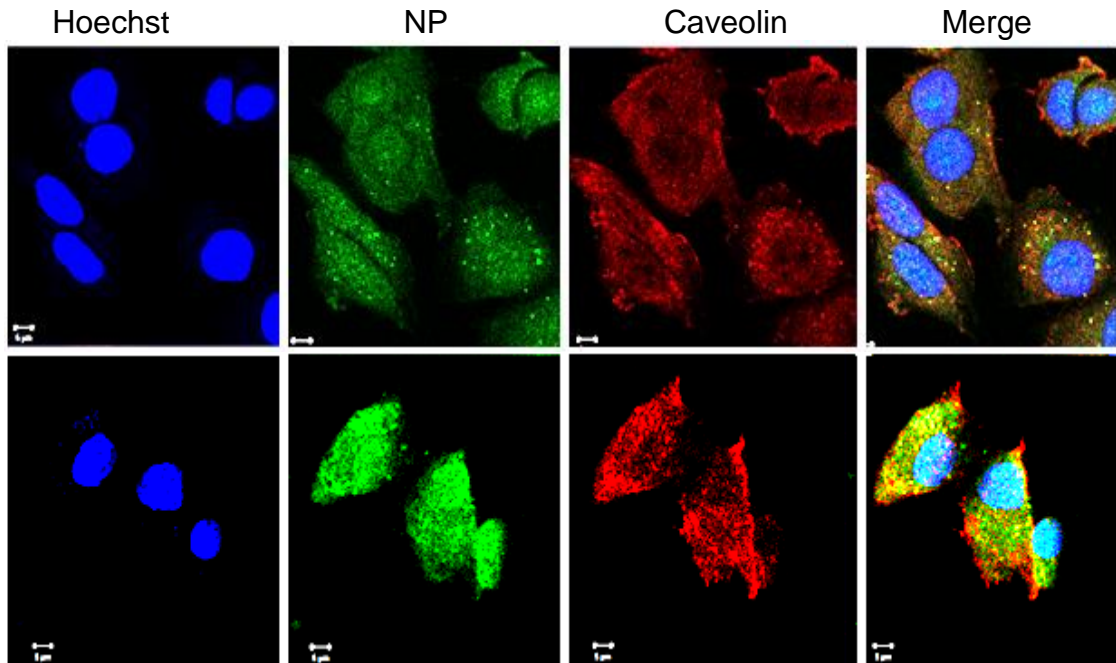


**Figure 26. TQ-NP Colocalization with Caveolin in MCF-7 and MDA-MB-231 Breast Cancer Cells.** MCF-7 (upper panel) and MDA-MB-231 (lower panel) breast cancer cells were incubated with 25  $\mu$ g/ml of NR-loaded TQ-NP in growth medium for 30 min before preparation for incubation with caveolin. Caveolin is shown in red, the NP in green and the nuclei stained with Hoechst, are shown in blue. The images were obtained using a Zeiss 710 confocal microscope and a 63x oil objective. Bar = 5  $\mu$ m.



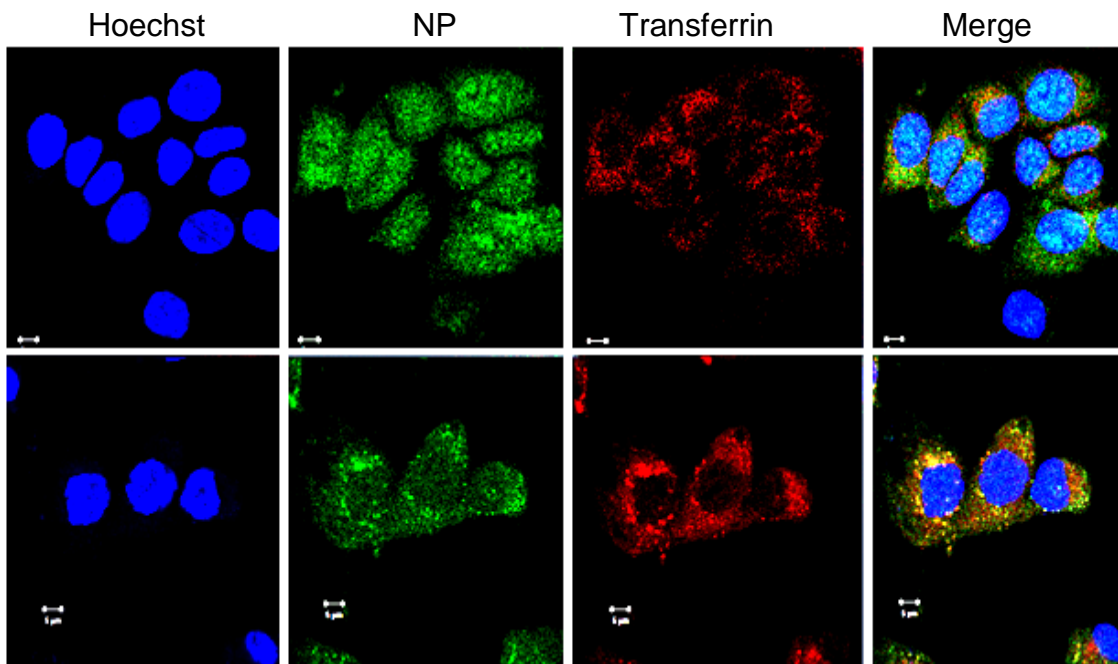


**Figure 27. TQ-NP Colocalization with Transferrin in MCF-7 and MDA-MB-231 Breast Cancer Cells.** MCF-7 (upper panel) and MDA-MB-231 (lower panel) breast cancer cells were incubated with 25  $\mu\text{g/ml}$  of NR-loaded TQ-NP in growth medium for 30 min before preparation for incubation with transferrin. Transferrin is shown in red, the NP in green and the nuclei stained with Hoechst, are shown in blue. The images were obtained using a Zeiss 710 confocal microscope and a 63x oil objective. Bar = 5  $\mu\text{m}$ .

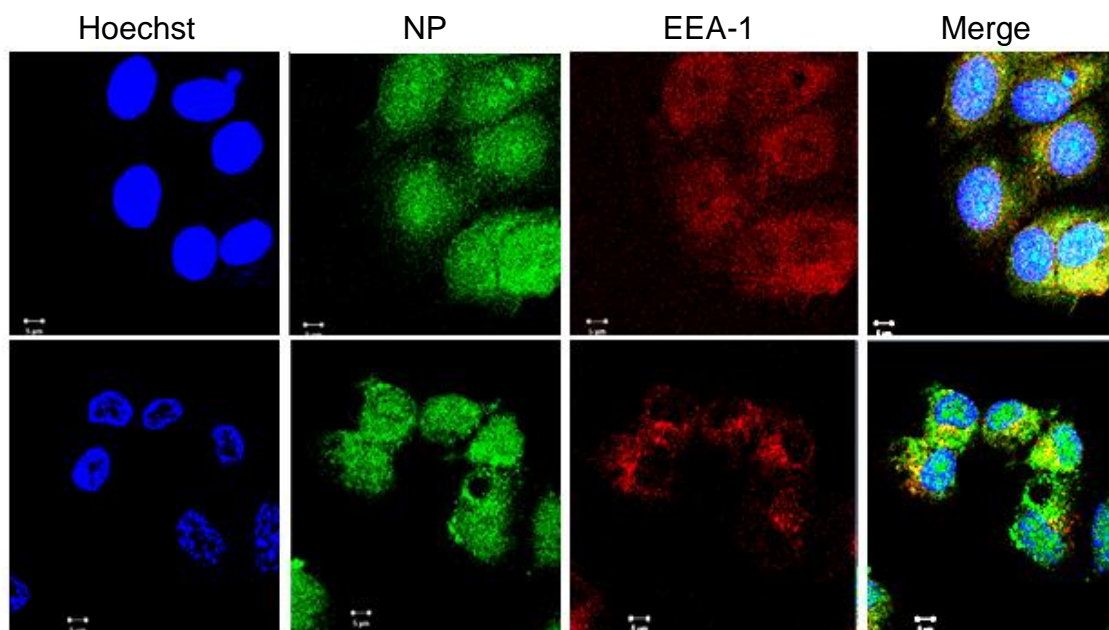


**Figure 28. TQ-NP Colocalization with EEA-1 in MCF-7 and MDA-MB-231 Breast Cancer Cells.** MCF-7 (upper panel) and MDA-MB-231 (lower panel) breast cancer cells were incubated with 25  $\mu\text{g/ml}$  of NR-loaded TQ-NP in growth medium for 30 min before preparation for incubation with EEA-1. EEA-1 is shown in red, the NP in green and the nuclei stained with Hoechst, are shown in blue. The images were obtained using a Zeiss 710 confocal microscope and a 63x oil objective. Bar = 5  $\mu\text{m}$ .

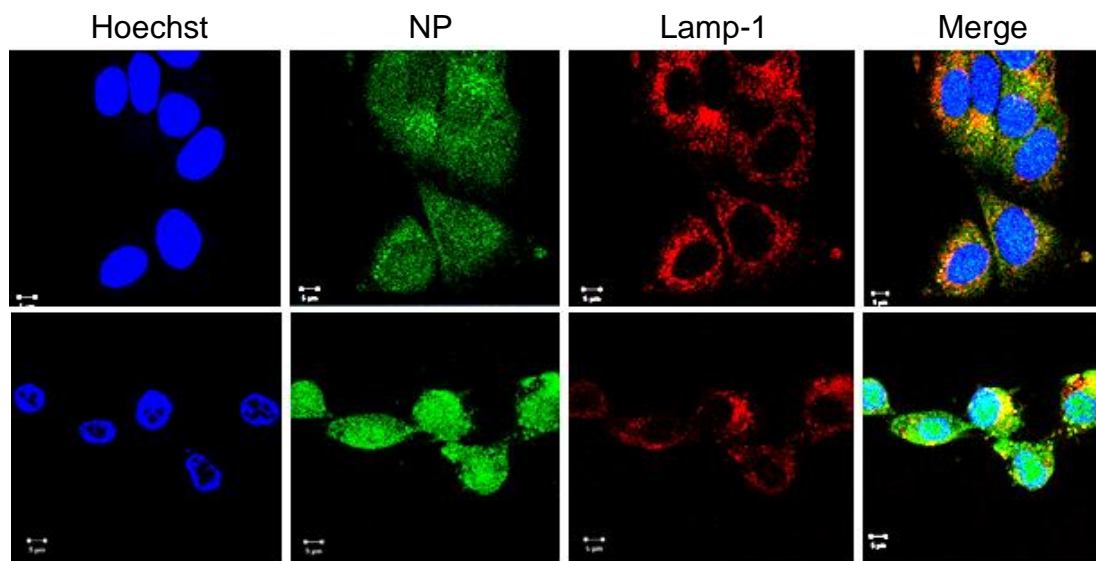


**Figure 29. TQ-NP Colocalization with Lamp-1 in MCF-7 and MDA-MB-231 Breast Cancer Cells.** MCF-7 (upper panel) and MDA-MB-231 (lower panel) breast cancer cells were incubated with 25  $\mu\text{g/ml}$  of NR-loaded TQ-NP in growth medium for 30 min before preparation for incubation with Lamp-1. Lamp-1 is shown in red, the NP in green and the nuclei stained with Hoechst, are shown in blue. The images were obtained using a Zeiss 710 confocal microscope and a 63x oil objective. Bar = 5  $\mu\text{m}$ .

## E. Discussion

This is the first comprehensive study of the cellular uptake mechanisms, the trafficking and the spatial distribution of fluorescent TQ-NP. In this study, polymeric TQ-NP were prepared using PS-PEO diblock copolymer via FNP. This formulation was non-toxic to non-tumorigenic MCF-10-A breast cell line up to 25  $\mu\text{M}$  and showed equal or enhanced activity against MDA-MB-231 and MCF-7 breast cancer cell lines respectively, in comparison to free TQ. Uptake studies suggest that inhibiting caveolin-

dependent endocytosis reduces the uptake of TQ-NP by 20-30% in MCF-7 and MDA-MB-231 cells and that caveolin-dependent endocytosis as well as clathrin-dependent endocytosis play a role in the uptake of TQ-NP in MDA-MB-231 breast cancer cells. Following internalization, TQ-NP can be found co-localizing with both endosomes (EEA-1) and lysosomes (Lamp-1).

The polymeric TQ-NP formulation described in this study holds great potential for *in vivo* application owing to their small size, long term stability and ability to be internalized to the cytoplasm and reach the nucleus of cells. Size control, high %EE and %LC are additional advantages conferred by the TQ-NP preparation described in the present work. FNP thus enabled the preparation of TQ-NP with average diameters suitable for cancer drug delivery applications as they are large enough to escape elimination by the kidney ( $> 10$  nm) and small enough to be sterilized ( $< 200$  nm) (Lammers et al., 2012; Nair et al., 2010; Shekunov et al., 2007). In comparison large TQ-NP were reported in previous studies (Abu-Dahab et al., 2013; Alam et al., 2012; Ravindran et al., 2010; Shah et al., 2011). Moreover, while some previously published TQ-NP papers do not assess the %EE and %LC of the formulations, FNP enabled the formulation of TQ-NP with considerably greater %EE and %LC than other polymeric and chitosan based TQ-NP (Alam et al., 2012; Ganea et al., 2010; Shah et al., 2010). Finally, the findings show that the TQ-NP formulations stability is maintained through steric stabilization provided by PS-PEO over 4 weeks which can potentially minimize non-specific interactions and prevent NP loss and side toxicity (Nair et al., 2010). The ethylene oxide component of the diblock copolymer is also expected to impart stealth capability of the NP.

Previously described TQ-NP have been tested against both MDA-MB-231 and MCF-7 cancer cell lines and have been shown to either have greater activity (Abu-Dahab et al., 2013; Dehghani et al., 2015; Ganea et al., 2010; Ravindran et al., 2010) or equal activity (Bhattacharya et al., 2015) in comparison to free TQ. For instance, a two fold increase in the activity of TQ-NP in MDA-MB-231 at 96 h was reported by Ganea et al (2010). The lack of enhancement in drug activity of PS-PEO TQ-NP in MDA-MB-231 cells observed in the present work is most likely due to the high sensitivity of these cells to TQ or to the difference in the genetic background of these cells. In the case of MCF-7 cells, Odeh et al (2012) have shown that liposomal TQ had much lower anticancer activity than free TQ, with an ED<sub>50</sub> five times higher than that of free TQ (Odeh et al., 2012), while Bhattacharya et al (2015) reported similar anticancer potential of TQ-NP in comparison to free TQ. Yet, the advantage of the latter formulation was its reduced cytotoxicity to normal PBMCs (Bhattacharya et al., 2015). Some formulations that increased TQ's anticancer potential in MCF-7 cells had larger average particle sizes. This was the case of beta-cyclodextrin TQ-NP (TQ-CD) which were six folds more active than TQ in inhibiting MCF-7 cell viability at 72 h (Abu-Dahab et al., 2013).

Imaging of TQ-NP in breast cancer cells revealed that NR-labeled TQ-NP internalize inside the cells. They were shown to accumulate both in the cytoplasm as well as in the nucleus and hence their activity can be linked to activation of elements in both compartments. Given that only small NP can pass the nuclear pore complexes which are around 10-25 nm in diameter (Elsabahy and Wooley, 2012), the data suggests that the smaller particles of the NP size distribution have freely diffused to those compartments and/or that a reduction in size of the NP have occurred. Drug diffusion from the NP to the cytoplasm and the nucleus after cellular intake could account for NP

size reduction. The distribution of the NP inside the cells can be very predictive of their mechanism of action.

Furthermore, NR-labeled TQ-NP uptake in breast cancer cells was shown to be time and concentration dependent. The uptake time represents the time required for the particles to come into contact with the cell membranes, the time for packaging the NP and their entry into the cells (Kievit and Zhang, 2011). In both cases, the uptake reached a maximum beyond which a plateau effect was observed. Saturation of the cells with NP or an equilibrium between NP uptake and their excretion by the cells could account for the plateau effect. The trend of increasing uptake with increasing concentration is in line with recently reported results for PEG TQ-NP uptake (Bhattacharya et al., 2015).

In addition, the fast uptake revealed by the high percentage of positive cells at 5 min, was shown to account for the enhanced anticancer potential of TQ-NP as compared with free TQ in MDA-MB-231 breast cancer cells. Indeed, treatment of MDA-MB-231 breast cancer cells with TQ or TQ-NP for 30 min followed by removal of treatment indicated that both TQ and TQ-NP are taken up by the cells at this incubation time. However, treatment with TQ-NP before removal of treatment caused an inhibition of cell viability similar to that observed with cells treated with TQ-NP for 24 h, while treatment with TQ and removal of treatment only caused around 20% cell death which is significantly different from the effect of treatment of MDA-MB-231 breast cancer cells with TQ for 24 h. This difference; attributed to the fast uptake of TQ-NP as compared with free TQ, thus confirms the advantage of TQ encapsulation. Moreover, the inhibition of uptake of labeled TQ-NP by co-treatment with the unlabeled ones, provided evidence that TQ-NP and NR-loaded TQ-NP are taken up by the same pathway in MDA-MB-231 and MCF-7 breast cancer cells. The competition assay

further showed that TQ and TQ-NP enter the cells using different routes, suggesting the involvement of endocytosis in the uptake of TQ-NP.

Encapsulation of therapeutic agents into NP with a particular affinity for an internalization pathway has the potential to increase the efficiency of membrane targeting given that the route of entry of nanocarriers in the cells has a direct impact on their fate after internalization (Kievit and Zhang, 2011; Xu et al., 2013). The use of inhibitors of endocytosis as well as the colocalization studies suggest a role for caveolin-dependent endocytosis in mediating the uptake of TQ-NP in MCF-7 and MDA-MB-231 cells and a role for clathrin-dependent endocytosis in mediating the uptake of TQ-NP in MDA-MB-231 cells. Clathrin-mediated endocytosis in MCF-7 cells has been reported recently (Bhattacharya et al., 2015). The results obtained with NR-loaded TQ-NP are consistent with previous results showing that the uptake of polystyrene nanoparticles by HeLa and human umbilical vein endothelial cells is clathrin and or caveolin-dependent (Lai et al., 2007). Additionally, a high expression of caveolin in breast cancer cells might account for the involvement of caveolae in the uptake of TQ-NP (Chung et al., 2015).

Interestingly, neurons and leukocytes do not express caveolins or possess caveolae, which could eliminate or reduce toxicity and side effects at those specific tissues in case of *in vivo* administration of NR-loaded TQ-NP (Xu et al., 2013). Nanomaterials that enter the cells in a caveolin-dependent manner can be delivered to the ER and subsequently the cytosol, and enter the nucleus via the nuclear pore complex (Xu et al., 2013). Compared with clathrin-dependent endocytosis, the trafficking along this pathway is longer and the nanomaterials are subjected to less degradation which increases drug concentration delivered at target sites, and results in an overall

improvement of the therapeutic effect (Kou et al., 2013). However, the reduction of 20-30% in the uptake of TQ-NP following pre-treatment with the inhibitors of endocytosis suggests that endocytosis might not account entirely for the uptake of TQ-NP.

Moreover, the inhibitors of endocytosis and the colocalization studies might not be specific enough for determining the mechanism of uptake of the NP. Hence it is still critical to investigate the uptake of TQ-NP in cells expressing mutated proteins implicated in the different pathways of endocytosis or in cells expressing siRNA against those targets for a conclusive understanding of TQ-NP mechanism of uptake.

In addition to the therapeutic advantage of TQ-NP, the NR-labeled TQ-NP developed in this study allows for imaging of the particles inside the cells. FNP can thus be exploited to produce multifunctional NP enabling co-formulation of imaging and anticancer agents, which is of great use in nanotheranostics; a field which integrates diagnostics and therapeutics tools in one system (Kim et al., 2013). For translation to the clinic, drug carriers that enable imaging are more advantageous than therapeutic NP alone given that physicians can monitor drug concentrations in off-target organs and in the tumor to adjust the type and dosing of drug for each patient and prevent over or under treatment that could result in harmful side effects, or incomplete cancer remission (Kievit and Zhang, 2011).

The co-localization of TQ-NP with both endosomes (EEA-1) and lysosomes (Lamp-1) suggests that TQ-NP can translocate from the endosomes and lysosomes to the cytoplasm after entering the cells by endocytosis. The process related to endosome maturation might therefore be making TQ in NP form accessible to the cytoplasm and the nucleus where they exert their anticancer activity in both compartments (Iversen et al., 2011).

In summary, the multifunctional nature of the polymeric TQ-NP prepared in this study, enables the imaging as well as the treatment of different cell lines which cannot be achieved with the administration of TQ in its free form. Furthermore, the overall advantages of the PS-PEO TQ-NP formulation in terms of size, stability, anticancer potential and dynamics of cellular uptake as well as their ability to be internalized to the cytoplasm and reach the nucleus of cells make it a potential candidate for cancer treatment, hence the need for further *in vivo* evaluation.



# CHAPTER IV

## SYNTHESIS, PRIMARY BIOEVALUATION AND COMPUTATIONAL ANALYSIS OF THYMOQUINONE PYRIMIDINE DERIVATIVES

### **A. Abstract**

Thymoquinone (TQ), the major constituent of black seed oil is a natural product which exhibits many biological activities including a chemotherapeutic potential. Recent studies have shown that TQ's anticancer efficacy is negatively affected by binding of TQ to off-targets. Drug conjugation is a strategy commonly used to overcome drugs non-specific binding as well as for increasing the potency and selectivity of many drugs. In this project, TQ pyrimidine hydrazides derivatives were synthesized and their anticancer potential was evaluated in a breast cancer model. The molecular targets of TQ and TQ derivatives and their mechanism of action were further investigated.

A Michael-type reaction was used to synthesize the derivatives. The anticancer potential was tested by MTT assay against MCF-7 and MDA-MB-231 breast cancer cells. Inverse docking by PharmMapper was performed to predict the potential targets of TQ and TQ derivatives and the functional comparative analysis of the targets was done in Protein ANalysis THrough Evolutionary Relationships (PANTHER).

The results show that TQ derivatives efficiently inhibit the viability of MCF-7 and MDA-MB-231 breast cancer cells. The *in silico* screening further enabled the identification of many potential TQ and TQ derivatives targets implicated in carcinogenesis. Specifically, the H-Ras protein which activates the MAPK/ERK pathway was among the top ranked target hits, with a pharmacophore model matching the molecular features of all TQ derivatives but not TQ. In addition, the data suggests that TQ binding to two proteins which inhibit its activity, namely, bovine serum albumin (BSA) and NADPH Quinone Oxidase 1 (NQO1) was abrogated upon conjugation.

Altogether, this study describes new active TQ derivatives as well as a fast approach for identifying the potential molecular targets and their mechanism of action. *In vitro* target validation however, is still warranted.

## **B. Introduction**

Thymoquinone (TQ), is a promising anticancer molecule whose mechanism of action has been thoroughly investigated (Schneider-Stock et al., 2014). However, little is known about the cellular and molecular targets which directly bind to TQ. Furthermore, the few studies investigating the consequences of TQ-target binding reveal undesirable effects of such interactions on the anticancer activity of TQ. For instance, we have shown that binding of TQ to BSA abrogates its activity (El-Najjar et al., 2011b). Another group has also reported resistance to treatment with TQ in cells expressing the quinone detoxifying flavoenzyme NQO1 which catalyzes the two-electron reduction of quinones to hydroquinones (Sutton et al., 2012). This suggests that

the development of TQ is hindered by shortcomings inherent to its chemical structure. Drug conjugation is an approach commonly used to overcome drugs physicochemical or biopharmaceuticals problems (Mahato et al., 2011; Singh et al., 2008). Many drug conjugates have even reached the clinic for the treatment of cancer. Literature also provides evidence for the enhancement of TQ's anticancer potential upon conjugation (Banerjee et al., 2010a; Effenberger et al., 2010; Wirries et al., 2010; Yusufi et al., 2013). For instance, conjugation of TQ with the triterpene betulinic acid; an active molecule which has reached clinical trials at the national cancer institute, enhances TQ's activity against HL-60 leukemia cells by up to 200 folds (Effenberger et al., 2010). Similarly, at least three potent TQ derivatives have been patented because of their increased activity in comparison with TQ (Banerjee et al., 2010a). All these studies mainly investigated the enhancement of the anticancer activity of TQ upon conjugation but did not provide insights to the effects of the conjugation on the molecular targets which are at the basis of drugs mechanisms of action.

In view of this gap in knowledge, this project aimed to design TQ conjugates, assess their anticancer potential in comparison with TQ as well as screen and analyze the potential TQ and TQ derivatives targets. We chose to add two active classes to TQ (carbocyclic nucleosides and acylhydrazones) to prepare TQ pyrimidine hydrazides derivatives. One attractive feature in carbocyclic nucleosides is the replacement of the furanose ring with a cycloalkane ring that is resistant to phosphorylases which cleave the *N*-glycosidic bond in natural nucleosides. Carbocyclic nucleosides display a wide range of biological activities including antitumor, antibiotic, antimicrobial, antiviral, antimetabolite, and herbicidal activities (Balzarini, 2000; Boutureira et al., 2013; De Clercq, 2005; Melroy and Nair, 2005; Shaw and Locarnini, 2004; Yuen et al., 2008). In

addition, hydrazone derivatives including TQ hydrazone derivatives constitute an important class of biologically active drug molecules with anticonvulsant, anti-inflammatory, anti-tuberculosis, anti-tumoral, anti-proliferative and antimalarial potential (Rollas and Kucukguzel, 2007; Seleem et al., 2011; Wirries et al., 2010).

The anticancer potential of TQ and the derivatives was evaluated in a breast cancer model consisting of non-aggressive MCF-7 and highly aggressive MDA-MB-231 human breast cancer cell lines. A computer-based approach was used to screen for TQ and TQ derivatives potential targets as well as to understand and compare their mechanisms of action.

## **C. Materials and methods**

### ***1. Materials***

RPMI 1640 and Dulbecco's Modified Eagle Medium (DMEM) were purchased from Lonza (Verviers, Belgium). Thymoquinone, trypsin-EDTA, Dulbecco's phosphate buffered saline (PBS), horse serum, fetal bovine serum (FBS), penicillin-streptomycin (P/S), MTT (3-(4,5-Dimethylthiazol-2-yl)-2,5-diphenyltetrazolium bromide), trypan blue and methanol, were purchased from Sigma Aldrich (St Louis, Missouri, USA).

### ***2. Cell Culture***

MDA-MB-231 breast cancer cells were grown in RPMI 1640 cell culture media supplemented with 10% heat-inactivated FBS and 1% P/S. MCF-7 breast cancer cells were grown in DMEM cell culture media supplemented with 10% heat-inactivated

FBS and 1% P/S. All cells were maintained in a humidified atmosphere of 5% CO<sub>2</sub> at 37°C. TQ was dissolved in methanol and then diluted in media as needed such that the final methanol concentration did not exceed 0.1%.

### ***3. TQ derivatives Synthesis***

The synthesis of TQ derivatives was initiated by allowing the commercially available pyrimidines uracil, thymine and cytosine, to undergo a Michael-type reaction with ethyl acrylate in the presence of catalytic amounts of sodium metal and form the corresponding esters. Hydrazinolysis of the esters with hydrazine under reflux conditions produced different 1-(2-hydrazidoethyl) pyrimidines. TQ derivatives were then prepared by coupling TQ with the corresponding 1-(2-hydrazidoethyl)pyrimidine in ethanol under reflux conditions.

### ***4. Characterization of TQ derivatives***

The purity of the TQ derivatives was assessed by TLC and the melting point of the expected solids. The structures of the compounds was also elucidated via FTIR, <sup>1</sup>H-NMR, <sup>13</sup>C-NMR and GC-MS.

### ***5. Viability Assay***

MTT assay was used to assess the anticancer potential of TQ and TQ derivatives in MCF-7 and highly aggressive MDA-MB-231 breast cancer cells as

described previously (Fakhoury et al., 2016). Briefly, cells were seeded in 96 well plates at a density of  $10^5$  cells/ml. All treatments were performed at 50% confluency and cells were treated separately with 10  $\mu$ M of each compound. At 24 h after treatment, the medium was removed and the cells were incubated overnight with an MTT solution (1 mg/ml prepared in PBS). The solution containing the MTT dye was removed the next day and replaced by isopropanol to dissolve the formazan crystal prior to measuring the colorimetric absorbance of the different wells at 595 nm using a microplate reader. Cellular viability was expressed as percentage of cell viability of treated cells relative to untreated controls.

#### ***6. Protein Target Prediction by PharmMapper***

PharmMapper (<http://59.78.96.61/pharmmapper>) was used to identify potential targets of TQ and TQ derivatives. 2D SDF files of TQ and the derivatives were entered for the reverse docking in PharmMapper. The structures were mapped against all the pharmacophore models of a repertoire of over 2200 human targets built from TargetBank, BindingDB, DrugBank. During the procedure, 300 conformations were generated. The best mapping poses of the TQ and TQ derivatives were listed by best-fitted hits.

#### ***7. Systems Biology***

VENNY (Venn's diagrams drawing tool) was used to determine the common targets between TQ and the derivatives. Classification of the genes common to all TQ

derivatives according to their biological processes, protein classes and molecular functions was done by PANTHER bioinformatics software (Protein ANalysis THrough Evolutionary Relationships). The pathway and interactions map was constructed in STRING (Search Tool for the Retrieval of Interacting Genes/Proteins). VENNY, PANTHER and STRING are freely available servers at the following addresses:

<http://bioinfogp.cnb.csic.es/tools/venny/>

<http://pantherdb.org/>

[http://string-db.org/newstring\\_cgi/show\\_input\\_page.pl](http://string-db.org/newstring_cgi/show_input_page.pl)

## **8. Statistical Analysis**

To determine the statistical significance between two samples, Two-sample t-test was used (Microsoft Office Excel). To determine the statistical significance between multiple samples, one way analysis of variance test (ANOVA) was used. Statistical significance was claimed when the p-value was  $< 0.05$ .

## **D. Results**

### ***1. TQ Pyrimidines Hydrazides Derivatives Synthesis***

The synthesis of TQ derivatives was performed in three steps which are outlined in Figure 30. First, reaction of uracil (1a), thymine (1b) and cytosine (1c) with ethyl acrylate allowed the formation of the corresponding pyrimidine esters 2a (uracil TQ intermediates), 2b (thymine TQ intermediates) and 2c (cytosine TQ intermediates), respectively. Hydrazinolysis converted these compounds into 1-(2-hydrazidoethyl)

uracil (3a), 1-(2-hydrazidoethyl) thymine (3b), and 1-(2-hydrazidoethyl) cytosine (3c), respectively. Finally, coupling of the intermediates 3a, 3b and 3c with TQ was required for the formation of the TQ pyrimidine hydrazides derivatives 4a (uracil TQ derivatives), 4b (thymine TQ derivatives) and 4c (cytosine TQ derivatives) as shown in Figure 30.

The structures of the final compounds referred to in the text as uracil TQ (U-TQ), thymine TQ (T-TQ) and cytosine TQ (C-TQ) are shown in Figure 31. U-TQ, T-TQ and C-TQ had molecular weights of 344.37 g/mol, 358.39 g/mol and 343 g/mol, respectively.

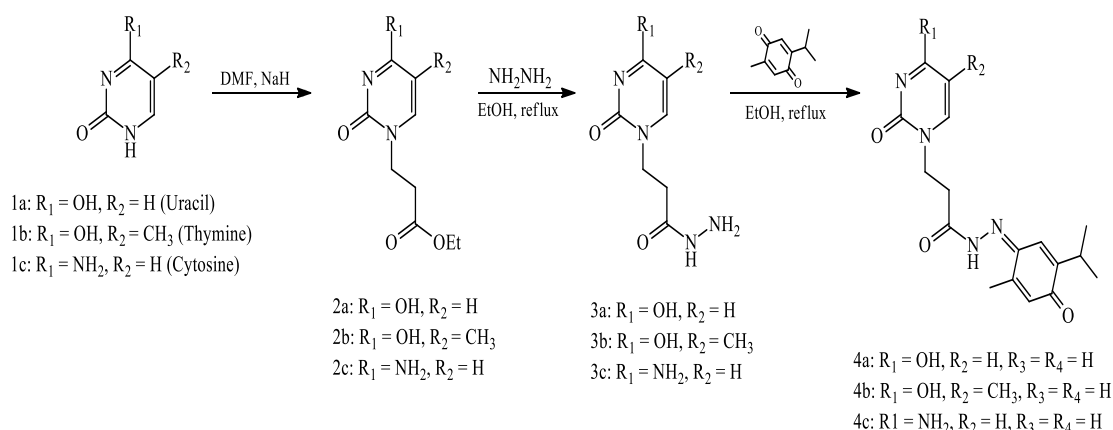
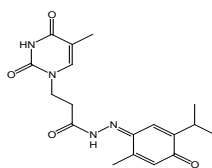


**Figure 30. Synthesis of TQ derivatives.** Pyrimidines 1a, 1b and 1c were subjected to a Michael-type reaction to form uracil ester (2a), thymine ester (2b) and cytosine ester (2c). Hydrazinolysis of the esters was used to form 1-(2-hydrazidoethyl) uracil (3a), 1-(2-hydrazidoethyl) thymine (3b) and 1-(2-hydrazidoethyl) cytosine (3c) intermediates. The last step consisted of coupling TQ with 3a, 3b and 3c to form TQ uracil hydrazides (4a), TQ thymine hydrazides (4b) and TQ cytosine hydrazides (4c).

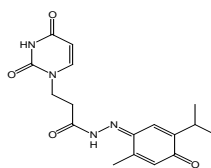


**Thymine thymoquinone**



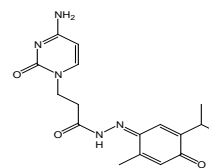
$C_{18}H_{22}N_4O_4$   
Mw: 358.39 g/mol

**Uracil thymoquinone**



$C_{17}H_{20}N_4O_4$   
Mw: 344.37 g/mol

**Cytosine thymoquinone**



$C_{17}H_{21}N_5O_3$   
Mw: 343 g/mol

**Figure 31. Representation of TQ derivatives structures and molecular weights.** TQ uracil hydrazides (4a), TQ thymine hydrazides (4b) and TQ cytosine hydrazides (4c) are referred to as thymine thymoquinone (T-TQ), uracil thymoquinone (U-TQ), and cytosine thymoquinone (C-TQ).

## ***2. TQ Derivatives Enhance TQ's Anticancer Potential***

To assess the anticancer potential of TQ derivatives, MCF-7 and MDA-MB-231 breast cancer cells were treated for 24 h with 10  $\mu$ M TQ or the derivatives. As shown in Figure 32, there was no effect on the viability of both cancer cell lines in response to treatment with TQ. However, treatment with the derivatives significantly reduced cell viability by up to 20-25% as compared to the untreated control.

## ***3. Protein Target Prediction of TQ and TQ derivatives***

To understand the difference between TQ and TQ derivatives, we sought to screen for the molecular targets which interact with each compound. PharmMapper, a web server designed for drug discovery and development, was used for ligand-protein inverse docking target prediction. PharmMapper enabled the extraction of TQ and TQ derivatives pharmacophores. All ligands-pharmacophore alignment models were accessible for visualization in 3D interactive mode. A ranked list of possible binding receptors was obtained for the top 300 molecules in descending order of fit score. Upon

examination, we noted that BSA was one of the top hits obtained for TQ and among the low hits for TQ derivatives. Furthermore, H-Ras was identified as top hit target for all TQ derivatives but not for TQ.

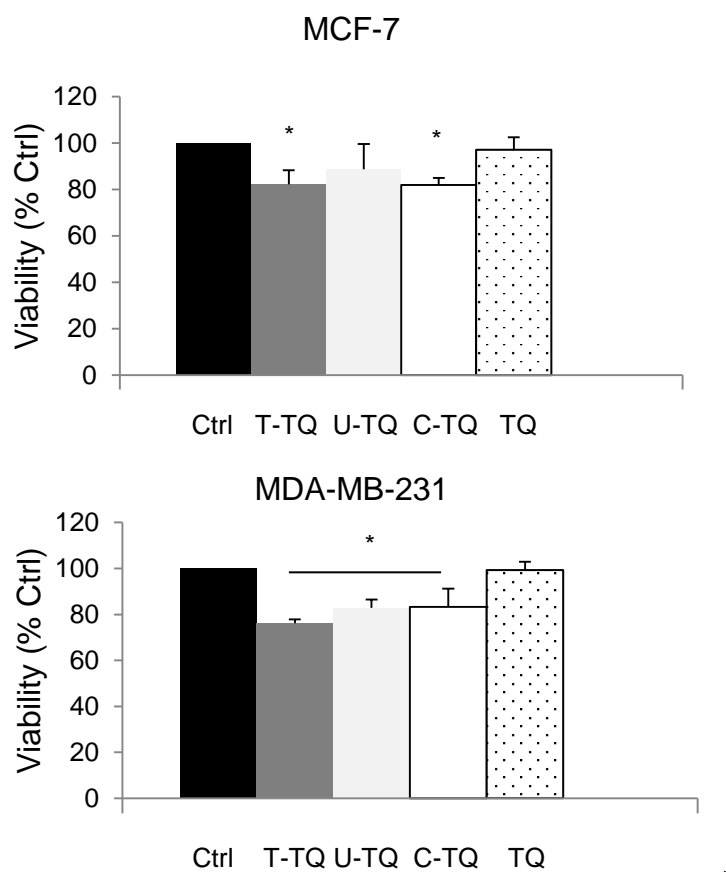


**Figure 32. TQ Pyrimidine Hydrazides Derivatives Enhance TQ’s Anticancer Potential.** The viability of MCF-7 and MDA-MB-231 breast cancer cells was determined in the presence of 10  $\mu$ M TQ or TQ derivatives. MTT viability assay was performed 24 h post-treatment and the values were normalized to the control. Each condition was done in triplicate and the experiment was repeated twice. The error bars represent the standard error. \* indicates  $p < 0.05$  with respect to the control.

Table 3 presents the top ten disease associated targets for each compound. As the results show, the top targets which bind TQ and TQ derivatives are implicated in a

variety of diseases. However, among TQ derivatives only, the top ten disease-related targets included targets implicated in human acute lymphocytic leukemia (Neprilysin) and T-cell acute lymphoblastic leukemia (IL-2). Furthermore, Table 3 shows the aldose reductase as a common target to all compounds. However, the nine remaining top targets of TQ were different from those obtained for the TQ derivatives. In total, TQ derivatives shared six common targets among each other including the aldose reductase, H-Ras, neprilysin (NEP), leukocyte elastase, renin and IL-2.

**Table 3: Classification of the Top 10 Disease-Related Targets for TQ and TQ Derivatives.** The Top 10 Disease-Related Targets were obtained by PharmMapper.

TQ		T-TQ	
Target	Disease	Target	Disease
Fibroblast growth factor receptor	Pfeiffer syndrome	H-Ras	Costello syndrome
Serum Albumin	Dysalbuminemic hyperthyroxinemia	Aldose reductase	In diabetes and galactosemia
Vitamin D3 Receptor	Type IIA rickets	Prothrombin	Dystrothrombenemia
Aldose Reductase	In diabetes and galactosemia	Neprilysin	Human acute lymphocytic leukemia
Androgen Receptor	Androgenetic alopecia	Cathepsin K	Pycnodystostosis
Prothrombin	Dysprothrombinemia	Interleukin 2	T-cell acute lymphoblastic leukemia
cAMP-specific 3,5-cyclic phosphodiesterase 4D	Susceptibility to stroke	Leukocyte elastase	Cyclic hematopoiesis
Carbonic anhydrase	Osteopetrosis type 3	Corticosteroid 11-beta-dehydrogenase isozyme 1	Cortisone reductase deficiency
Glucocorticoid receptor	Glucocorticoid resistance	Renin	Renal tubular dysgenesis

Complement factor D	Predisposition to invasive meningococcal disease	Tyrosine-protein kinase ZAP-70	Selective T-cell defect
C-TQ		U-TQ	
Target	Disease	Target	Disease
Aldose reductase	In diabetes and galactosemia	Aldose reductase	In diabetes and galactosemia
H-Ras	Costello syndrome	H-Ras	Costello syndrome
Neprilysin	Human acute lymphocytic leukemia	Prothrombin	Dystrothrombenemia
Leukocyte elastase	Cyclic hematopoiesis	Leukocyte elastase	Cyclic hematopoiesis
Vitamin D3 receptor	Type IIA rickets	Neprilysin	Human acute lymphocytic leukemia
Renin	Renal tubular dysgenesis	Renin	Renal tubular dysgenesis
Mitogen activated protein kinase 10	Epileptic encephalopathy Lennox-Gastaut type	Uridine 5-monophosphate synthase	Hereditary orotic aciduria
Retinol-binding protein 4	Retinol binding protein deficiency – Night vision problems	Interleukin 2	T-cell acute lymphoblastic leukemia
Interleukin 2	T-cell acute lymphoblastic leukemia	Carbonic anhydrase 2	Osteoporosis type 3
Mast/Stem cell growth factor receptor	Piebaldism	Corticosteroid 11-beta-dehydrogenase isozyme 1	Cortisone reductase deficiency

Next, Venn's diagram was used to compare the similarities and differences between all identified targets (Figure 33). Approximately 23% (48 proteins) of all targets identified were common to all ligands. In contrast, 23% of all targets were common to all TQ derivatives (excluding TQ) among which the top hit target H-Ras implicated in carcinogenesis was identified. Similarly, 6% (13 proteins) of the targets were exclusive to TQ only among which the NQO1 protein. Both BSA and NQO1

proteins, responsible for resistance to TQ were detected by this approach among the top TQ targets but not among TQ derivatives targets (NQO1), or among the low hits for TQ derivatives targets (BSA).

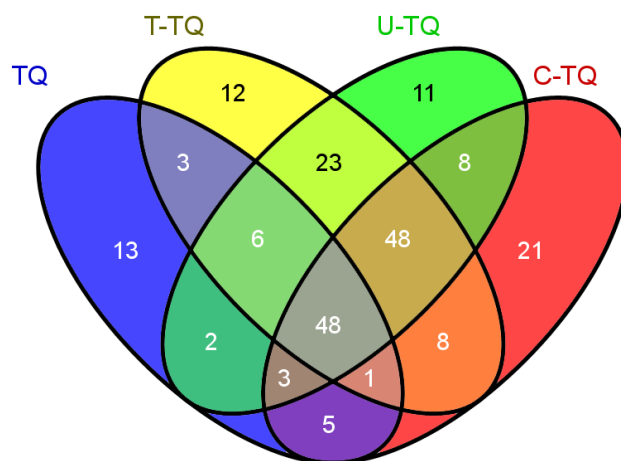


**Figure 33: Common Targets among the Different Compounds.** All Uniplot identifications names of obtained by PharmMapper for each compound, were used generate the Venn's diagram. The numbers in the diagram represent the number of common and unique targets to TQ, T-TQ, C-TQ and U-TQ compounds.

#### 4. Targets Ontology

Using bioinformatics tools, we explored if the targets obtained by reverse docking approach could pinpoint specific functions or pathways differentially modulated by TQ derivatives as compared to TQ. Functional analysis was done by the Protein ANalysis THrough Evolutionary Relationships (PANTHER) bioinformatics software. Targets ontology analysis provided insights with regards to the biological processes, the protein classes and the molecular functions of TQ derivatives common targets. As presented in the pie charts, a number of targets was involved in biogenesis (36%) apoptosis (6%), regulation processes, localization (10%), metabolism and

adhesion (Figure 34). Examples of molecules involved in apoptosis include transforming growth factor beta TGF- $\beta$ , serine/threonine protein kinase 1 (PIM1), death associated protein kinase (DAPK1) and EGFR. Regulator of metabolic processes such as adenosine kinase (ADK), cytochrome P450, histidine triad nucleotide binding protein (HINT1), and NEP. These targets comprised of hydrolases, proteases, phosphatases, kinases, oxidoreductases, cytoskeletal proteins, receptors and enzymes (Figure 35). The prominent molecular function of TQ derivatives common targets was catalytic activity (53%), followed by binding activities (19%) and translation regulator activity (6%) (Figure 36). Cancer-related protein with catalytic activity include GTPase H-Ras, lymphocyte-specific kinase Lck, DAPK1, Ras-related protein (Rap-2A) and mitogen activated protein kinase kinase 1 (MP2K1). Binding proteins included IL-2, TGF- $\beta$ , and nuclear receptor ROR-alpha. Eukaryotic translation initiation factor 4E EIF4E involved in translation regulation was also a potential target common to all TQ derivatives. Among these targets, the cancer-related key players were Src, MAPK, MMPs, EIF4E, EGFR, TGFR, Lck, Hck, CHEK, H-Ras, IL, PDPK1 and KDR, among others. TQ only targets, TQ derivatives common targets and TQ and TQ derivatives common targets had similar biological and molecular functions as seen in Table 4. However, protein classes differed among these targets whereby TQ only targets comprised mostly of receptors, TQ and TQ derivatives common targets of hydrolases, and TQ derivatives common targets of hydrolases and transferases, respectively as summarized in Table 4.

### Biological Processes of Targets Common to all TQ derivatives

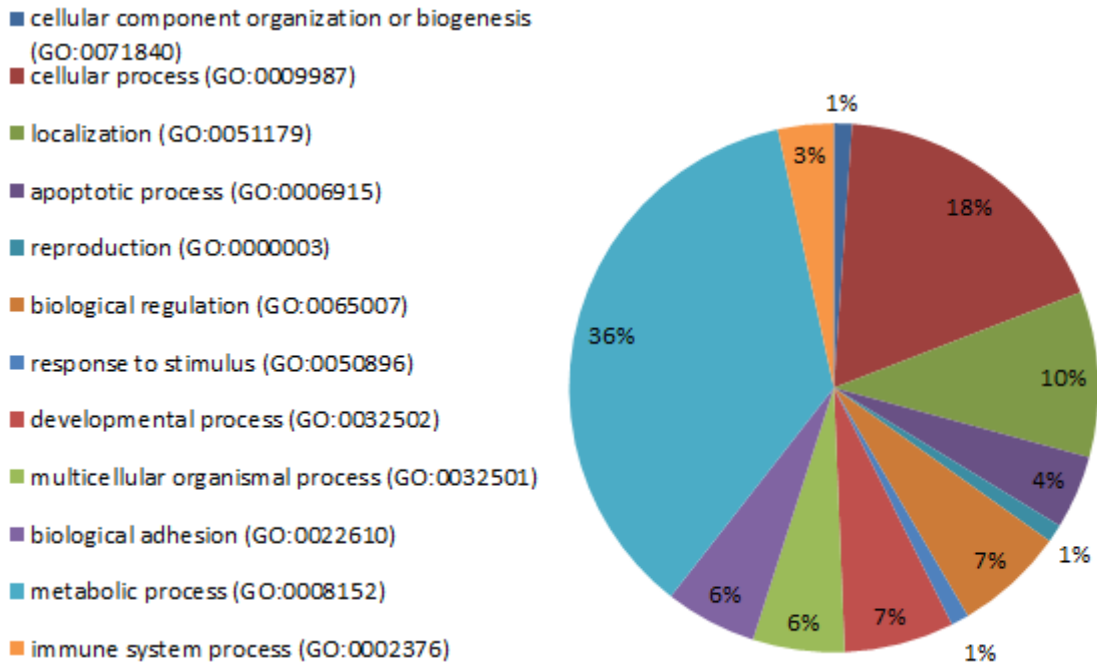


**Figure 34: Biological Processes of TQ Derivatives Common Targets.** Gene Ontology Analysis of TQ derivatives was performed in PANTHER. The percentages listed in the pie chart are calculated as the number of proteins associated with a particular biological process normalized to the total number of proteins.

### Protein Classes of Targets Common to all TQ derivatives

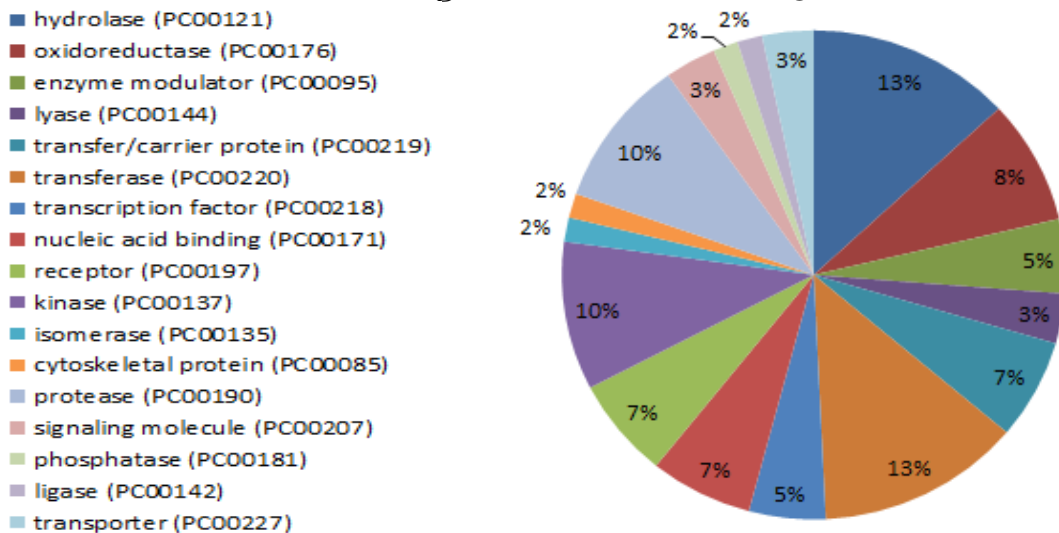


**Figure 35: Protein Classes of TQ Derivatives Common Targets.** Gene Ontology Analysis of TQ derivatives was performed in PANTHER. The percentages listed in the

pie chart are calculated as the number of proteins belonging to a particular protein class normalized to the total number of proteins.

### Molecular Functions of Targets Common to All Derivatives

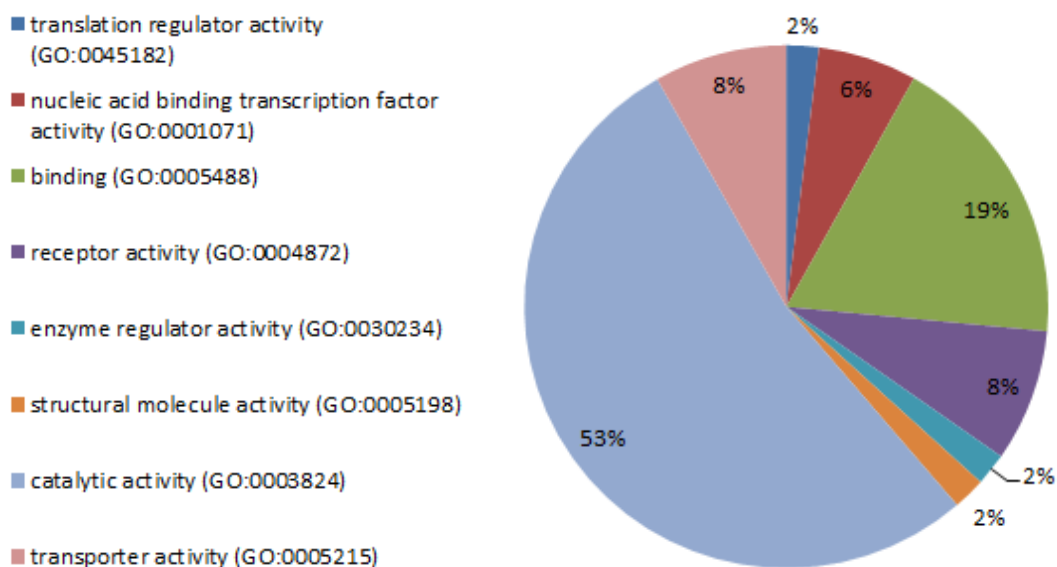


**Figure 36: Molecular Functions of TQ Derivatives Common Targets.** Gene Ontology Analysis of TQ derivatives was performed in PANTHER. The percentages listed in the pie chart are calculated as the number of proteins associated with a particular molecular function normalized to the total number of proteins.

**Table 4: Comparative Gene Ontology Analysis.** Gene Ontology of TQ derivatives common targets was performed in PANTHER. The percentages listed are calculated as the number of proteins associated with a particular category normalized to the total number of proteins

	Molecular Function	Biological Processes	Protein Class
<b>TQ Targets Only</b>	Catalytic Activity (54%)	Metabolic Processes (77%)	Receptor (38.5%)
<b>Common TQ and TQ Derivatives</b>	Catalytic Activity (62%)	Metabolic Processes (39%)	Hydrolase (17%)
<b>Common TQ Derivatives Targets</b>	Catalytic Activity (53%)	Metabolic Processes (36%)	Hydrolase (13%) Transferase (13%)



Finally, STRING database was used to search for possible protein-protein interactions and regulators of TQ derivatives common targets and construct pathways and interaction maps of these proteins. The global interaction proteome network of these key regulators is presented in Figure 37. By this approach, we found that proteins belonging to different structural and functional families involved in processes such as angiogenesis, inflammation, apoptosis and proliferation are enriched. This further shows that TQ derivatives common targets are key proteins in the Ras, insulin, EGFR, TGF- $\beta$ , and MAPK signaling pathways.

## **E. Discussion**

In this study, the synthesis of TQ pyrimidine derivatives, the preliminary bioevaluation as well as the identification of the binding targets by inverse docking were described. The results show that TQ pyrimidine derivatives are active and reveal key molecules differentially targeted by TQ and TQ derivatives.

*In silico* studies have greatly contributed to drug discovery and drug development and are systemically used for identification of drug targets (Caldwell, 2015). To our knowledge however, this is the first study to investigate the anticancer potential of TQ pyrimidine derivatives as well as carry out inverse docking to identify therapeutic targets of TQ and the derivatives. Inverse docking is a relatively new technique for drug repurposing, available for academic and industrial researches by several servers including CPI, GOLD, FlexX, Tarfisdock and PharmMapper (Kamper et al., 2006; Hui-fang et al., 2010; Liu et al., 2010). PharmMapper inverse docking

approach is based on the pharmacophore repositioning which allows the spatial re-arrangement of ligands against the targets of a protein database (Liu et al., 2010).

Disease information indicate that TQ derivatives targets are involved in acute lymphocytic leukemia and acute T-cell lymphoblastic leukemia. TQ has been previously tested against leukemia and shown to play a role in the treatment of leukemia as well as upregulation of IL-2 production among others (Banerjee et al., 2010b; Schneider-Stock et al., 2014; Woo et al., 2012).

Thorough analysis further revealed the protein classes as well as biological and molecular functions of TQ derivatives targets and we were able to map the pathways in which these proteins are involved. According to our preliminary results, H-Ras appears to be the potential disease-related target as well as anticancer target of TQ derivatives (Table 3). The pharmacophore models aligned to molecule features of TQ derivatives further supported the inverse docking results (Data not shown). The Ras GTPase proteins family consists of H-Ras, N-Ras and K-Ras proteins. The main function of these proteins is to translate the extracellular responses into biological signals critical for proliferation, differentiation, and survival (Adjei, 2001; Lo, 2010; Takashima and Faller, 2013). H-Ras regulates key signaling pathways which are often mutated in cancers, specifically the MAPK pathway (Lo, 2010; Takashima and Faller, 2013). Many potent anticancer agents including quinones, modulate the H-Ras signaling pathway and downstream targets to inhibit tumor growth and viability (Adjei, 2001; Cavalieri and Rogan, 2004; Lo, 2010; Takashima and Faller, 2013). In addition, mutations which abrogate H-Ras can cause the Costello syndrome, a rare disorder characterized by coarse facial appearance, disrupted intellectual abilities as well as predisposition to

cancers (Schubbert et al., 2007). There are no reports to date investigating the effects of TQ or TQ derivatives on this disease.

In addition to H-Ras, several other targets differentially bound TQ or TQ derivatives. TQ derivatives synthesis for instance resulted in the abrogation of binding to BSA and NQO1 proteins. Binding to BSA has been shown to reduce TQ's anticancer activity while cells expressing NQO1 have exhibited resistance to treatment with TQ (El-Najjar et al., 2011b; Sutton et al., 2012). The enhancement of anticancer potential of TQ pyrimidine derivatives might thus result in part from the disruption of binding of TQ to these two inhibitory targets.

Systems biology and targets ontology analysis have also identified a number of TQ derivatives targets implicated in cancer modulation. Although these TQ derivatives common targets and partners were not obtained by inverse docking in the top 300 binding targets for TQ, literature indicates that TQ is capable of modulating the expression levels of many of these molecules. For instance, TQ has been shown to deregulate the phosphorylation or expression levels of 4E EIF4E, Src, MAPK, MMPs, EGFR, TGFR, Lck, cytochrome P450, UHRF1 and PDEA1 among others (Abusnina et al., 2011; Alhosin et al., 2010; El-Najjar et al., 2010; Rajput et al., 2013a; Schneider-Stock et al., 2014; Sethi et al., 2008). Interestingly, Lck is another leukemia-related target of TQ derivatives. This tyrosine kinase belongs to the Src family and expressed in T cells and natural killers (Zamoyska et al., 2003).

In conclusion, the comparative analysis of TQ and TQ derivatives targets presented here provide a guide for further biological and biochemical investigations which can greatly contribute to the understanding of cell response to treatment with these compounds. Further testing however is still warranted for the validation of TQ and

TQ derivatives targets as well as the mechanisms underlying the anticancer activity of each structure.

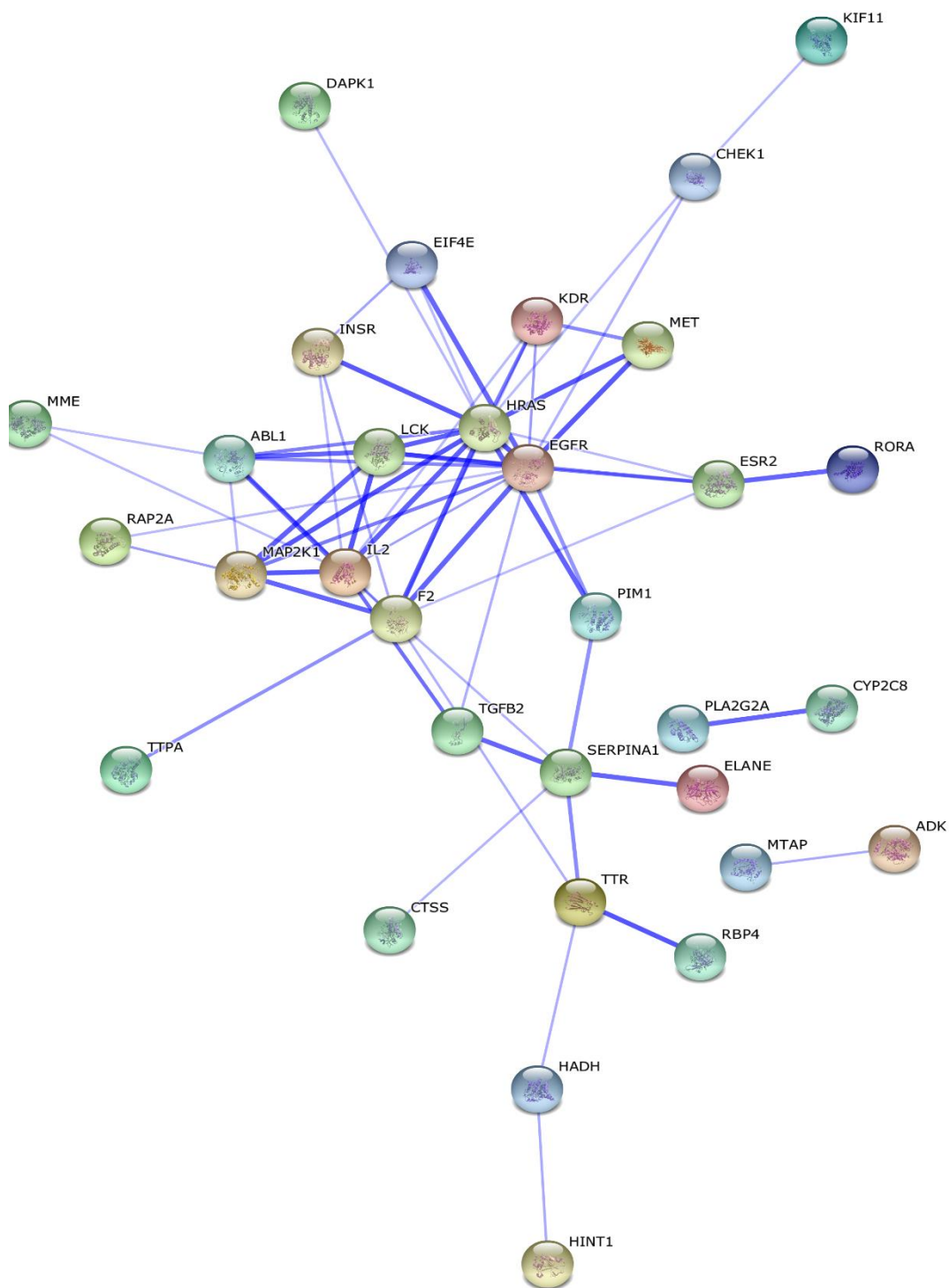


**Figure 37: Pathways and Networks Modulated by TQ derivatives Common Targets.** Global pathway analysis of the 48 potential targets common to TQ derivatives was performed using STRING database. The network nodes are proteins whose final position in the network is computed by minimization of the energy of the system. The thickness of the lines indicate the degree of confidence prediction of the interaction.

## CHAPTER V

### DISCUSSION AND PERSPECTIVES

The main aim of this thesis was to set up the grounds for testing TQ-NP in combination therapy with Dox. NP in combination therapy are designed to enable the use of lower doses of a drug as well as reduce drug exposure to the normal tissues by targeted delivery (Hu et al., 2010). In fact, several NP in combination therapies have reached the clinic. For instance, the CPX351 formulation which consists of cytarabine and daunorubicin (5:1) have reached phase III clinical trials for the treatment of acute myeloid leukemia after showing enhanced therapeutic effect and lower toxicity than the free drug combinations (Ma et al., 2013). Similarly, CPX1 formulation consisting of irinotecan and floxuridine have reached phase II clinical trials for the treatment of colorectal cancer (Ma et al., 2013). TQ and Dox have been selected for several reasons. First, both drugs are commonly used in the treatment of various forms of cancers, including leukemia and breast cancer, the main focus of our studies. Second, Dox dosage is limited by its toxicity to the heart and liver, among other side effects (Octavia et al., 2012). Moreover, TQ has been shown to reduce Dox side effects *in vivo* (al-Shabanah et al., 1998; Badary et al., 2000; Nagi and Mansour, 2000).

Our preliminary results show that the TQ and Dox combination treatment is active against ATL and that cell death is enhanced in comparison to treatment with TQ or Dox alone. The effects of the combination on ROS, the mitochondria as well as key molecular targets however were similar to those observed in response to treatment with TQ alone. The Dox doses used for combination treatment induce G2/M arrest but do not

have a significant effect on ROS, mitochondrial integrity or the regulation of molecular targets. Several experiments do however need more replicates and independent repeats to confirm these findings. Nevertheless, in all experiments, the combination anticancer potential is enhanced as compared to treatment with Dox alone. Moreover, the degree of inhibition of cell viability by the combination treatment was very similar to that observed in cells treated with high doses of Dox (up to two folds higher than the dose used for combination with TQ). The effect of the high doses of Dox on apoptosis, ROS, mitochondrial integrity, the expression levels of key targets and cytotoxicity against normal PBMCs or cardiomyocytes were not carried out to allow further comparison. The cytotoxicity of the combination treatment against normal PBMCs or cardiomyocytes has not been investigated either in this study. In literature however, both TQ and Dox used at the indicated concentrations are not significantly toxic to normal cells (Brown et al., 2014; Dergarabetian et al., 2013; Georgakis et al., 2005). In parallel, some studies have reported that pre-exposure with TQ prior to treatment with a clinically approved drug is more efficient than simultaneous treatment with TQ. For instance, pre-exposure with TQ prior to treatment with topotecan significantly enhances the anticancer potential the drugs used at non-toxic doses against acute myelogenous leukemia (Khalife et al., 2014). This has not been investigated in our study but is being considered for future projects.

In addition, TQ is known to be active against breast cancer including Dox resistant MCF-7 cells. TQ has also been tested in combination with Dox against the MCF-7 cell line. The results indicate that 20  $\mu$ M of TQ in combination treatment with 2  $\mu$ M of Dox for 24 h enhance the anticancer potential of both drugs by approximately 2.6 folds in MCF-7 breast cancer cells (Woo et al., 2011). Breast cancer thus appeared to be

a good model for testing TQ-NP in combination treatment with Dox. MCF-7 and MDA-MB-231 breast cancer cells were chosen to test the anticancer potential and NP uptake and efficiency based on the differences in the metastatic and endocytic potential of the two cell lines.

We have shown that TQ-NP enhance TQ activity in MCF-7 and not in MDA-MB-231 breast cancer cells. However, our findings also indicate that MCF-7 cells take up less NP than MDA-MB-231 cells. This suggests that the mechanism underlying enhanced activity could be related to the genomic profile of the cell line. To this aim, the mechanism of cell death will be investigated in MCF-7 versus MDA-MB-231 cells. We also plan to test the anticancer potential of TQ-NP against a panel of luminal A and triple-negative tumors from patients to determine the range of activity of TQ NP.

To investigate the uptake of TQ-NP we had to choose between three main tools commonly used for investigating endocytosis: 1) Using Pharmacological inhibitors of endocytosis 2) Using markers of different endocytic compartments and 3) Inhibition of the expression of key proteins specific to the pathways of endocytosis (generally achieved by siRNA) (Iversen et al., 2011). Many inhibitors are available for testing the route endocytosis. However, the specificity of the inhibitors to one mechanism of uptake remains controversial. For instance, cholesterol binding agents, filipin and nystatin are commonly used to check for the involvement of clathrin-independent and cholesterol-dependent entry routes (Doherty and McMahon, 2009; Grimmer et al., 2002; Iversen et al., 2011; Sandvig et al., 2008). However, cholesterol is involved in caveolin-mediated endocytosis, as well as clathrin-mediated endocytosis (Doherty and McMahon, 2009; Grimmer et al., 2002; Iversen et al., 2011; Sandvig et al., 2008). Genistein on the other hand, is an inhibitor of several tyrosine kinases among which

enzymes that are required for caveolae pinching (Iversen et al., 2011; Pelkmans et al., 2002). Genistein is used for assessing the involvement of caveolin-mediated uptake although the mechanism of action of genistein does not make it selective for caveolin-mediated endocytosis pathway only. Many tyrosine kinases are involved in the phosphorylation of cargo which are taken up by CME (Iversen et al., 2011; Zhang and Monteiro-Riviere, 2009). For instance, phosphorylation of EGF is critical for the accumulation and uptake of this molecule by clathrin-coated pits (Iversen et al., 2011; Vercauteren et al., 2010). Similarly, amiloride specificity to the macropinocytosis route can be questioned. In fact, amiloride lowers the cytosolic pH close to the membrane disrupting thus the Rac1 and cdc42 signaling (Sabharanjak et al., 2002; Vercauteren et al., 2010). Given the broad spectrum of actions of these molecules, the inhibition of uptake is prone to misinterpretation. Moreover, literature suggests that the efficacy of many inhibitors of endocytosis depends on the cell line (Kumari et al., 2010; Vercauteren et al., 2010). This is the case for example for chlorpromazine, a RhoGTPase inhibitor used to study CME although many other inhibitors suffer from the same limitation (Iversen et al., 2011; Kumari et al., 2010).

Determining the mechanism of endocytosis by colocalization studies of NP with intracellular organelles can be challenging as well. False positives can occur because of the low resolution of fluorescent microscopes. Concluding whether the NP are taken up by the cells and colocalize or whether the NP are on the surface becomes difficult. Even colocalization measurements can be misleading if two structures are close enough and more so when the fluorescent markers display large and diffuse fluorescent signals (Balasubramanian et al., 2007; Iversen et al., 2011). Tomographic scans using confocal microscopy can however indicate whether NP are internalized or



are instead localized on the cell membrane. But, high resolution electron microscopy still need to be used for determining the colocalization of NP with organelles more accurately (Iversen et al., 2011).

Finally, using siRNA has also some limitations. For instance, results obtained after silencing of specific proteins might be linked to unwanted signaling changes in the cells and not directly linked to endocytosis (Iversen et al., 2011). Moreover, silencing of proteins involved in a specific route of endocytosis can affect or upregulate the signaling of other endocytic pathways (Damke et al., 1995; Iversen et al., 2011).

Taking into consideration all these limitations, we chose to combine two methods to consolidate the findings and interpret the results with more confidence. In fact, Dox NP uptake in the literature has been investigated using one or more of these methods separately or simultaneously. For instance, inhibitors and fluorescence microscopy were used simultaneously to show clathrin and caveolin mediated uptake of Dox NP and Dox conjugates and hence we based our studies accordingly (Cheng et al., 2015; Cui et al., 2015; Gautier et al., 2015; Hu et al., 2016).

Our uptake studies are the first to illustrate the dynamics and uptake mechanism of TQ-NP by the cells. We have combined two methods for the investigation of endocytosis. The doses of inhibitors used conforms to the ones described in literature. We have also shown a dose-dependent response to treatment of MCF-7 and MDA-MB-231 breast cancer cells with genistein (data not shown). Our results however suggest that endocytosis is involved to a small extent in the uptake of TQ-NP (around 20-30%). We think that this observation can be linked to the inhibitor dose used or it can stem from the drug release kinetics from the PS-PEO polymer. In fact, drug release kinetics from PS-PEO NP have been recently investigated *in vitro* and *in vivo*. Using a fluorescence

resonance energy transfer (FRET) imaging approach (Zou et al., 2013), one group showed a rapid release of donor and acceptor dyes from PS-PEO NP as evidenced by the high FRET signals in membranes and subcellular endocytic organelles in MDA-MB-231 cells. *In vivo*, the release half-life of the cargo was 9.2 min, with no significant change in FRET signal noted when the NP were incubated with cell culture medium or plasma. This study highlighted the role of cell membranes in triggering of the release of cargo from the PS-PEO NP and also showed that the release to the membrane can be slowed or eliminated by increasing the hydrophobicity of the NP core (Zou et al., 2013).

Another group however have radiolabeled PS-PEO NP by incorporation of  $^{111}\text{In}$ -tropolone in the NP (Laan et al., 2016) and showed that the NP are stable for two days in saline, with 95% of the radiolabel retained inside the NP. In contrast, a minor rapid loss of radiolabel occurs when the NP are exposed to the serum the first 24 h, followed by a negligible release the following day whereby 81% radiolabel is still retained in the NP. Dynamic single photon emission computed tomography images in mice *in vivo*, further showed that the radiolabel is detectable in blood and the heart chamber the first 4 h while most radioactivity accumulated in the liver and spleen by 24 h. Biodistribution analysis further confirmed the uptake of the NP by the spleen, the liver and the stomach and that the blood still retained NP in circulation (Laan et al., 2016).

In light of these two studies, it can be inferred that a part of TQ-NP might be taken up by kiss and run and a part are being internalized through the endocytic machinery. Further increasing of the hydrophobicity of TQ-NP can be attempted in the future to investigate the effect on the release of the drug from the NP and the amount of NP which are taken up by endocytosis.

An illustration of the model we proposed for TQ-NP internalization and cargo delivery in the cytoplasm as well as the nucleus of the cells is presented in Figure 38. *In vivo* studies to assess the potential of the NP in an animal model of breast cancer are still planned. We also aim to investigate the delivery and uptake of NP *in vivo*. Labeled NP will be used to trace the biodistribution of the NP and assess the targeting of the tumor tissue.

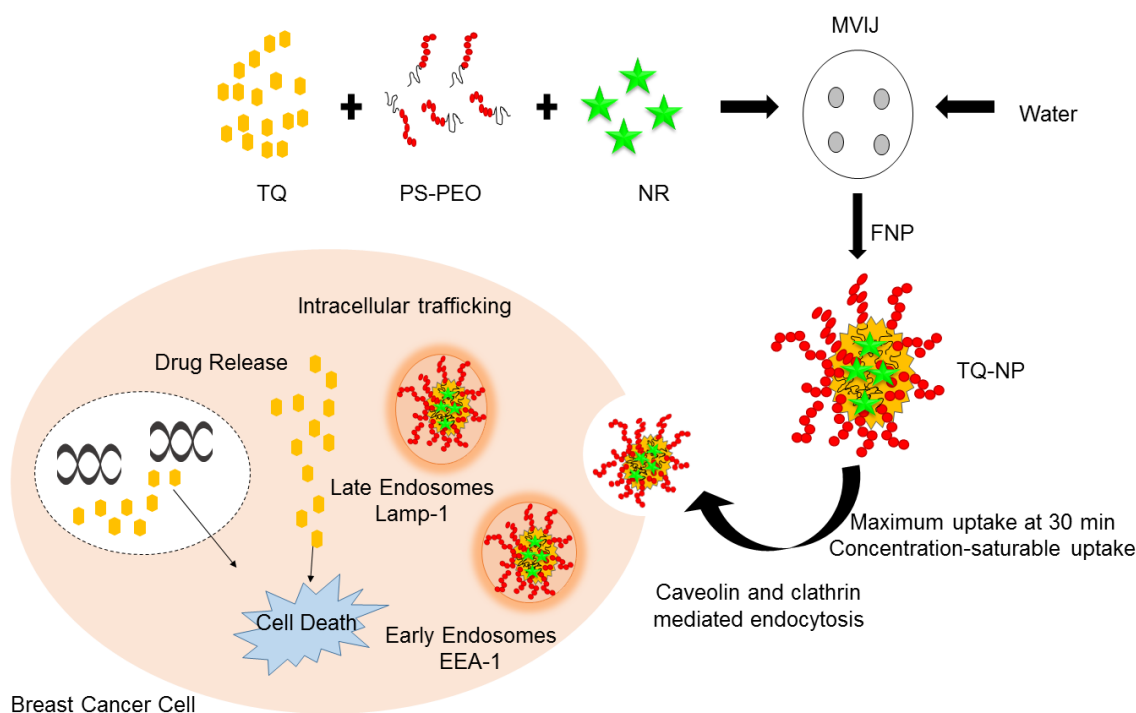


**Figure 38. Model for TQ-NP Uptake.** FNP is used for the preparation of NR-loaded TQ-NP. Fluorescent NP can be internalized by caveolin-mediated endocytosis in MCF-7 and caveolin and clathrin-mediated endocytosis in MDA-MB-231 breast cancer cells. After intake, the NP are trafficked into the endosomes, the lysosomes and manage to reach the cytosol and the nucleus where TQ can potentially exert its activity.

Finally, the derivatives study describes the synthesis of new active TQ pyrimidine derivatives. The preliminary results need further validation *in vitro*, to test

TQ derivatives binding to H-Ras by calorimetric and binding assays or the potential modulation of the expression levels of the protein by Western blot. Calorimetric and binding assays have also to be performed to compare TQ and TQ derivatives binding to the BSA and NQO1 proteins which inhibit TQ activity. TQ derivatives can also be assessed in combination treatment with Dox or formulated in NP.

In summary, the projects presented in this manuscript highlight the importance of enhancing TQ's activity by encapsulating the molecule in NP, conjugating it to active classes or combining it with FDA approved drugs. For each method of drug enhancement we discussed the advantages with regards to TQ and the novelty of the work. TQ-NP, TQ derivatives and TQ combination show enhanced activity in comparison to TQ when tested against different cancer models. Combining TQ further provides means for using sub-toxic doses of Dox. Similarly, the biocomputational work on TQ derivatives suggests that TQ and TQ derivatives differentially modulate key targets in carcinogenesis and pinpoints to specific pathways that might account for the different compounds mechanisms of action. Our future work now aim at using these strategies simultaneously, namely nanotechnology for targeted delivery of combination treatment and investigate the effects of such approach with regards to the anticancer potential of TQ.

## BIBLIOGRAPHY

- Abdel-Wahab WM (2014) Thymoquinone attenuates toxicity and oxidative stress induced by bisphenol A in liver of male rats. *Pakistan journal of biological sciences : PJBS* **17**(11): 1152-1160.
- Abu-Dahab R, Odeh F, Ismail SI, Azzam H and Al Bawab A (2013) Preparation, characterization and antiproliferative activity of thymoquinone-beta-cyclodextrin self assembling nanoparticles. *Die Pharmazie* **68**(12): 939-944.
- Abusnina A, Alhosin M, Keravis T, Muller CD, Fuhrmann G, Bronner C and Lugnier C (2011) Down-regulation of cyclic nucleotide phosphodiesterase PDE1A is the key event of p73 and UHRF1 deregulation in thymoquinone-induced acute lymphoblastic leukemia cell apoptosis. *Cellular signalling* **23**(1): 152-160.
- Adjei AA (2001) Blocking oncogenic Ras signaling for cancer therapy. *Journal of the National Cancer Institute* **93**(14): 1062-1074.
- Agudelo D, Berube G and Tajmir-Riahi HA (2016) An overview on the delivery of antitumor drug doxorubicin by carrier proteins. *International journal of biological macromolecules*.
- Ahmad F, Baloch MK, Jamil M and Jeon YJ (2010) Characterization of polystyrene-b-poly(ethylene oxide) diblock copolymer and investigation of its micellization behavior in water. *Journal of Applied Polymer Science*: n/a-n/a.
- Ahmad I, Muneer KM, Tamimi IA, Chang ME, Ata MO and Yusuf N (2013) Thymoquinone suppresses metastasis of melanoma cells by inhibition of NLRP3 inflammasome. *Toxicology and applied pharmacology* **270**(1): 70-76.
- Akbulut M, Ginart P, Gindy ME, Theriault C, Chin KH, Soboyejo W and Prud'homme RK (2009) Generic Method of Preparing Multifunctional Fluorescent Nanoparticles Using Flash NanoPrecipitation. *Advanced Functional Materials* **19**(5): 718-725.
- Al-Ali A, Alkhawajah AA, Randhawa MA and Shaikh NA (2008) Oral and intraperitoneal LD50 of thymoquinone, an active principle of *Nigella sativa*, in mice and rats. *Journal of Ayub Medical College, Abbottabad : JAMC* **20**(2): 25-27.
- Al-Amri AM and Bamosa AO (2009) Phase I Safety and Clinical Activity Study of Thymoquinone in Patients with Advanced Refractory Malignant Disease. *Shiraz E-Med J* **10**(3): 107-111.
- al-Shabanah OA, Badary OA, Nagi MN, al-Gharably NM, al-Rikabi AC and al-Bekairi AM (1998) Thymoquinone protects against doxorubicin-induced cardiotoxicity without compromising its antitumor activity. *Journal of experimental & clinical cancer research : CR* **17**(2): 193-198.
- Alam S, Khan ZI, Mustafa G, Kumar M, Islam F, Bhatnagar A and Ahmad FJ (2012) Development and evaluation of thymoquinone-encapsulated chitosan nanoparticles for nose-to-brain targeting: a pharmacoscintigraphic study. *International journal of nanomedicine* **7**: 5705-5718.
- Alhosin M, Abusnina A, Achour M, Sharif T, Muller C, Peluso J, Chataigneau T, Lugnier C, Schini-Kerth VB, Bronner C and Fuhrmann G (2010) Induction of apoptosis

- by thymoquinone in lymphoblastic leukemia Jurkat cells is mediated by a p73-dependent pathway which targets the epigenetic integrator UHRF1. *Biochemical pharmacology* **79**(9): 1251-1260.
- Alhosin M, Ibrahim A, Boukhari A, Sharif T, Gies JP, Auger C and Schini-Kerth VB (2012) Anti-neoplastic agent thymoquinone induces degradation of alpha and beta tubulin proteins in human cancer cells without affecting their level in normal human fibroblasts. *Investigational new drugs* **30**(5): 1813-1819.
- Allouche J (2013) Synthesis of Organic and Bioorganic Nanoparticles: An Overview of the Preparation Methods. 27-74.
- Allred DC (2010) Ductal carcinoma in situ: terminology, classification, and natural history. *Journal of the National Cancer Institute Monographs* **2010**(41): 134-138.
- Angsutararux P, Luanpitpong S and Issaragrisil S (2015) Chemotherapy-Induced Cardiotoxicity: Overview of the Roles of Oxidative Stress. *Oxidative medicine and cellular longevity* **2015**: 795602.
- Anothaisintawee T, Wiratkapun C, Lerdsittichai P, Kasamesup V, Wongwaisayawan S, Srinakaran J, Hirunpat S, Woodtichartpreecha P, Boonlikit S, Teerawattananon Y and Thakkestian A (2013) Risk factors of breast cancer: a systematic review and meta-analysis. *Asia-Pacific journal of public health / Asia-Pacific Academic Consortium for Public Health* **25**(5): 368-387.
- Arafa el SA, Zhu Q, Shah ZI, Wani G, Barakat BM, Racoma I, El-Mahdy MA and Wani AA (2011) Thymoquinone up-regulates PTEN expression and induces apoptosis in doxorubicin-resistant human breast cancer cells. *Mutation research* **706**(1-2): 28-35.
- Attoub S, Sperandio O, Raza H, Arafat K, Al-Salam S, Al Sultan MA, Al Safi M, Takahashi T and Adem A (2013) Thymoquinone as an anticancer agent: evidence from inhibition of cancer cells viability and invasion in vitro and tumor growth in vivo. *Fundamental & clinical pharmacology* **27**(5): 557-569.
- Badary OA (1999) Thymoquinone attenuates ifosfamide-induced Fanconi syndrome in rats and enhances its antitumor activity in mice. *Journal of ethnopharmacology* **67**(2): 135-142.
- Badary OA, Abdel-Naim AB, Abdel-Wahab MH and Hamada FM (2000) The influence of thymoquinone on doxorubicin-induced hyperlipidemic nephropathy in rats. *Toxicology* **143**(3): 219-226.
- Badary OA, Nagi MN, al-Shabanah OA, al-Sawaf HA, al-Sohaibani MO and al-Bekairi AM (1997) Thymoquinone ameliorates the nephrotoxicity induced by cisplatin in rodents and potentiates its antitumor activity. *Canadian journal of physiology and pharmacology* **75**(12): 1356-1361.
- Badr G, Lefevre EA and Mohany M (2011) Thymoquinone inhibits the CXCL12-induced chemotaxis of multiple myeloma cells and increases their susceptibility to Fas-mediated apoptosis. *PloS one* **6**(9): e23741.
- Balasubramanian N, Scott DW, Castle JD, Casanova JE and Schwartz MA (2007) Arf6 and microtubules in adhesion-dependent trafficking of lipid rafts. *Nature cell biology* **9**(12): 1381-1391.
- Balzarini J (2000) Effect of antimetabolite drugs of nucleotide metabolism on the anti-human immunodeficiency virus activity of nucleoside reverse transcriptase inhibitors. *Pharmacology & therapeutics* **87**(2-3): 175-187.
- Banerjee S, Azmi AS, Padhye S, Singh MW, Baruah JB, Philip PA, Sarkar FH and Mohammad RM (2010a) Structure-activity studies on therapeutic potential of

- Thymoquinone analogs in pancreatic cancer. *Pharmaceutical research* **27**(6): 1146-1158.
- Banerjee S, Padhye S, Azmi A, Wang Z, Philip PA, Kucuk O, Sarkar FH and Mohammad RM (2010b) Review on molecular and therapeutic potential of thymoquinone in cancer. *Nutrition and cancer* **62**(7): 938-946.
- Bazarbachi A, Suarez F, Fields P and Hermine O (2011) How I treat adult T-cell leukemia/lymphoma. *Blood* **118**(7): 1736-1745.
- Bertos NR and Park M (2011) Breast cancer - one term, many entities? *The Journal of clinical investigation* **121**(10): 3789-3796.
- Bhattacharya S, Ahir M, Patra P, Mukherjee S, Ghosh S, Mazumdar M, Chattopadhyay S, Das T, Chattopadhyay D and Adhikary A (2015) PEGylated-thymoquinone-nanoparticle mediated retardation of breast cancer cell migration by deregulation of cytoskeletal actin polymerization through miR-34a. *Biomaterials* **51**: 91-107.
- Boutureira O, Matheu MI, Diaz Y and Castillon S (2013) Advances in the enantioselective synthesis of carbocyclic nucleosides. *Chemical Society reviews* **42**(12): 5056-5072.
- Brannon-Peppas L and Blanchette JO (2004) Nanoparticle and targeted systems for cancer therapy. *Advanced drug delivery reviews* **56**(11): 1649-1659.
- Breyer S, Effenberger K and Schobert R (2009) Effects of thymoquinone-fatty acid conjugates on cancer cells. *ChemMedChem* **4**(5): 761-768.
- Brown RK, Wilson G, Tucci MA and Benghuzzi HA (2014) The effects of thymoquinone and Doxorubicin on leukemia and cardiomyocyte cell lines. *Biomedical sciences instrumentation* **50**: 391-396.
- Cambon A, Rey-Rico A, Barbosa S, Soltero JF, Yeates SG, Brea J, Loza MI, Alvarez-Lorenzo C, Concheiro A, Taboada P and Mosquera V (2013) Poly(styrene oxide)-poly(ethylene oxide) block copolymers: From "classical" chemotherapeutic nanocarriers to active cell-response inducers. *Journal of controlled release : official journal of the Controlled Release Society* **167**(1): 68-75.
- Cavalieri EL and Rogan EG (2004) A unifying mechanism in the initiation of cancer and other diseases by catechol quinones. *Annals of the New York Academy of Sciences* **1028**: 247-257.
- Chehl N, Chipitsyna G, Gong Q, Yeo CJ and Arafat HA (2009) Anti-inflammatory effects of the *Nigella sativa* seed extract, thymoquinone, in pancreatic cancer cells. *HPB : the official journal of the International Hepato Pancreato Biliary Association* **11**(5): 373-381.
- Cheng L, Hu Q, Cheng L, Hu W, Xu M, Zhu Y, Zhang L and Chen D (2015) Construction and evaluation of PAMAM-DOX conjugates with superior tumor recognition and intracellular acid-triggered drug release properties. *Colloids and surfaces B, Biointerfaces* **136**: 37-45.
- Coleman MP, Quaresma M, Berrino F, Lutz J-M, De Angelis R, Capocaccia R, Baili P, Rachet B, Gatta G, Hakulinen T, Micheli A, Sant M, Weir HK, Elwood JM, Tsukuma H, Koifman S, e Silva GA, Francisci S, Santaquilani M, Verdecchia A, Storm HH and Young JL (2008) Cancer survival in five continents: a worldwide population-based study (CONCORD). *The Lancet Oncology* **9**(8): 730-756.
- Cook LB, Elemans M, Rowan AG and Asquith B (2013) HTLV-1: persistence and pathogenesis. *Virology* **435**(1): 131-140.

- Cremer D, Hausen BM and Schmalte HW (1987) Toward a rationalization of the sensitizing potency of substituted p-benzoquinones: reaction of nucleophiles with p-benzoquinones. *Journal of medicinal chemistry* **30**(9): 1678-1681.
- Cui C, Yu P, Wu M, Zhang Y, Liu L, Wu B, Wang CX, Zhuo RX and Huang SW (2015) Reduction-sensitive micelles with sheddable PEG shells self-assembled from a Y-shaped amphiphilic polymer for intracellular doxorubicin release. *Colloids and surfaces B, Biointerfaces* **129**: 137-145.
- D'Addio SM, Saad W, Ansell SM, Squiers JJ, Adamson DH, Herrera-Alonso M, Wohl AR, Hoye TR, Macosko CW, Mayer LD, Vauthier C and Prud'homme RK (2012) Effects of block copolymer properties on nanocarrier protection from in vivo clearance. *Journal of controlled release : official journal of the Controlled Release Society* **162**(1): 208-217.
- Damke H, Baba T, van der Blik AM and Schmid SL (1995) Clathrin-independent pinocytosis is induced in cells overexpressing a temperature-sensitive mutant of dynamin. *The Journal of cell biology* **131**(1): 69-80.
- Danaei G, Vander Hoorn S, Lopez AD, Murray CJL and Ezzati M (2005) Causes of cancer in the world: comparative risk assessment of nine behavioural and environmental risk factors. *The Lancet* **366**(9499): 1784-1793.
- Darwiche N, El-Banna S and Gali-Muhtasib H (2007) Cell cycle modulatory and apoptotic effects of plant-derived anticancer drugs in clinical use or development. *Expert opinion on drug discovery* **2**(3): 361-379.
- Das S, Dey KK, Dey G, Pal I, Majumder A, MaitiChoudhury S, Kundu SC and Mandal M (2012) Antineoplastic and apoptotic potential of traditional medicines thymoquinone and diosgenin in squamous cell carcinoma. *PloS one* **7**(10): e46641.
- Davis SS, Round HP and Purewal TS (1981) Ostwald ripening and the stability of emulsion systems: an explanation for the effect of an added third component. *Journal of colloid and interface science* **80**(2): 508-511.
- De Clercq E (2005) John Montgomery's legacy: carbocyclic adenosine analogues as SAH hydrolase inhibitors with broad-spectrum antiviral activity. *Nucleosides, nucleotides & nucleic acids* **24**(10-12): 1395-1415.
- De Jong WH and Borm PJA (2008) Drug delivery and nanoparticles: Applications and hazards. *International journal of nanomedicine* **3**(2): 133-149.
- Dergarabetian EM, Ghattass KI, El-Sitt SB, Al-Mismar RM, El-Baba CO, Itani WS, Melhem NM, El-Hajj HA, Bazarbachi AA, Schneider-Stock R and Gali-Muhtasib HU (2013) Thymoquinone induces apoptosis in malignant T-cells via generation of ROS. *Frontiers in bioscience (Elite edition)* **5**: 706-719.
- Doherty GJ and McMahon HT (2009) Mechanisms of endocytosis. *Annual review of biochemistry* **78**: 857-902.
- Effenberger-Neidnicht K, Breyer S, Mahal K, Diestel R, Sasse F and Schobert R (2011) Cellular localisation of antitumoral 6-alkyl thymoquinones revealed by an alkyne-azide click reaction and the streptavidin-biotin system. *Chembiochem : a European journal of chemical biology* **12**(8): 1237-1241.
- Effenberger-Neidnicht K and Schobert R (2011) Combinatorial effects of thymoquinone on the anti-cancer activity of doxorubicin. *Cancer chemotherapy and pharmacology* **67**(4): 867-874.



- Effenberger K, Breyer S and Schobert R (2010) Terpene conjugates of the *Nigella sativa* seed-oil constituent thymoquinone with enhanced efficacy in cancer cells. *Chemistry & biodiversity* **7**(1): 129-139.
- Ekkapongpisit M, Giovia A, Follo C, Caputo G and Isidoro C (2012) Biocompatibility, endocytosis, and intracellular trafficking of mesoporous silica and polystyrene nanoparticles in ovarian cancer cells: effects of size and surface charge groups. *International journal of nanomedicine* **7**: 4147-4158.
- El-Baba C, Mahadevan V, Fahlbusch FB, S SM, Rau TT, Gali-Muhtasib H and Schneider-Stock R (2014) Thymoquinone-induced conformational changes of PAK1 interrupt pro-survival MEK-ERK signaling in colorectal cancer. *Molecular cancer* **13**: 201.
- El-Mahdy MA, Zhu Q, Wang QE, Wani G and Wani AA (2005) Thymoquinone induces apoptosis through activation of caspase-8 and mitochondrial events in p53-null myeloblastic leukemia HL-60 cells. *International journal of cancer Journal international du cancer* **117**(3): 409-417.
- El-Najjar N, Chatila M, Moukadem H, Vuorela H, Ocker M, Gandesiri M, Schneider-Stock R and Gali-Muhtasib H (2010) Reactive oxygen species mediate thymoquinone-induced apoptosis and activate ERK and JNK signaling. *Apoptosis : an international journal on programmed cell death* **15**(2): 183-195.
- El-Najjar N, Gali-Muhtasib H, Ketola RA, Vuorela P, Urtti A and Vuorela H (2011a) The chemical and biological activities of quinones: overview and implications in analytical detection. *Phytochemistry Reviews* **10**(3): 353-370.
- El-Najjar N, Ketola RA, Nissila T, Mauriala T, Antopolsky M, Janis J, Gali-Muhtasib H, Urtti A and Vuorela H (2011b) Impact of protein binding on the analytical detectability and anticancer activity of thymoquinone. *Journal of chemical biology* **4**(3): 97-107.
- El Gazzar MA, El Mezayen R, Nicolls MR and Dreskin SC (2007) Thymoquinone attenuates proinflammatory responses in lipopolysaccharide-activated mast cells by modulating NF-kappaB nuclear transactivation. *Biochimica et biophysica acta* **1770**(4): 556-564.
- El Saghir NS, Khalil MK, Eid T, El Kinge AR, Charafeddine M, Geara F, Seoud M and Shamseddine AI (2007) Trends in epidemiology and management of breast cancer in developing Arab countries: a literature and registry analysis. *International journal of surgery (London, England)* **5**(4): 225-233.
- El Saghir NS, Seoud M, Khalil MK, Charafeddine M, Salem ZK, Geara FB and Shamseddine AI (2006) Effects of young age at presentation on survival in breast cancer. *BMC cancer* **6**: 194.
- Elsabahy M and Wooley KL (2012) Design of polymeric nanoparticles for biomedical delivery applications. *Chemical Society reviews* **41**(7): 2545-2561.
- Elsherbiny NM and El-Sherbiny M (2014) Thymoquinone attenuates Doxorubicin-induced nephrotoxicity in rats: Role of Nrf2 and NOX4. *Chemico-biological interactions* **223c**: 102-108.
- Gali-Muhtasib H, Diab-Assaf M, Boltze C, Al-Hmaira J, Hartig R, Roessner A and Schneider-Stock R (2004a) Thymoquinone extracted from black seed triggers apoptotic cell death in human colorectal cancer cells via a p53-dependent mechanism. *International journal of oncology* **25**(4): 857-866.
- Gali-Muhtasib H, Kuester D, Mawrin C, Bajbouj K, Diestel A, Ocker M, Habold C, Foltzer-Jourdainne C, Schoenfeld P, Peters B, Diab-Assaf M, Pommrich U, Itani

- W, Lippert H, Roessner A and Schneider-Stock R (2008a) Thymoquinone triggers inactivation of the stress response pathway sensor CHEK1 and contributes to apoptosis in colorectal cancer cells. *Cancer research* **68**(14): 5609-5618.
- Gali-Muhtasib H, Ocker M, Kuester D, Krueger S, El-Hajj Z, Diestel A, Evert M, El-Najjar N, Peters B, Jurjus A, Roessner A and Schneider-Stock R (2008b) Thymoquinone reduces mouse colon tumor cell invasion and inhibits tumor growth in murine colon cancer models. *Journal of cellular and molecular medicine* **12**(1): 330-342.
- Gali-Muhtasib H, Roessner A and Schneider-Stock R (2006) Thymoquinone: a promising anti-cancer drug from natural sources. *The international journal of biochemistry & cell biology* **38**(8): 1249-1253.
- Gali-Muhtasib HU, Abou Kheir WG, Kheir LA, Darwiche N and Crooks PA (2004b) Molecular pathway for thymoquinone-induced cell-cycle arrest and apoptosis in neoplastic keratinocytes. *Anti-cancer drugs* **15**(4): 389-399.
- Ganea GM, Fakayode SO, Losso JN, van Nostrum CF, Sabliov CM and Warner IM (2010) Delivery of phytochemical thymoquinone using molecular micelle modified poly(D, L lactide-co-glycolide) (PLGA) nanoparticles. *Nanotechnology* **21**(28): 285104.
- Ganji-Harsini S, Khazaei M, Rashidi Z and Ghanbari A (2016) Thymoquinone Could Increase The Efficacy of Tamoxifen Induced Apoptosis in Human Breast Cancer Cells: An In Vitro Study. *Cell journal* **18**(2): 245-254.
- Gautier J, Allard-Vannier E, Burlaud-Gaillard J, Domenech J and Chourpa I (2015) Efficacy and Hemotoxicity of Stealth Doxorubicin-Loaded Magnetic Nanovectors on Breast Cancer Xenografts. *Journal of biomedical nanotechnology* **11**(1): 177-189.
- Georgakis GV, Li Y, Humphreys R, Andreeff M, O'Brien S, Younes M, Carbone A, Albert V and Younes A (2005) Activity of selective fully human agonistic antibodies to the TRAIL death receptors TRAIL-R1 and TRAIL-R2 in primary and cultured lymphoma cells: induction of apoptosis and enhancement of doxorubicin- and bortezomib-induced cell death. *British journal of haematology* **130**(4): 501-510.
- Giam CZ and Semmes OJ (2016) HTLV-1 Infection and Adult T-Cell Leukemia/Lymphoma-A Tale of Two Proteins: Tax and HBZ. *Viruses* **8**(6).
- Goncalves DU, Proietti FA, Ribas JG, Araujo MG, Pinheiro SR, Guedes AC and Carneiro-Proietti AB (2010) Epidemiology, treatment, and prevention of human T-cell leukemia virus type 1-associated diseases. *Clinical microbiology reviews* **23**(3): 577-589.
- Gottesman MM (2002) Mechanisms of cancer drug resistance. *Annual review of medicine* **53**: 615-627.
- Grimmer S, van Deurs B and Sandvig K (2002) Membrane ruffling and macropinocytosis in A431 cells require cholesterol. *Journal of cell science* **115**(Pt 14): 2953-2962.
- Guler E, Barlas FB, Yavuz M, Demir B, Gumus ZP, Baspinar Y, Coskunol H and Timur S (2014) Bio-active nanoemulsions enriched with gold nanoparticle, marigold extracts and lipoic acid: In vitro investigations. *Colloids and surfaces B, Biointerfaces* **121**: 299-306.
- Gupta VK, Karar PK, Ramesh S, Misra SP and Gupta A (2010) Nanoparticle Formulation for Hydrophilic & Hydrophobic Drugs. *Int J Res Pharm* **1**(2): 163-169.

- Han K, Miah MA, Shanmugam S, Yong CS, Choi HG, Kim JA and Yoo BK (2007) Mixed micellar nanoparticle of amphotericin B and poly styrene-block-poly ethylene oxide reduces nephrotoxicity but retains antifungal activity. *Archives of pharmacol research* **30**(10): 1344-1349.
- Harpole JL, Tucci M and Benghuzzi H (2015) Pathophysiological Effects of Thymoquinone and Epigallocatechin-3-Gallate on SK-OV-3 Ovarian Cancer Like Cell Line. *Biomedical sciences instrumentation* **51**: 31-39.
- Hofmann D, Messerschmidt C, Bannwarth MB, Landfester K and Mailander V (2014) Drug delivery without nanoparticle uptake: delivery by a kiss-and-run mechanism on the cell membrane. *Chemical communications (Cambridge, England)* **50**(11): 1369-1371.
- Holliday DL and Speirs V (2011) Choosing the right cell line for breast cancer research. *Breast cancer research : BCR* **13**(4): 215.
- Hu CM, Aryal S and Zhang L (2010) Nanoparticle-assisted combination therapies for effective cancer treatment. *Therapeutic delivery* **1**(2): 323-334.
- Hu W, Qiu L, Cheng L, Hu Q, Liu Y, Hu Z, Chen D and Cheng L (2016) Redox and pH dual responsive poly(amidoamine) dendrimer-poly(ethylene glycol) conjugates for intracellular delivery of doxorubicin. *Acta biomaterialia* **36**: 241-253.
- Hwang N-M, Jung J-S and Lee D-K (2012) Thermodynamics and Kinetics in the Synthesis of Monodisperse Nanoparticles.
- Iversen T-G, Skotland T and Sandvig K (2011) Endocytosis and intracellular transport of nanoparticles: Present knowledge and need for future studies. *Nano Today* **6**(2): 176-185.
- Jafri SH, Glass J, Shi R, Zhang S, Prince M and Kleiner-Hancock H (2010) Thymoquinone and cisplatin as a therapeutic combination in lung cancer: In vitro and in vivo. *Journal of experimental & clinical cancer research : CR* **29**: 87.
- Johnson BK and Prud'homme RK (2003) Mechanism for rapid self-assembly of block copolymer nanoparticles. *Physical review letters* **91**(11): 118302.
- Johnson BK, Prud, #39 and homme RK (2003) Flash NanoPrecipitation of Organic Actives and Block Copolymers using a Confined Impinging Jets Mixer. *Australian Journal of Chemistry* **56**(10): 1021-1024.
- Kaseb AO, Chinnakannu K, Chen D, Sivanandam A, Tejwani S, Menon M, Dou QP and Reddy GP (2007) Androgen receptor and E2F-1 targeted thymoquinone therapy for hormone-refractory prostate cancer. *Cancer research* **67**(16): 7782-7788.
- Kensara OA, El-Shemi AG, Mohamed AM, Refaat B, Idris S and Ahmad J (2016) Thymoquinone subdues tumor growth and potentiates the chemopreventive effect of 5-fluorouracil on the early stages of colorectal carcinogenesis in rats. *Drug design, development and therapy* **10**: 2239-2253.
- Kfoury Y, Nasr R, Hermine O, de The H and Bazarbachi A (2005) Proapoptotic regimes for HTLV-I-transformed cells: targeting Tax and the NF-kappaB pathway. *Cell death and differentiation* **12 Suppl 1**: 871-877.
- Khalife R, El-Hayek S, Tarras O, Hodroj MH and Rizk S (2014) Antiproliferative and proapoptotic effects of topotecan in combination with thymoquinone on acute myelogenous leukemia. *Clinical lymphoma, myeloma & leukemia* **14 Suppl**: S46-55.
- Khan MA, Tania M, Wei C, Mei Z, Fu S, Cheng J, Xu J and Fu J (2015) Thymoquinone inhibits cancer metastasis by downregulating TWIST1 expression to reduce epithelial to mesenchymal transition. *Oncotarget*.

- Kievit FM and Zhang M (2011) Cancer nanotheranostics: improving imaging and therapy by targeted delivery across biological barriers. *Advanced materials (Deerfield Beach, Fla)* **23**(36): H217-247.
- Kou L, Sun J, Zhai Y and He Z (2013) The endocytosis and intracellular fate of nanomedicines: Implication for rational design. *Asian Journal of Pharmaceutical Sciences* **8**(1): 1-10.
- Kumari S, Mg S and Mayor S (2010) Endocytosis unplugged: multiple ways to enter the cell. *Cell research* **20**(3): 256-275.
- Laan AC, Santini C, Jennings L, de Jong M, Bernsen MR and Denkova AG (2016) Radiolabeling polymeric micelles for in vivo evaluation: a novel, fast, and facile method. *EJNMMI research* **6**(1): 12.
- Lakkis NA, Adib SM, Osman MH, Musharafieh UM and Hamadeh GN (2010) Breast cancer in Lebanon: incidence and comparison to regional and Western countries. *Cancer epidemiology* **34**(3): 221-225.
- Lammers T (2012) Nanomedicine on the move: from monotherapeutic regimens to combination therapies. *Expert review of clinical pharmacology* **5**(2): 105-108.
- Lammers T, Kiessling F, Hennink WE and Storm G (2012) Drug targeting to tumors: principles, pitfalls and (pre-) clinical progress. *Journal of controlled release : official journal of the Controlled Release Society* **161**(2): 175-187.
- Lehar J, Krueger AS, Avery W, Heilbut AM, Johansen LM, Price ER, Rickles RJ, Short GF, 3rd, Staunton JE, Jin X, Lee MS, Zimmermann GR and Borisy AA (2009) Synergistic drug combinations tend to improve therapeutically relevant selectivity. *Nature biotechnology* **27**(7): 659-666.
- Li F, Rajendran P and Sethi G (2010) Thymoquinone inhibits proliferation, induces apoptosis and chemosensitizes human multiple myeloma cells through suppression of signal transducer and activator of transcription 3 activation pathway. *British journal of pharmacology* **161**(3): 541-554.
- Liu P, Sun Y, Wang Q, Sun Y, Li H and Duan Y (2014) Intracellular trafficking and cellular uptake mechanism of mPEG-PLGA-PLL and mPEG-PLGA-PLL-Gal nanoparticles for targeted delivery to hepatomas. *Biomaterials* **35**(2): 760-770.
- Lo HW (2010) Targeting Ras-RAF-ERK and its interactive pathways as a novel therapy for malignant gliomas. *Current cancer drug targets* **10**(8): 840-848.
- Lopez-Davila V, Seifalian AM and Loizidou M (2012) Organic nanocarriers for cancer drug delivery. *Current opinion in pharmacology* **12**(4): 414-419.
- Ma L, Kohli M and Smith A (2013) Nanoparticles for combination drug therapy. *ACS nano* **7**(11): 9518-9525.
- Mahato R, Tai W and Cheng K (2011) Prodrugs for improving tumor targetability and efficiency. *Advanced drug delivery reviews* **63**(8): 659-670.
- Marshall E (2014) Breast cancer. Dare to do less. *Science (New York, NY)* **343**(6178): 1454-1456.
- Mateo-Mateo C, #xe1, zquez-V, #xe1, zquez C, #xe9, rez-Lorenzo M, #xe9, Salgueiri, #xf1, o V, #xf3, nica and Correa-Duarte MA (2012) Ostwald Ripening of Platinum Nanoparticles Confined in a Carbon Nanotube/Silica-Templated Cylindrical Space. *Journal of Nanomaterials* **2012**: 6.
- Melroy J and Nair V (2005) The antiviral activity, mechanism of action, clinical significance and resistance of abacavir in the treatment of pediatric AIDS. *Current pharmaceutical design* **11**(29): 3847-3852.

- Mohanraj VJ and Chen Y (2006) Nanoparticles - A review. *Trop J Pharm Res* **5**(1): 561-573.
- Motaghed M, Al-Hassan FM and Hamid SS (2013) Cellular responses with thymoquinone treatment in human breast cancer cell line MCF-7. *Pharmacognosy research* **5**(3): 200-206.
- Motaghed M, Al-Hassan FM and Hamid SS (2014) Thymoquinone regulates gene expression levels in the estrogen metabolic and interferon pathways in MCF7 breast cancer cells. *International journal of molecular medicine* **33**(1): 8-16.
- Mu GG, Zhang LL, Li HY, Liao Y and Yu HG (2015) Thymoquinone Pretreatment Overcomes the Insensitivity and Potentiates the Antitumor Effect of Gemcitabine Through Abrogation of Notch1, PI3K/Akt/mTOR Regulated Signaling Pathways in Pancreatic Cancer. *Digestive diseases and sciences* **60**(4): 1067-1080.
- Muhleisen A, Giaisi M, Kohler R, Krammer PH and Li-Weber M (2014) Tax contributes apoptosis resistance to HTLV-1-infected T cells via suppression of Bid and Bim expression. *Cell death & disease* **5**: e1575.
- Nagi MN and Mansour MA (2000) Protective effect of thymoquinone against doxorubicin-induced cardiotoxicity in rats: a possible mechanism of protection. *Pharmacological research : the official journal of the Italian Pharmacological Society* **41**(3): 283-289.
- Nair HB, Sung B, Yadav VR, Kannappan R, Chaturvedi MM and Aggarwal BB (2010) Delivery of antiinflammatory nutraceuticals by nanoparticles for the prevention and treatment of cancer. *Biochemical pharmacology* **80**(12): 1833-1843.
- Nekkanti V, Vabalaboina V and Pillai R (2012) Drug Nanoparticles – An Overview, in *The Delivery of Nanoparticles* (Hashim AA ed), InTech.
- Ng WK, Saiful Yazan L, Yap LH, Wan Nor Hafiza WA, How CW and Abdullah R (2015) Thymoquinone-loaded nanostructured lipid carrier exhibited cytotoxicity towards breast cancer cell lines (MDA-MB-231 and MCF-7) and cervical cancer cell lines (HeLa and SiHa). *BioMed research international* **2015**: 263131.
- Nielsen UB, Kirpotin DB, Pickering EM, Hong K, Park JW, Refaat Shalaby M, Shao Y, Benz CC and Marks JD (2002) Therapeutic efficacy of anti-ErbB2 immunoliposomes targeted by a phage antibody selected for cellular endocytosis. *Biochimica et biophysica acta* **1591**(1-3): 109-118.
- Nounou MI, ElAmrawy F, Ahmed N, Abdelraouf K, Goda S and Syed-Sha-Qhattal H (2015) Breast Cancer: Conventional Diagnosis and Treatment Modalities and Recent Patents and Technologies. *Breast cancer : basic and clinical research* **9**(Suppl 2): 17-34.
- Octavia Y, Tocchetti CG, Gabrielson KL, Janssens S, Crijns HJ and Moens AL (2012) Doxorubicin-induced cardiomyopathy: from molecular mechanisms to therapeutic strategies. *Journal of molecular and cellular cardiology* **52**(6): 1213-1225.
- Odeh F, Ismail SI, Abu-Dahab R, Mahmoud IS and Al Bawab A (2012) Thymoquinone in liposomes: a study of loading efficiency and biological activity towards breast cancer. *Drug delivery* **19**(8): 371-377.
- Oh N and Park JH (2014) Endocytosis and exocytosis of nanoparticles in mammalian cells. *International journal of nanomedicine* **9** **Suppl 1**: 51-63.
- Parbin S, Shilpi A, Kar S, Pradhan N, Sengupta D, Deb M, Rath SK and Patra SK (2015) Insights into the molecular interactions of thymoquinone with histone

- deacetylase: evaluation of the therapeutic intervention potential against breast cancer. *Molecular bioSystems* **12**(1): 48-58.
- Pathan SA, Jain GK, Zaidi SM, Akhter S, Vohora D, Chander P, Kole PL, Ahmad FJ and Khar RK (2011) Stability-indicating ultra-performance liquid chromatography method for the estimation of thymoquinone and its application in biopharmaceutical studies. *Biomedical chromatography : BMC* **25**(5): 613-620.
- Pelkmans L, Puntener D and Helenius A (2002) Local actin polymerization and dynamin recruitment in SV40-induced internalization of caveolae. *Science (New York, NY)* **296**(5567): 535-539.
- Petschauer JS, Madden AJ, Kirschbrown WP, Song G and Zamboni WC (2015) The effects of nanoparticle drug loading on the pharmacokinetics of anticancer agents. *Nanomedicine (London, England)* **10**(3): 447-463.
- Pinder MC and Ibrahim NK (2006) Nanoparticle albumin-bound paclitaxel for treatment of metastatic breast cancer. *Drugs of today (Barcelona, Spain : 1998)* **42**(9): 599-604.
- Rajput S, Kumar BN, Banik P, Parida S and Mandal M (2015a) Thymoquinone restores radiation-induced TGF-beta expression and abrogates EMT in chemoradiotherapy of breast cancer cells. *Journal of cellular physiology* **230**(3): 620-629.
- Rajput S, Kumar BN, Dey KK, Pal I, Parekh A and Mandal M (2013a) Molecular targeting of Akt by thymoquinone promotes G(1) arrest through translation inhibition of cyclin D1 and induces apoptosis in breast cancer cells. *Life sciences* **93**(21): 783-790.
- Rajput S, Kumar BN, Sarkar S, Das S, Azab B, Santhekadur PK, Das SK, Emdad L, Sarkar D, Fisher PB and Mandal M (2013b) Targeted apoptotic effects of thymoquinone and tamoxifen on XIAP mediated Akt regulation in breast cancer. *PloS one* **8**(4): e61342.
- Rajput S, Puvvada N, Kumar BN, Sarkar S, Konar S, Bharti R, Dey G, Mazumdar A, Pathak A, Fisher PB and Mandal M (2015b) Overcoming Akt Induced Therapeutic Resistance in Breast Cancer through siRNA and Thymoquinone Encapsulated Multilamellar Gold Niosomes. *Molecular pharmaceutics* **12**(12): 4214-4225.
- Ravindran J, Nair HB, Sung B, Prasad S, Tekmal RR and Aggarwal BB (2010) Thymoquinone poly (lactide-co-glycolide) nanoparticles exhibit enhanced anti-proliferative, anti-inflammatory, and chemosensitization potential. *Biochemical pharmacology* **79**(11): 1640-1647.
- Reynolds AR, Moein Moghimi S and Hodivala-Dilke K (2003) Nanoparticle-mediated gene delivery to tumour neovasculature. *Trends in molecular medicine* **9**(1): 2-4.
- Roepke M, Diestel A, Bajbouj K, Walluscheck D, Schonfeld P, Roessner A, Schneider-Stock R and Gali-Muhtasib H (2007) Lack of p53 augments thymoquinone-induced apoptosis and caspase activation in human osteosarcoma cells. *Cancer biology & therapy* **6**(2): 160-169.
- Rollas S and Kucukguzel SG (2007) Biological activities of hydrazone derivatives. *Molecules (Basel, Switzerland)* **12**(8): 1910-1939.
- Ryan SM and Brayden DJ (2014) Progress in the delivery of nanoparticle constructs: towards clinical translation. *Current opinion in pharmacology* **18**: 120-128.
- Saad WS and Prud'homme RK (2016) Principles of nanoparticle formation by Flash Nanoprecipitation. *Nano Today*.

- Sabharanjak S, Sharma P, Parton RG and Mayor S (2002) GPI-anchored proteins are delivered to recycling endosomes via a distinct cdc42-regulated, clathrin-independent pinocytic pathway. *Developmental cell* **2**(4): 411-423.
- Sakalar C, Izgi K, Iskender B, Sezen S, Aksu H, Cakir M, Kurt B, Turan A and Canatan H (2015) The combination of thymoquinone and paclitaxel shows anti-tumor activity through the interplay with apoptosis network in triple-negative breast cancer. *Tumour biology : the journal of the International Society for Oncodevelopmental Biology and Medicine*.
- Salim LZ, Mohan S, Othman R, Abdelwahab SI, Kamalidehghan B, Sheikh BY and Ibrahim MY (2013) Thymoquinone induces mitochondria-mediated apoptosis in acute lymphoblastic leukaemia in vitro. *Molecules (Basel, Switzerland)* **18**(9): 11219-11240.
- Salim LZ, Othman R, Abdulla MA, Al-Jashamy K, Ali HM, Hassandarvish P, Dehghan F, Ibrahim MY, Omer FA and Mohan S (2014) Thymoquinone inhibits murine leukemia WEHI-3 cells in vivo and in vitro. *PloS one* **9**(12): e115340.
- Sandvig K, Torgersen ML, Raa HA and van Deurs B (2008) Clathrin-independent endocytosis: from nonexistent to an extreme degree of complexity. *Histochemistry and cell biology* **129**(3): 267-276.
- Schneider-Stock R, Fakhoury IH, Zaki AM, El-Baba CO and Gali-Muhtasib HU (2014) Thymoquinone: fifty years of success in the battle against cancer models. *Drug discovery today* **19**(1): 18-30.
- Schubbert S, Bollag G and Shannon K (2007) Deregulated Ras signaling in developmental disorders: new tricks for an old dog. *Current opinion in genetics & development* **17**(1): 15-22.
- Seleem HS, El-Inany GA, El-Shetary BA and Mousa MA (2011) The ligational behavior of a phenolic quinolyl hydrazone towards copper(II)- ions. *Chemistry Central journal* **5**(1): 2.
- Sethi G, Ahn KS and Aggarwal BB (2008) Targeting nuclear factor-kappa B activation pathway by thymoquinone: role in suppression of antiapoptotic gene products and enhancement of apoptosis. *Molecular cancer research : MCR* **6**(6): 1059-1070.
- Shah M, Choi MH, Ullah N, Kim MO and Yoon SC (2011) Synthesis and characterization of PHV-block-mPEG diblock copolymer and its formation of amphiphilic nanoparticles for drug delivery. *Journal of nanoscience and nanotechnology* **11**(7): 5702-5710.
- Shah M, Naseer MI, Choi MH, Kim MO and Yoon SC (2010) Amphiphilic PHA-mPEG copolymeric nanocontainers for drug delivery: preparation, characterization and in vitro evaluation. *International journal of pharmaceuticals* **400**(1-2): 165-175.
- Shapira A, Livney YD, Broxterman HJ and Assaraf YG (2011) Nanomedicine for targeted cancer therapy: towards the overcoming of drug resistance. *Drug resistance updates : reviews and commentaries in antimicrobial and anticancer chemotherapy* **14**(3): 150-163.
- Shaw T and Locarnini S (2004) Entecavir for the treatment of chronic hepatitis B. *Expert review of anti-infective therapy* **2**(6): 853-871.
- Shoieb AM, Elgayyar M, Dudrick PS, Bell JL and Tithof PK (2003) In vitro inhibition of growth and induction of apoptosis in cancer cell lines by thymoquinone. *International journal of oncology* **22**(1): 107-113.
- Singh A, Ahmad I, Akhter S, Jain GK, Iqbal Z, Talegaonkar S and Ahmad FJ (2013) Nanocarrier based formulation of Thymoquinone improves oral delivery: stability

- assessment, in vitro and in vivo studies. *Colloids and surfaces B, Biointerfaces* **102**: 822-832.
- Singh Y, Palombo M and Sinko PJ (2008) Recent trends in targeted anticancer prodrug and conjugate design. *Current medicinal chemistry* **15**(18): 1802-1826.
- Siveen KS, Mustafa N, Li F, Kannaiyan R, Ahn KS, Kumar AP, Chng WJ and Sethi G (2014) Thymoquinone overcomes chemoresistance and enhances the anticancer effects of bortezomib through abrogation of NF-kappaB regulated gene products in multiple myeloma xenograft mouse model. *Oncotarget* **5**(3): 634-648.
- Sugimoto K, Tamayose K, Sasaki M, Hayashi K and Oshimi K (2002) Low-dose doxorubicin-induced necrosis in Jurkat cells and its acceleration and conversion to apoptosis by antioxidants. *British journal of haematology* **118**(1): 229-238.
- Sutton KM, Doucette CD and Hoskin DW (2012) NADPH quinone oxidoreductase 1 mediates breast cancer cell resistance to thymoquinone-induced apoptosis. *Biochemical and biophysical research communications* **426**(3): 421-426.
- Sutton KM, Greenshields AL and Hoskin DW (2014) Thymoquinone, a bioactive component of black caraway seeds, causes G1 phase cell cycle arrest and apoptosis in triple-negative breast cancer cells with mutant p53. *Nutrition and cancer* **66**(3): 408-418.
- Swami A, Shi J, Gadde S, Votruba A, Kolishetti N and Farokhzad O (2012) Nanoparticles for Targeted and Temporally Controlled Drug Delivery, in *Multifunctional Nanoparticles for Drug Delivery Applications* (Svenson S and Prud'homme RK eds) pp 9-29, Springer US.
- Tadros T, Izquierdo P, Esquena J and Solans C (2004) Formation and stability of nano-emulsions. *Advances in colloid and interface science* **108-109**: 303-318.
- Takashima A and Faller DV (2013) Targeting the RAS oncogene. *Expert opinion on therapeutic targets* **17**(5): 507-531.
- Uozumi K (2010) Treatment of adult T-cell leukemia. *Journal of clinical and experimental hematopathology : JCEH* **50**(1): 9-25.
- Utsunomiya A, Choi I, Chihara D and Seto M (2015) Recent advances in the treatment of adult T-cell leukemia-lymphomas. *Cancer science* **106**(4): 344-351.
- van Vlerken LE and Amiji MM (2006) Multi-functional polymeric nanoparticles for tumour-targeted drug delivery. *Expert Opin Drug Deliv* **3**(2): 205-216.
- Velho-Pereira R, Kumar A, Pandey BN, Jagtap AG and Mishra KP (2011) Radiosensitization in human breast carcinoma cells by thymoquinone: role of cell cycle and apoptosis. *Cell biology international* **35**(10): 1025-1029.
- Vercauteren D, Vandenbroucke RE, Jones AT, Rejman J, Demeester J, De Smedt SC, Sanders NN and Braeckmans K (2010) The use of inhibitors to study endocytic pathways of gene carriers: optimization and pitfalls. *Molecular therapy : the journal of the American Society of Gene Therapy* **18**(3): 561-569.
- Wang B, Rosano JM, Cheheltani R, Achary MP and Kiani MF (2010) Towards a targeted multi-drug delivery approach to improve therapeutic efficacy in breast cancer. *Expert opinion on drug delivery* **7**(10): 1159-1173.
- Wilson AJ, Saskowski J, Barham W, Yull F and Khabele D (2015) Thymoquinone enhances cisplatin-response through direct tumor effects in a syngeneic mouse model of ovarian cancer. *Journal of ovarian research* **8**: 46.
- Wirries A, Breyer S, Quint K, Schobert R and Ocker M (2010) Thymoquinone hydrazone derivatives cause cell cycle arrest in p53-competent colorectal cancer cells. *Experimental and therapeutic medicine* **1**(2): 369-375.



- Woo CC, Kumar AP, Sethi G and Tan KH (2012) Thymoquinone: potential cure for inflammatory disorders and cancer. *Biochemical pharmacology* **83**(4): 443-451.
- Woo CC, Loo SY, Gee V, Yap CW, Sethi G, Kumar AP and Tan KH (2011) Anticancer activity of thymoquinone in breast cancer cells: possible involvement of PPAR-gamma pathway. *Biochemical pharmacology* **82**(5): 464-475.
- World Health Organization (2015) Cancer Fact sheet N°297.
- World Health Organization (2016) Breast cancer: prevention and control.
- Worthen DR, Ghosheh OA and Crooks PA (1998) The in vitro anti-tumor activity of some crude and purified components of blackseed, *Nigella sativa* L. *Anticancer research* **18**(3a): 1527-1532.
- Wu ZH, Chen Z, Shen Y, Huang LL and Jiang P (2011) [Anti-metastasis effect of thymoquinone on human pancreatic cancer]. *Yao xue xue bao = Acta pharmaceutica Sinica* **46**(8): 910-914.
- Xu S, Olenyuk BZ, Okamoto CT and Hamm-Alvarez SF (2013) Targeting receptor-mediated endocytotic pathways with nanoparticles: rationale and advances. *Advanced drug delivery reviews* **65**(1): 121-138.
- Yi T, Cho SG, Yi Z, Pang X, Rodriguez M, Wang Y, Sethi G, Aggarwal BB and Liu M (2008) Thymoquinone inhibits tumor angiogenesis and tumor growth through suppressing AKT and extracellular signal-regulated kinase signaling pathways. *Molecular cancer therapeutics* **7**(7): 1789-1796.
- Yoshida M (2001) Multiple viral strategies of HTLV-1 for dysregulation of cell growth control. *Annual review of immunology* **19**: 475-496.
- Yuan J, Sanhaji M, Kramer A, Reindl W, Hofmann M, Kreis NN, Zimmer B, Berg T and Strebhardt K (2011) Polo-box domain inhibitor poloxin activates the spindle assembly checkpoint and inhibits tumor growth in vivo. *The American journal of pathology* **179**(4): 2091-2099.
- Yuen GJ, Weller S and Pakes GE (2008) A review of the pharmacokinetics of abacavir. *Clinical pharmacokinetics* **47**(6): 351-371.
- Yusufi M, Banerjee S, Mohammad M, Khatal S, Venkateswara Swamy K, Khan EM, Aboukameel A, Sarkar FH and Padhye S (2013) Synthesis, characterization and anti-tumor activity of novel thymoquinone analogs against pancreatic cancer. *Bioorganic & medicinal chemistry letters* **23**(10): 3101-3104.
- Zamboni WC, Torchilin V, Patri AK, Hrkach J, Stern S, Lee R, Nel A, Panaro NJ and Grodzinski P (2012) Best practices in cancer nanotechnology: perspective from NCI nanotechnology alliance. *Clinical cancer research : an official journal of the American Association for Cancer Research* **18**(12): 3229-3241.
- Zamoyska R, Basson A, Filby A, Legname G, Lovatt M and Seddon B (2003) The influence of the src-family kinases, Lck and Fyn, on T cell differentiation, survival and activation. *Immunological reviews* **191**: 107-118.
- Zeng X, Morgenstern R and Nystrom AM (2014) Nanoparticle-directed sub-cellular localization of doxorubicin and the sensitization breast cancer cells by circumventing GST-mediated drug resistance. *Biomaterials* **35**(4): 1227-1239.
- Zhang LW and Monteiro-Riviere NA (2009) Mechanisms of quantum dot nanoparticle cellular uptake. *Toxicological sciences : an official journal of the Society of Toxicology* **110**(1): 138-155.
- Zou P, Chen H, Paholak HJ and Sun D (2013) Noninvasive fluorescence resonance energy transfer imaging of in vivo premature drug release from polymeric nanoparticles. *Molecular pharmaceutics* **10**(11): 4185-4194.

